

**PREPARATION OF SOME SUPRAMOLECULAR  
ASSEMBLIES OF AN ADAMANTANEDICARBOXYLIC  
ACID**

**A THESIS  
SUBMITTED FOR THE DEGREE OF  
DOCTOR OF PHILOSOPHY  
(IN CHEMISTRY)**

**TO  
UNIVERSITY OF PUNE**

**BY  
Mr. Yogesh Shivdas Manjare**

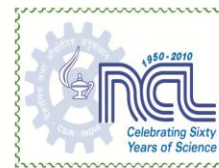
**DIVISION OF ORGANIC CHEMISTRY  
NATIONAL CHEMICAL LABORATORY  
DR. HOMI BHABHA ROAD  
PUNE-411008**

**May-2012**

*Dedicated*  
*To*  
*MY*  
*Parents*



राष्ट्रीय रासायनिक प्रयोगशाला  
(वैज्ञानिक तथा औद्योगिक अनुसंधान परिषद)  
डॉ. होमी भाभा रोड, पुणे - 411 008. भारत  
**NATIONAL CHEMICAL LABORATORY**  
(Council of Scientific & Industrial Research)  
Dr. Homi Bhabha Road, Pune - 411008. India



## CERTIFICATE

This is to certify that the work presented in this thesis entitled “**Preparation of Some Supramolecular Assemblies of an Adamantanedicarboxylic Acid**” submitted by **Mr. Yogesh Shivdas Manjare**, has been carried out by the candidate at National Chemical Laboratory, Pune, India, under my supervision. Such materials as obtained from other sources have been duly acknowledged in the thesis. This work is original and has not been submitted for any other degree or diploma of this or any other university.

May 2012  
Pune

Dr. V. R. Pedireddi

## CANDIDATE'S DECLARATION

I hereby declare that the research work presented in the thesis entitled "Preparation of Some Supramolecular Assemblies of an Adamantanedicarboxylic Acid" was carried out by me at the National Chemical Laboratory, Pune, India, under the supervision of **Dr. V. R. Pedireddi**, Scientist, Division of Organic Chemistry, National Chemical Laboratory, Pune, India and submitted for the degree of Doctor of Philosophy in Chemistry to the University of Pune. This work is original and has not been submitted in part or full by me for any other degree or diploma of this or any other university.

May 2012  
Pune

Yogesh Manjare



## Acknowledgements

With deep sense of gratitude and profound respect, I express my sincere thanks to my mentor, Prof. V. R. Pedireddi for his inspiring guidance and constant encouragement throughout my Ph.D. He has been my source of inspiration in many aspects. I have been able to learn many things from him and consider my association with him a rewarding experience.

It is my privilege to thank Dr. Ganesh Pandey Head of the Division of Organic Chemistry, NCL for his constant support and encouragement during the progress of this work. Also I thank Dr. K. N. Ganesh, former Head of the Division of Organic Chemistry, NCL, and current director, IISER, Pune, for his support.

I thank Dr. Sourav Pal, present Director NCL, and Dr. S. Sivaram, former Director NCL, for their support as for giving infrastructure facilities, and University Grand Commission, New Delhi for financial support.

My heartfelt thanks to Dr. Ramana for his support to carry out research work. I thank Dr. P. A. Joy and Dr. C. V. V. Sathyanarayana for their assistance toward the use of characterization techniques. I also thank Dr. Avinash Kumbhar for his support in many aspects.

I am grateful to Dr. Mohan Bhadbhade, Dr. Mrs. Vedavathi Puranik and Dr. Rajesh Gonnade for their assistance in the single crystal X-ray diffraction.

I wish to thank my friendly and cooperative labmates, Prakash Reddy, Kapil Arora, Sunil Varughese, Seetha Lekshmi, S. Marivel, Sathyanarayana Reddy, Amit Delori, Manishkumar Shimpi, V. Nagrajan, Manish Raut, Prince Ravat, Ketaki Upadhey, Mayura Talwelkar, Sharmita Bishwas, Amrita Nayak, Purnendu Nandy and others for their help in various capacities and providing me with an excellent working ambience.

I am thankful to all the teachers and lecturers, who taught me throughout my career. I thank to Shree Jaganale, Wagh and Ingle. I thank Dr. Mahajan, Dr. Rajaput, Dr. Parate, Dr. Doshi, Dr. Bolakhe, Dr. Mohad, Dr. Jayprakash and others who ignited my interest in chemistry through excellent chemistry lectures.

It gives me great pleasure to thank my beloved parents, for their love, tremendous patience, trust and encouragement during many years of studies. They have been my constant source of strength and have brought a great deal of happiness to my life.

Special thank to my wife, Hrushali who has provided me with that extra bit of inspiration when I really needed it.

I thank to my sisters, Varsha, Sarika, Sanjivani, Ashwini and Brothers-in-law, Subhash Munde, Nana Lad, Gajanan Bande and Ankush Shete for their expectation and hope, that kept me awake all along.

Special thanks to my father-in-law, Mahedevrao Turak, mother-in-law, Latabai Turak, sister-in-law, Ashwini and brothers-in-law, Ashish and Vikas Shelake for their expectations and hope that kept me awake all along.

I thank all my friends Sudesh Manjare, Mangesh Mahajan, Lenin, Bhausahab Tawade, Bala, Edwin, Vivek Humane, Vilas, Ajay Jha, Amol Nerkar, Viyay Masand and others for their support.

The blessings and best wishes of my parents keep me active throughout my life. They made me what I am and I owe everything to them. Dedicating this thesis to them is a minor recognition for their invaluable support and encouragement.

I thank all of you once again for your kind support and cooperation.

Yogesh

# CONTENTS

---

---

---

## Chapter I

### An Overview of Contemporary Research in Supramolecular Chemistry

1.1 Introduction	2
1.2 Supramolecular Chemistry	3
1.3 Hydrogen bond	6
1.4 Co-crystals	11
1.5 Pharmaceutical Cocrystallization	23
1.6 Conclusions	31
1.7 References	32

---

---

## Chapter II

### Preparation and Analysis of Co-crystals of 1,3-Adamantanedicarboxylic Acid with N-Oxide and Aza Compounds

2.1 Introduction	41
2.2 Co-crystals of 1,3-Adamantanedicarboxylic Acid with 1,3-di(pyridin-4-yl)propane	49
2.3 Co-crystals of 1,3-Adamantanedicarboxylic Acid with <i>E</i> -1,2-di(pyridine-4yl)diazene	51
2.4 Co-crystals of 1,3-Adamantanedicarboxylic Acid with <i>E</i> -2,2'-(ethene-1,2-diyl)dipyridine 1-oxide	54
2.5 Polymorphs of Co-crystals of 1,3-Adamantanedicarboxylic Acid with 1,7-Phenanthroline	57
2.6 Conclusions	62
2.7 Experimental Section	62
2.8 References	66

---

---

### Chapter III

#### Host-Guest Assemblies of 1,3-Adamantanedicarboxylic Acid in the Presence of Various Hydrogen Bond Donor and Acceptor Compounds

---

3.1 Introduction	72
3.2 Host-Guest Complex of 1,3-Adamantanedicarboxylic Acid and 4,7-Phenanthroline with Water	86
3.3 Host-Guest Complex of 1,3-Adamantanedicarboxylic Acid and 4,7-Phenanthroline with Phenol	89
3.4 Host-Guest Complex of 1,3-Adamantanedicarboxylic Acid and 4,7-Phenanthroline with 1,4-dihydroxybenzene	92
3.5 Host-Guest Complex of 1,3-Adamantanedicarboxylic Acid and 4,7-Phenanthroline with 1,2-dihydroxybenzene	94
3.6 Host-Guest Complex of 1,3-Adamantanedicarboxylic Acid and 4,7-Phenanthroline with 1,3-dihydroxybenzene	96
3.7 Host-Guest Complex of 1,3-Adamantanedicarboxylic Acid and 4,7-Phenanthroline with 4-Aminophenol	98
3.8 Host-Guest Complex of 1,3-Adamantanedicarboxylic Acid and 4,7-Phenanthroline with 1,4-Dioxane	100
3.9 Conclusions	102
3.10 Experimental Section	103
3.11 References	108

---

### Chapter IV

#### Preparation and Analysis of Anhydrous and Hydrated Forms of 1,3-Adamantanedicarboxylic Acid with Different Aza Compounds

---

4.1 Introduction	112
4.2 Hydrated and Anhydrous Co-crystal of 1,3-Adamantanedicarboxylic Acid with 4,7-Phenanthroline	116
4.3 Hydrated and Anhydrous Co-crystal of 1,3-Adamantanedicarboxylic Acid with 1,4-diazabicyclo(2.2.2)octane	124
4.4 Hydrated and Anhydrous Co-crystal of 1,3-Adamantanedicarboxylic Acid with Piperazine	131
4.5 Hydrated and Anhydrous Co-crystal of 1,3-Adamantanedicarboxylic Acid with Norfloxacin	138
4.6 Conclusions	144
4.7 Experimental Section	145
4.8 References	150
Publications	154
Symposia/Poster presentation	155

---

The thesis entitled “**Preparation of Some Supramolecular Assemblies of an Adamantanedicarboxylic Acid**” contains following four chapters. Chapter I is an overview of contemporary supramolecular chemistry highlighting various strategies towards target directed synthesis of supramolecular assemblies. Chapter II deals with preparation and analysis of co-crystals of 1,3-adamantanedicarboxylic acid with *N*-oxide and aza compounds. In Chapter III, host guest assemblies of 1,3-adamantanedicarboxylic acid and 4,7-phenanthroline in the presence of various other organic ligands are described. Finally in Chapter IV, preparation and analysis of anhydrous and hydrated forms of 1,3-adamantanedicarboxylic acid with different aza compounds are discussed.

### **Chapter I**

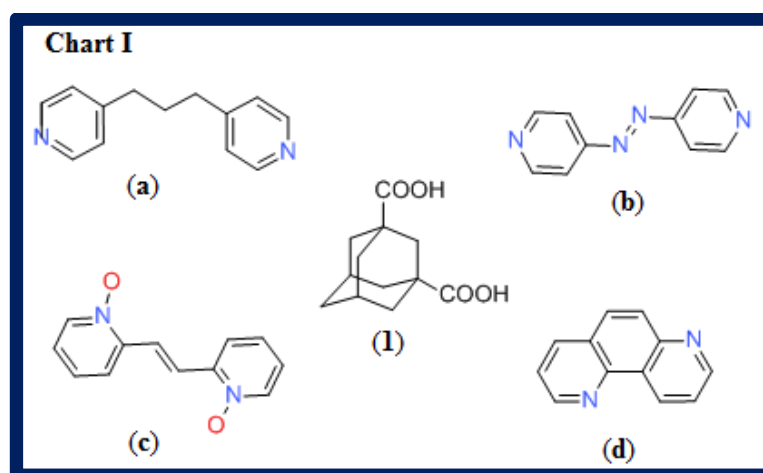
Supramolecular assembly, an aggregate of different types of components, such as ions, atoms, molecules, etc., is due to the intermolecular forces, often being referred as noncovalent interactions. In recent decades, the aggregation behaviour of the organic molecules has been extensively studied to evaluate the influence of noncovalent interactions towards the arrangement of molecules in the crystalline solids, as the physical and chemical properties of crystalline solids depend on the packing of molecular components within the crystal structure. For examples (1) a nonlinear optical (NLO) property of a crystalline solid is due to the non-centrosymmetric arrangement of its molecules. (2) Also the physical properties such as solubility, thermal stability, hygroscopicity, etc., of an active pharmaceutical ingredient (API) vary with different (polymorphic) arrangements of

its molecules in solid state. However, prediction of a specific type of aggregation, in other words, a crystal form, of a solid is not yet well established. Thus, structural chemists thrive to achieve control over the directed arrangement of molecules to alter the properties of different types of functional molecules by co-crystallization processes. In recent times, the impact of co-crystals has been found to be enormous in the pharmaceutical industry, as the properties of several APIs could be tailored in the presence of appropriate co-formers. Besides, study of metal-organic assemblies for the generation of materials of contemporary needs such as gas storage devices, catalytic reaction vessels, etc., also have gained much attention under the umbrella of supramolecular chemistry. Salient features of these processes would be elaborated in this Chapter.

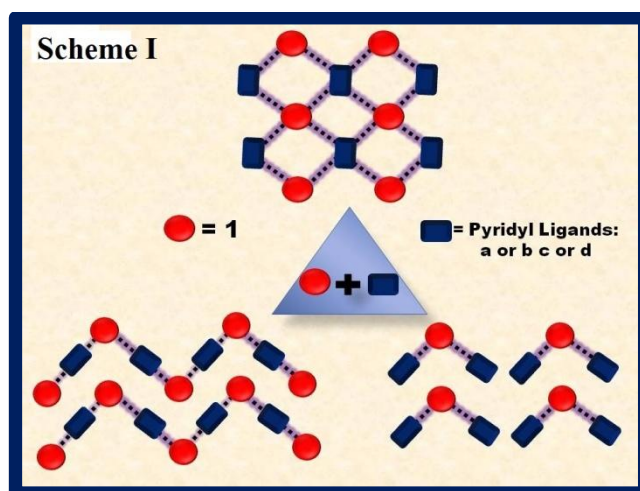
## **Chapter II**

The design and synthesis of molecular materials, with desired properties, by systematic variation of functional moieties on molecular structure, is one of the other attractive themes of supramolecular chemistry. The constituent molecules within a material, thus, are the fundamental building blocks for the creation of network structures with a desired arrangement and dimensionality, through non-covalent interactions such as hydrogen bonds, coordinate bonds, halogen bonds, etc. Several examples of extended hydrogen bonding assemblies have been reported, illustrating the importance and influence of such interactions to facilitate the organization of molecules into supramolecular assemblies. In supramolecular synthesis, in general, molecular topology and the strength of intermolecular

interactions like hydrogen bonds play a significant role in the formation of extended structures in one, two and three dimensions. Thus, various aromatic and aliphatic carboxylic acids mediated supramolecular assemblies, (particularly, utilizing O-H $\cdots$ N / C-H $\cdots$ O pair wise hydrogen bonding patterns, evolved due to the interaction of –COOH moieties with aza-donor compounds) are well explored as reported in the literature. In this regard, only a few assemblies of 1,3-adamantanedicarboxylic acid (**adc**) with different pyridyl ligands like 4,4'-bipyridine and its higher analogues like 1,2-di-4-pyridylethylene / ethane are known in the recent literature. Thus to explore a landscape of co-crystals of 1,3-adamantanedicarboxylic acid, we have prepared molecular adducts of it with some pyridine based compounds having variable molecular conformations, like 1,3-di(pyridin-4-yl)propane (**a**), *E*-1,2-di(pyridine-4yl)diazene, *E*-2,2'-(ethene-1,2-diyl)dipyridine 1-oxide and 1,7-phenanthroline, as listed in Chart I, which are good hydrogen bond acceptors as well as show ability to form secondary interactions of appreciable characteristics.



These assemblies have been characterized by single crystal X-ray diffraction method. The analyses of the 3D structures reveal that, in all the co-crystals the basic interaction between the constituent molecules is established through a pair-wise hydrogen bond ( $\text{O-H}\cdots\text{N}$  or  $\text{O-H}\cdots\text{O}$  /  $\text{C-H}\cdots\text{O}$ ), which is further extended in two and three-dimensions by  $\text{C-H}\cdots\text{O}$  hydrogen bonds,  $\text{C-H}\cdots\pi$  and  $\pi\cdots\pi$  interactions. The schematic representation of the assemblies has been shown in Scheme I. The packing features of all these assemblies have been elaborated in this Chapter.



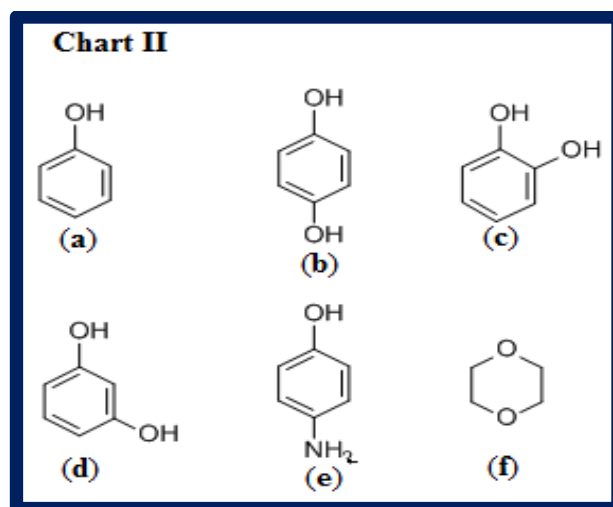
### Chapter III

In general, host framework in host-guest complexes can be divided into two different structural categories — rigid hosts (such as cyclodextrins, crownethers, cryptands and spherands, etc.) which are due to the covalent linkages and flexible hosts (such as ensembles of trimesic acid, trithiocyanuric acid, etc.) which are essentially formed due to the noncovalent interactions like hydrogen bonds. Although, the later type of hosts, often, are guest specific, in recent times the co-



crystallization of components of host and guest has unrestricted the guest exchange in organic inclusion compounds. Such approach leads to the preparation of various kinds of functional materials with tailor made properties for the evaluation in the area of catalysis, gas storage devices etc. Thus, identification of suitable host(s) for the guest inclusion is the area of interest. In such a process, we have identified a host which is formed due to the aggregation of 1,3-adamantanedicarboxylic acid (**adc**) and 4,7-phenanthroline (**phen**) with void space of approximately  $7 \times 8 \text{ \AA}^2$ .

We report, herein, preparation of co-crystals of **adc** and **phen** in the presence of various organic compounds as listed in Chart II and evaluation of structural features in terms of host-guest complexation.



In all the complexes, the molecules of **adc** and **phen** form a four membered host network through a pair-wise hydrogen bonding patterns ( $\text{O-H}\cdots\text{O}$  and  $\text{C-H}\cdots\text{O}$ ). The resultant ensemble is shown in Figure 1.

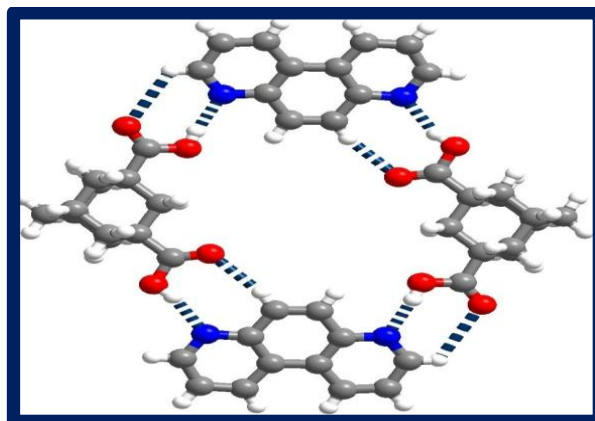


**Figure 1.** Representation of four membered cyclic host of **adc** and **phen** obtained through a pair-wise hydrogen bonding patterns.

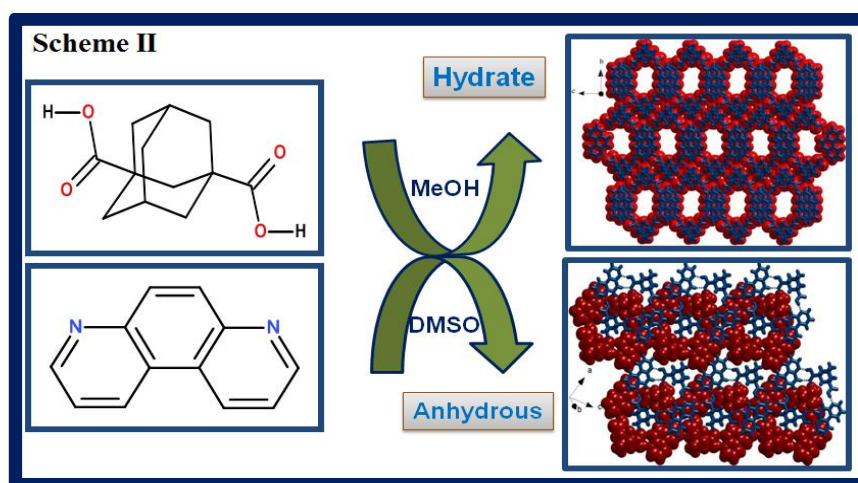
Among all the complexes, except with 1,4-dioxane the ensembles are stacked to yield channels, in which guest molecules are inserted. But in the dioxane structure the host entities are packed in the crystal lattice in such a manner that the cavities are effectively being shadowed by the host molecules from the adjacent layers, thus precluding the formation of channels. Salient features of these host guest assemblies are illustrated in detail in this Chapter.

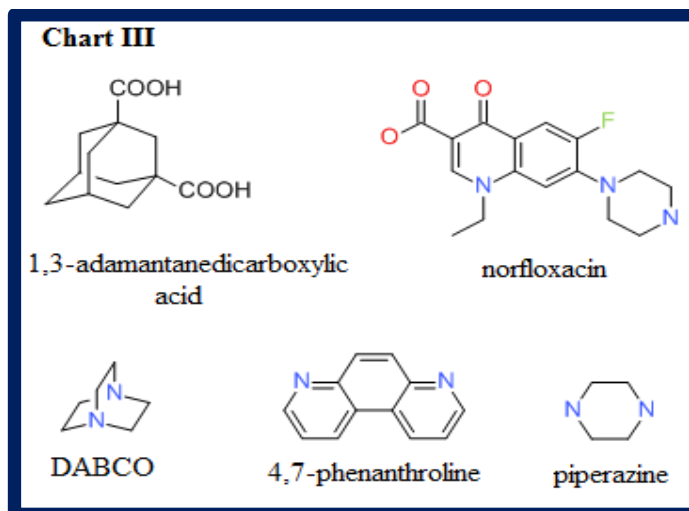
#### **Chapter IV**

In most of the solvated structures, water is found to be incorporated more frequently than any other solvents, even though water is not being used in the crystallization process. In general, such hydration influences the internal energy, enthalpy, entropy, solubility, dissolution rate, stability of the compounds, etc. For example, it is known that the anhydrous forms of many pharmaceutically important compounds are found to be more soluble in water than the corresponding hydrate forms. Thus, preparation of specifically anhydrous forms corresponding to the

hydrated forms may provide an opportunity to expand the applications of even other classes of the organic compounds. For this purpose, dehydration of a hydrate, often being carried out by thermal treatment, may consider to be a viable method to obtain an anhydrous form. However, the structural characterization of such anhydrous forms is often a complex process due to the formation of microcrystalline or amorphous materials, which could not be characterized by single crystal X-ray diffraction method. Thus, it necessitates the development of methodologies and techniques to prepare anhydrous forms in the form of single crystals for elucidation of structural features by single crystal X-ray diffraction method.

In this regard, we demonstrate by a deliberate choice of a specific reaction medium, as exemplified in Scheme II, preparation of anhydrous assemblies for the corresponding hydrated assemblies of 1,3-adamantanedicarboxylic acid (**adc**) with complementary ligands, as listed in Chart III. The structural features of both the hydrated and anhydrous assemblies are illustrated in detail in this Chapter.





## References

- (1) Desiraju, G. R. *Crystal Engineering: The Design of Organic Solids*; Elsevier: Amsterdam, 1989. (2) Lehn, J. M. *Supramolecular Chemistry: Concepts and Perspectives*; VCH: Weinheim, 1995. (3) Atwood J. L.; Davies J. E. D.; MacNicol D. D.; Vögtle F. *Comprehensive Supramolecular Chemistry*, Pergamon, Oxford, 1996. (4) Steiner, T. *Angew. Chem., Int. Ed.* **2002**, *41*, 48. (5) Prins, L. J.; Reinhoudt, D. N.; Timmerman, P. *Angew. Chem., Int. Ed.* **2001**, *40*, 2382. (6) Desiraju, G. R. *Angew. Chem., Int. Ed.* **1995**, *34*, 2311. (7) Metrangolo, P.; Meyer, F.; Pilati, T.; Resnati, G.; Terraneo, G. *Angew. Chem., Int. Ed.* **2008**, *47*, 6114. (8) Jeffrey, G. A.; Saenger, W. *Hydrogen Bonding in Biological Structures*, Springer, Berlin, 1991. (9) Jeffrey, G. A. *An Introduction to Hydrogen Bonding*, Oxford University Press, New York, 1997. (10) MacDonald, J. C.; Whitesides, G. M. *Chem. Rev.* **1994**, *94*, 2383. (11) Brunet, P.; Simard, M.; Wuest, J. D. *J. Am. Chem. Soc.* **1997**, *119*, 2737. (12) Khankari R. K.; Grant D. J. W. *Thermochim. Acta* **1995**,

- 248, 61. (13) Martí-Rujas J.; Harris K. D. M. *Cryst. Growth Des.* **2010**, *10*, 3176. (14) SeethaLekshmi L.; Pedireddi V. R. *Cryst. Growth Des.* **2007**, *7*, 944. (15) Hulliger, J.; Konig, O.; Hoss, R. *Adv. Mater.* **1995**, *7*, 719. (16) Sozzani, P.; Racco, S.; Omotti, A.; Erretti, L.; Simonutti, R. *Angew. Chem. Int. Ed.* **2005**, *44*, 1816. (17) Sada, K.; Inoue, K.; Tanaka, T.; Epergyes, A.; Tanaka, A.; Tohnai, N.; Matsumoto, A.; Miyata, M. *Angew. Chem. Int. Ed.* **2005**, *44*, 7059. (18) Msayib, K.; Book, D.; Budd, P.; Chaukura, N.; Harris, K. D. M.; Helliwell, M.; Tedds, S.; Walton, A.; Warren, J. E.; Xu, M.; McKeown, N. B. *Angew. Chem. Int. Ed.* **2009**, *48*, 3273. (19) Harris, K. D. M. *Chem. Sec. Rev.* **1997**, *26*, 279. (20) Pedireddi, V. R.; Chatterjee, S.; Ranganathan, A.; Rao, C. N. R. *J. Am. Chem. Soc.* **1997**, *119*, 10867. (21) Ranganathan, A.; Pedireddi, V. R.; Rao, C. N. R. *J. Am. Chem. Soc.* **1999**, *121*, 1752. (22) Pedireddi, V. R. *Cryst. Growth Des.* **2001**, *1*, 383.

# CHAPTER ONE

An Overview of Contemporary Research in Supramolecular Chemistry

## 1.1 Introduction

Solids are composed of entities such as atoms, ions, molecules, etc., which are bound through a variety of forces of different in energy. For example, in inorganic solids, anions and cations are held together by strong electrostatic interactions, while in molecular solids, in particularly, organic in nature, molecules are held together primarily by weak intermolecular forces, which are often being referred as noncovalent interactions such as hydrogen bonds, halogen bonds, van der Waals interactions, etc.<sup>1</sup> In general, since the energy of the noncovalent interactions is considerably low, in the range of 0.1-40 kcal/mole, aggregation of molecules is so facile, hence plays a significant role for the accounted properties of the materials.<sup>2</sup> In fact, noncovalent interactions are primarily responsible for various biological processes, such as enzymatic reactions, protein folding, selective transport of ions and small molecules across membranes, etc.<sup>3</sup> Indeed, such interactions also determine the specific patterns of packing of molecules in various bulk materials, by which materials properties like solubility thermal stability, etc., could be tuned.<sup>4</sup>

The importance of noncovalent interactions in materials or solids is well recognized with the Noble prize awarded discovery of crown ethers<sup>5</sup>, cryptands<sup>6</sup> and spherands<sup>7</sup> by Charles Pederson, Jean-Marie Lehn and Donald J. Cram, which were demonstrated as potential hosts for selective binding of ions through noncovalent interactions and lead to the evaluation of a major research area in science spectrum “*Supramolecular Chemistry*”.

## 1.2 Supramolecular Chemistry

Supramolecular chemistry is one of the facets of chemical sciences involving the study of physical and chemical properties of supermolecules of different types, like macromolecules with well defined covalent frameworks, as well as macrostructures due to the self-assembly of small molecules by intermolecular interactions.<sup>8</sup> However, in the process of evaluation, the studies are more directed towards interaction between different components, with one of them being a host while the other functions as guest. It is well established that, the formation of supermolecule is highly selective and self driving process, like that of a complex formation between enzyme and substrate.<sup>6</sup> Such selective binding process between substrate and receptor, in general, depends on the availability of bonding sites, molecular dimension, etc., which is defined as molecular recognition as conceptualized by Emil Fischer in 1894 through “lock and key” model for the explanation of geometrical features prerequisite for enzyme catalysis.<sup>9</sup> According to this model, a specific substrate fits into only one receptor (enzyme), like a key fits in one lock, as shown in Figure 1.1.

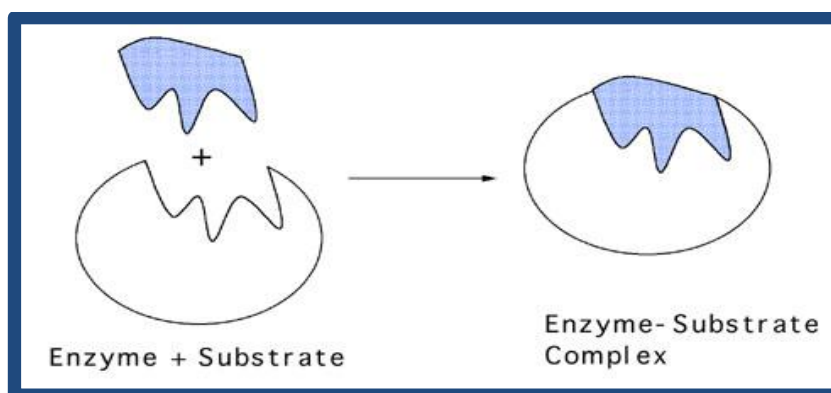


**Figure 1.1.** Schematic representation of lock and key model of Emil Fischer.



In general, such recognition is often a function or task specific; hence established knowledge of various process, Jean-Marie Lehn defined molecular recognition as “a process involving both binding and selection of substrate by a given receptor molecule, as well as possibly a specific function”.<sup>8b</sup>

Thus, molecular complementarity<sup>10</sup> and precise recognition<sup>11</sup> between the entities, is a kind of prerequisite to undergo recognition process, as one may realized in the structure of a well known biologically significant polymer, DNA (deoxyribonucleic acid), which exist in a double helical form, with entwining of complementary stands by means of noncovalent forces (hydrogen bonds), as shown in Figure 1.2, is the best example to demonstrate function oriented recognition process.<sup>3e</sup> In fact, structure of DNA further illustrates the effectiveness of multiple binding sites for the unusual co-operative effect of noncovalent interactions perhaps due to the stability to the supermolecules/supramolecular assembly, as DNA is known to be associated with numerous hydrogen bonds with a double helix structure.

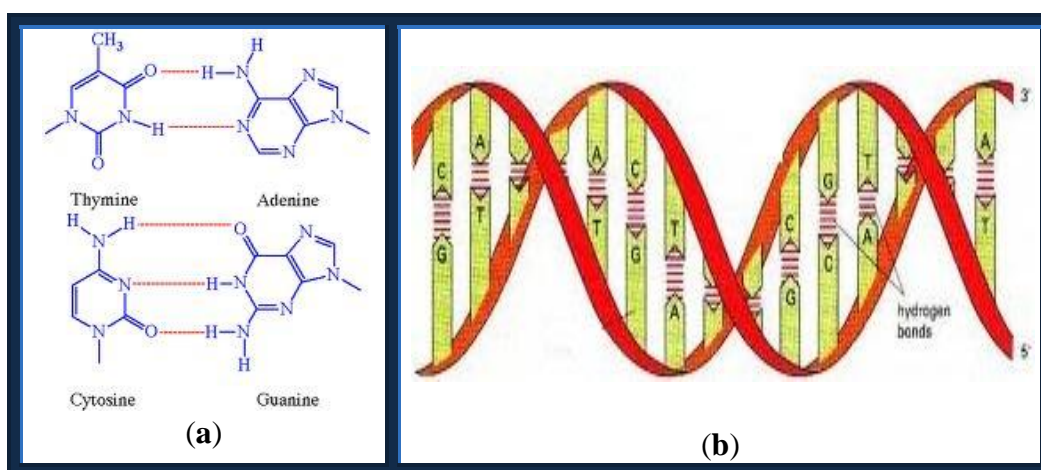


**Figure 1.2.** a) Recognition between DNA base-pairs, b) DNA double helix.

Such co-operativity of noncovalent interactions mediated non-biological molecules are also well known in the literature. For example, supramolecular assembly formed between cyanuric acid and melamine with a total of eighteen hydrogen bonds is one of the best known examples in the class of organic assemblies for its unusual structural integrity and thermal stability known still date.<sup>2b, 12</sup> The elegant assembly in the form of ‘rosette’ is shown in Figure 1.3.

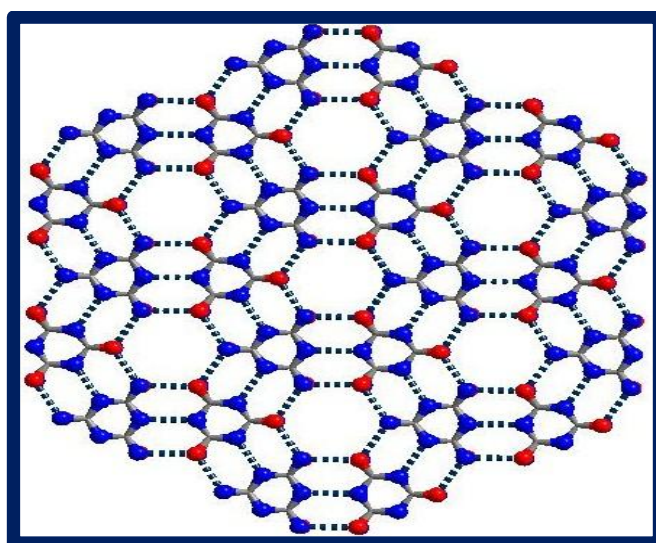
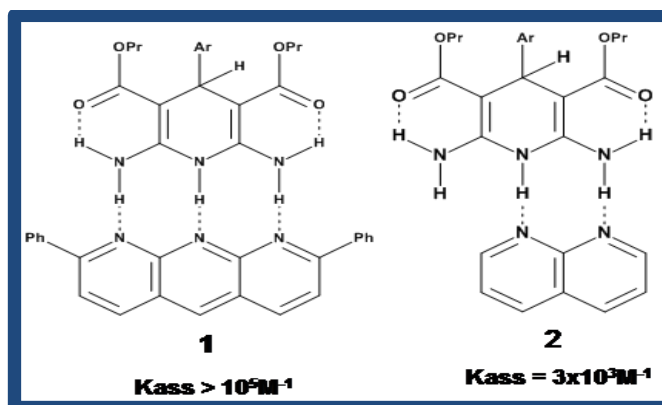


**Figure 1.3.** Molecular arrangement in the complex of cyanuric acid and melamine.

Further, Zimmerman, Hans-Jorg Schneider, J. D. Wuest, Meijer and P. Timmerman, etc., demonstrated by the quantitative measurement of stability constants for different complexes, essentially formed through variable number of hydrogen bonds. The stability of an assembly increases with the increased number of hydrogen bond between the substrates.<sup>13</sup> For example, the complex **1** ( $K_a, 10^5 M^{-1}$ ) is found to be more stable than complex **2** ( $K_a, 3 \times 10^3 M^{-1}$ ), as the components in the complexes are associated through three and two hydrogen bonds, respectively, Scheme 1.1.<sup>13a</sup>

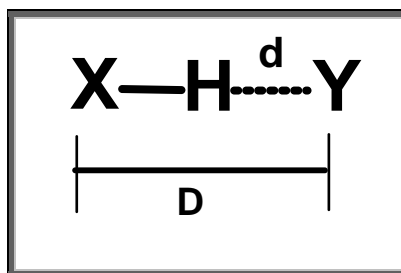


**Scheme 1.1.** Recognition pattern between the molecules through double and triple hydrogen bonds.

Among the noncovalent interactions, the hydrogen bond is the premier interaction that appears in a majority of known supramolecular assemblies, due to thorough understanding of the features of such bonds in terms of energy, robustness, topology, etc.

### 1.3 Hydrogen Bond

The term Hydrogen bond is proposed by Bernal<sup>14</sup> and Huggins<sup>15</sup> to define interaction between a polar X–H group and an electron pair donor, Y where atoms X and Y are connected through the H atom as represented in Scheme 1.2. However, it has been further extended substantially to a variety of functionalities with X and Y like F, O, N, C, Cl, I, S, etc.<sup>1i, 2d, 16</sup> Thus, in general, in a hydrogen bond, X–H···Y, X–H is often being referred as hydrogen bond donor and Y as hydrogen bond acceptor.



**Scheme 1.2.** A typical representation of the hydrogen bond.

In fact, the strength of the hydrogen bond is generally related to electronegativity of donor and acceptor atoms. Thus, hydrogen bonds have been classified into weak, moderate and strong by Jeffrey.<sup>17</sup> For example, hydrogen bonds of the types  $O-H\cdots O$ ,  $N-H\cdots O$ ,  $N-H\cdots N$  are generally considered to be stronger as the atoms to which the hydrogen is attached are of high electronegativity, over  $C-H\cdots O$ ,  $C-H\cdots N$ , etc., since electronegativity of C is lower than oxygen and nitrogen atoms. The relative energy scale and other characteristic features of different hydrogen bonds are represented in Table 1.1.

**Table 1.1.** Comparison of strong, moderate and weak hydrogen bonds.

	Strong	Moderate	weak
Bond energy (kcal/mol)	15 to 40	4 to 15	< 4
$H\cdots A$ bond Length (Å)	1.2 to 1.5	1.5 to 2.2	> 2.2
$D\cdots A$ bond Length (Å)	2.2 to 2.5	2.5 to 3.2	> 3.2
$\angle DHA$ bond angles (deg)	170 to 180	>130	> 90
D-H versus $H\cdots A$	$D-H \approx H\cdots A$	$D-H < H\cdots A$	$D-H \ll H\cdots A$
Lengthening of D-H (Å)	0.08 to 0.25	0.02 to 0.08	< 0.02

In general, distances and angles obtained from the complementary X-ray/neutron diffraction methods play a significant role for the evaluation of the hydrogen bonds. However, some other techniques also play a significant role in the characterization of hydrogen bonds.

### **1.3.1 Infrared Spectroscopy**

It is apparent from Table 1.1 that, formation of a hydrogen bond between X-H and Y affects bond length of X-H bond, which in turn affects its vibrational frequency. In a typical hydrogen bond, X-H $\cdots$ Y, the bond length of X-H is increased as compared to free X-H bond, as hydrogen atom is attracted by Y, reflecting a red-shift in the absorption band with either broadening or intensification. The difference between the stretching frequency value of the X-H of free and hydrogen bonded increases systematically with decreasing H $\cdots$ Y distance. Thus, IR spectroscopy is one of the cheap techniques, especially for the estimation of energy of the strong hydrogen bonds.

### **1.3.2 $^1\text{H}$ NMR Spectroscopy**

The electron density of the protons involved in hydrogen bonding decreases, and which influences the NMR (Nuclear Magnetic Resonance) signals by shifting to higher chemical shift. Thus, magnitude of the chemical shift is also indicative of the strength of the hydrogen bond. However, hydrogen bonds are mostly characterized by monitoring  $^1\text{H}$  NMR shifts as a function of concentration.

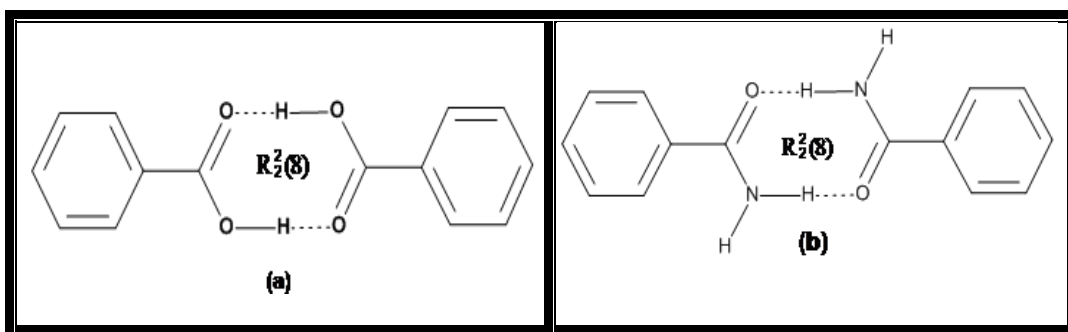
Because of directionality, strength and facile techniques for the characterization, the hydrogen bond has become a powerful tool in supramolecular synthesis.<sup>1c, 18</sup> Thus, several studies of systematic analysis of hydrogen bonding patterns have been carried out for the development of methodologies towards target oriented synthesis of supramolecular assemblies. The interpretation of hydrogen bonding analysis is originated with the formulation of a graph set analysis, proposed by Etter and further refined by Bernstein.<sup>20</sup> The purpose of graph set assignment is to define the patterns of hydrogen-bonded arrays through numerical coding, followed by some recognition principle, often, referred as Etter rules as describe below.

**Etter Rules:**

- 1) *All good proton donors and acceptors are used in hydrogen bonding.*
- 2) *Six-membered-ring intramolecular hydrogen bonds form in preference to intermolecular hydrogen bonds.*
- 3) *The best proton donors and acceptors remaining after intramolecular hydrogen-bond formation form intermolecular hydrogen bonds to one another.*

The process of assigning a graph set begins with identification of the number of different types of hydrogen bonds, as defined by the nature of the donors and acceptors in a hydrogen bond, that are present in the structure of interest. A hydrogen bond that connects set of molecules is called a motif and is characterized by one of four designators that indicating whether the motif is infinite or finite and

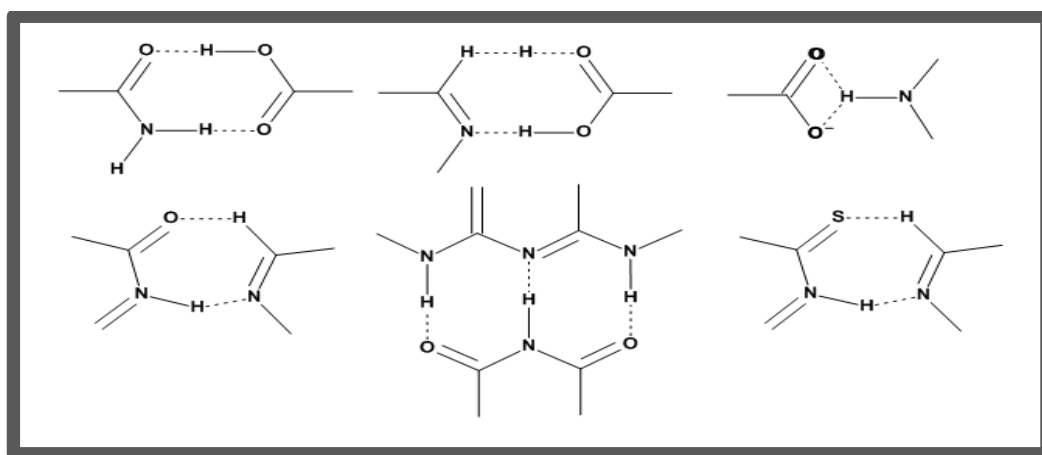
cyclic or not. For motifs generated from intermolecular hydrogen bonds, these designators are **C** (chain), **R** (ring), and **D** (dimer or other finite set), while **S** denotes an intramolecular hydrogen bond. The number of donors (**d**) and acceptors (**a**) present in each motif are assigned as subscripts and superscripts, respectively, and the size or degree of the motif (corresponding to the number of atoms in the repeat unit) is indicated in parentheses. Thus, a hydrogen bond pattern formed by either  $\text{-COOH}$  or  $\text{-CONH}_2$ , as shown in Scheme 1.3, will have the graph set notation as  $R_2^2(8)$ , which indicates that network is a ring with eight atoms and comprises of two acceptors and two donors of each.



**Scheme 1.3.**  $R_2^2(8)$  Hydrogen bonding patterns in a) carboxylic acid dimer and b) amide dimer.

Although, the patterns exemplified in the Scheme 1.3 are of homomeric type, in fact heteromeric patterns could also be synthesized, by replacing one of the moieties with an appropriate complimentary ligand. Thus, an acid-amide heteromeric pattern, as shown in Scheme 1.4 could be realized. Such an analysis leads to the exploration of solids by crystallization of multiple components, which are referred as co-crystals. In continuum, some of the other heteromeric hydrogen

bonding patterns are shown in Scheme 1.4, which have been well utilized for the preparation of various supramolecular assemblies of exotic and functional in nature.<sup>16b, 21</sup>



**Scheme 1.4.** Hydrogen bonding patterns.

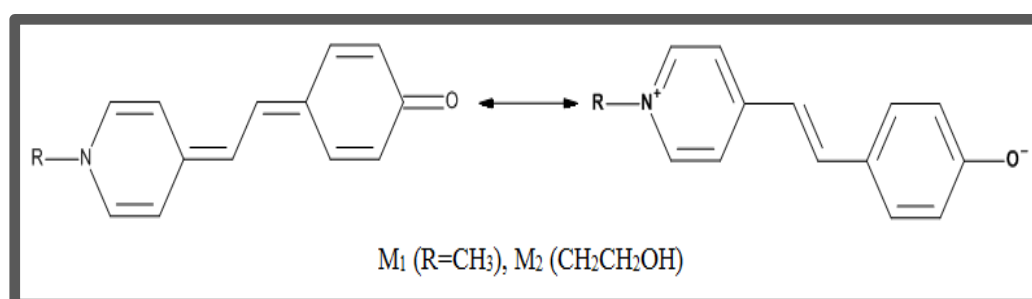
## 1.4 Co-crystals

A study of co-crystals may be considered to be originated with the report of a complex between benzoquinone and hydroquinone as reported by Wohler in 1844 during the studies on quinine.<sup>22</sup> He found that by mixing the solutions of benzoquinone and hydroquinone, a crystalline substance was formed that he called “green hydroquinone”. Based on the unit cell information obtained, it is confirmed that the complex is made up of discrete benzoquinone and hydroquinone moieties, while chemists were unsure about the types of intermolecular chemical bonds holding quinhydrone together, not knowing if they were covalent, ionic, or dipole in nature.<sup>23</sup> In 1958 the full crystal structure of quinhydrone was published in which benzoquinone and hydroquinone molecules were found to alternate in zigzag



chains held together by O–H $\cdots$ O hydrogen bonds.<sup>24</sup> The planar molecules pack parallel to one another, with an intermolecular distance considerably shorter than those found in many other crystals of aromatic compounds. Therefore, it was concluded that, such chains are stacked through  $\pi\cdots\pi$  interactions. In recent times, the co-crystals are defined as a multiple components crystal in which all components are solid under ambient conditions when in their pure form.<sup>25</sup>

In the last few decades, a large numbers of co-crystals have been reported in the literature, which are evaluated for various types of specific applications.<sup>26</sup> Among such systems, merocyanine dye (**M**<sub>1</sub>), an outstanding nonlinear optical (NLO) material, exhibits a very high molecular hyperpolarizability as well as good thermal and photo stabilities. The merocyanine dye exists in two resonance forms, quinoid and zwitterionic (Scheme 1.5). The electronic structure of **M**<sub>1</sub> depends on the relative contribution of these two resonance forms: the quinoid form being favoured in nonpolar media and the zwitterionic form being favoured in polar media. However, compound **M**<sub>1</sub> packs centrosymmetrically in its crystal, and in addition forms poor quality single crystals that are unsuitable for NLO applications.



**Scheme 1.5.**

Feng Pan, Christian Bosshard and co-workers prepared co-crystals of  $\mathbf{M}_1$  with either 2-amino-5-nitrophenol or 2-amino-4-nitrophenol from ethanol solution. The packing in each co-crystal is different, but the presence of the nitrophenols altered the structures in a positive NLO point of view, relative to the structure of  $\mathbf{M}_1$  alone. A study of those structures led to the further development of co-crystals, containing compounds  $\mathbf{M}_2$  (Scheme 1.5) and 2,4-dihydroxybenzaldehyde, which exhibited strong second-harmonic signal generation, suggesting noncentrosymmetric packing of  $\mathbf{M}_2$ .<sup>27</sup>

Similarly Huang et al. reported a number of phenol-pyridine co-crystals and investigated their NLO properties. Many of those are salts, apparently depending on the  $\Delta pK_a$  between the constituents. However, the salts tend to hydrogen bond to a third molecule, forming either 2:1 co-crystals or hydrates. For example, one of the co-crystals is composed of a 2-methoxy-4-nitrophenoxy anion and a 4-(dimethylamino) pyridinium cation along with a unionized 2-methoxy-4-nitrophenol molecule. This co-crystal, and three others like it, are packed noncentrosymmetrically and, thus, exhibit second harmonic generation activity. It was postulated that ionic co-crystals of the type discussed above might have a greater chance of forming noncentrosymmetric structures than do achiral organic molecules in general.<sup>28</sup>

Hulliger and co-workers found that, racemic perhydrotriphenylene (*phtp*) acts like a host, and forms polar host-guest compounds by accommodating more than 90% of the NLO molecules investigated, as guests, in co-crystallization

experiments. For instance, co-crystallization of racemic perhydrotriphenylene (*phtp*) with 1-(4-nitrophenyl)piperazine as a guest, forms a polar compound in which homochiral stacks of *phtp*, the host molecules, surround polar chains of hydrogen bonded 1-(4-nitrophenyl)piperazine molecules in a channel type, hexagonal architecture, as shown in Figure 1.3. The co-crystals of complex show second harmonic generation (SHG) for incident light of wavelength 1064nm.<sup>29</sup>

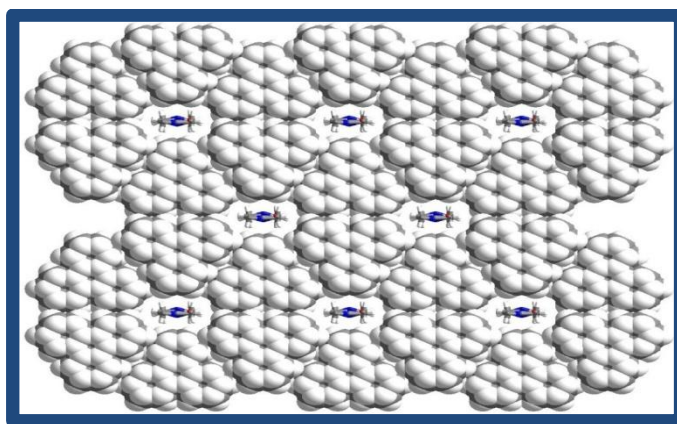
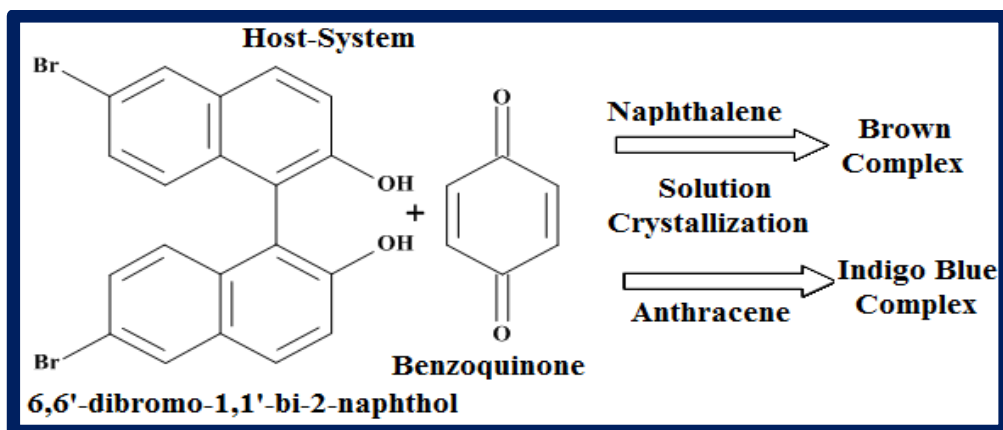


**Figure 1.3.** Arrangement of molecules of host (*phtp*) and guest in the co-crystals of perhydrotriphenylene with 1-(4-nitrophenyl)piperazine.

Co-crystals are not only used in optimization of optical properties, but also used as colorimetric indicators to identify, visually, some aromatic compounds. Imai and co-workers have revealed the ability of the host network, formed by derivatives of 1,1'-*bis*-2-naphthol and *p*-benzoquinone, towards selective visual recognition of aromatic guest molecules via charge transfer  $\pi \cdots \pi$  interactions. The charge transfer complex composed of 6,6'-dibromo-1,1'-*bi*-2-naphthol as an electron donor and *p*-benzoquinone as an electron acceptor serve as host for the inclusion of guest molecules such as naphthalene and anthracene. The host-guest

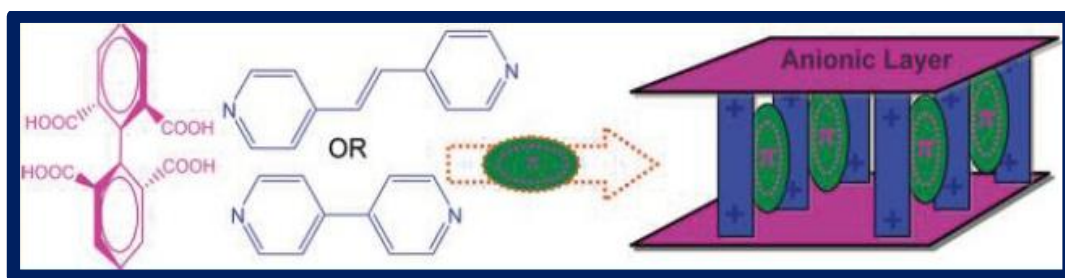
complex obtained from components of host and naphthalene, by conventional crystallization method, produced crystals which were brown in colour. However, crystals of anthracene containing host-guest complex were indigo blue. The study has been represented in Scheme 1.6.<sup>30</sup>



**Scheme 1.6.**

Recently, Biradha and co-workers prepared two components host networks from 2,2',6,6'-tetracarboxybiphenyl / 4,4'-bipyridylethylene and 2,2',6,6'-tetracarboxybiphenyl / 4,4'-bipyridine which were shown to recognise various aromatic guest molecules.<sup>31</sup> Further, they have shown that, these hosts were able to form coloured complexes with various aromatic compounds, even though all the components are colourless. It is proven that, the colouration is due to the formation of charge transfer complex between cations of aza-donors and aromatic guest molecules, as shown in Scheme 1.7. Further, the host formed by 2,2',6,6'-tetracarboxybiphenyl and bipyridylethylene was found to include only solid aromatic guest molecules, while the 2,2',6,6'-tetracarboxybiphenyl and bipyridine host system was found to include both solid and liquid aromatic guests, in

particular those containing phenolic moieties. The different colors observed in these complexes indicate that these hosts may serve as colorimetric indicators for various aromatic moieties in the solid state as shown by Imai and co-workers.

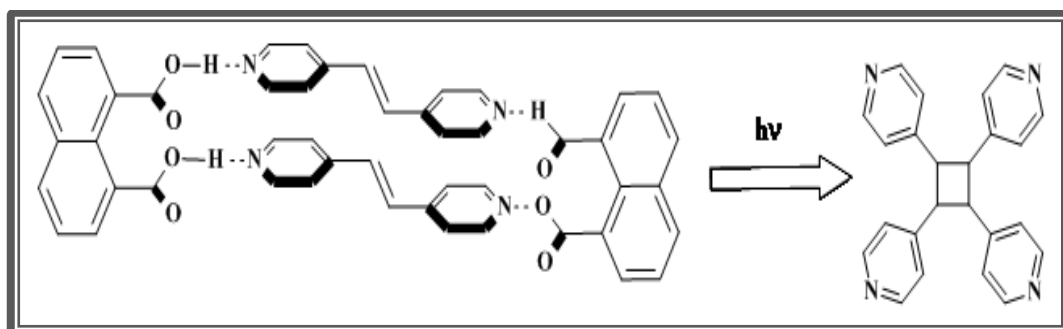


**Scheme 1.7.**

Further, co-crystallization approaches also have been utilised to control the isomerisation of molecules in solid state. For example, Pedireddi and co-workers have synthesised the co-crystals of maleic acid with 4,4'-bipyridine (**bpy**) by crystallizing from various solvents such as acetone, chloroform, ethylacetate and methanol, dimethylformamide and dimethylsulfoxide.<sup>32</sup> Co-crystallization of maleic acid and **bpy** from acetone, chloroform, ethylacetate and methanol gave expected co-crystals, where the molecules of constituents interact through O–H···N hydrogen bonds. However, co-crystallization of the components from solution of dimethylformamide (DMF) or dimethylsulfoxide (DMSO) gave an unexpected result wherein maleic acid isomerises to fumaric acid. Such isomerisation did not encounter when the acid is refluxed in either DMF or DMSO. Thus, it is concluded that, the highly polar DMF/DMSO solvents is primarily involve in breaking of the intramolecular hydrogen bond in maleic acid. The **bpy** molecule being a good nucleophile adds on to the hydrogen-bond free maleic acid forming a zwitterionic

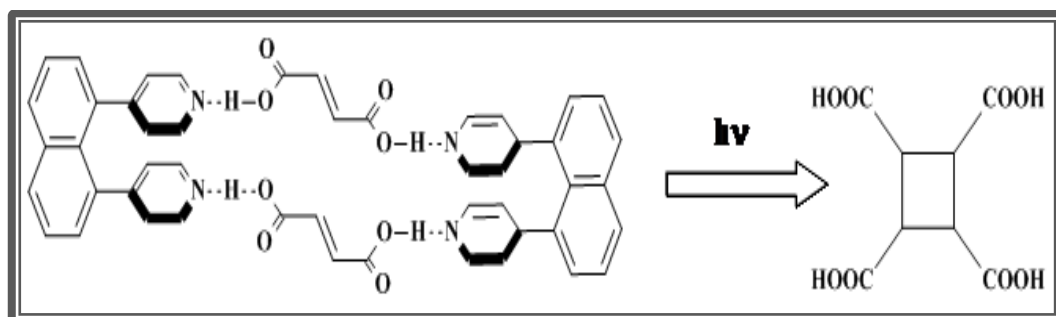
species which then isomerizes to the *trans* form, followed by the elimination of the bipyridine molecule. This is one of the examples which is explained the crucial role of co-former in the isomerisation process.

In recent times, co-crystallization approach has been directed towards even to develop carbon-carbon bond formation by atom economy process, through solid state photochemical reactions. For a [2+2] photochemical cycloaddition reaction to occur in solid state, the adjacent olefinic bonds should conform to the geometry criteria outlined by Schmidt.<sup>33</sup> Following crystal structure studies involving cinnamic acids, Schmidt forwarded that the adjacent olefinic bonds should be parallel to each other and lie at distance less than 4.2 Å. MacGillivray and co-workers demonstrated that, 1,8-naphthalenedicarboxylic acid (**1,8-nap**) can serve as a template, to induce [2+2] photochemical cycloaddition reaction for compounds like *trans*-1,2-*bis*(4-pyridyl)ethylene (**bpe**), which is otherwise photostable because of unfavourable arrangement of molecules for photodimerization.<sup>34</sup> Thus, co-crystallization of **1,8-nap** with **bpe** gave a discrete four-component molecular assembly through O-H $\cdots$ N hydrogen bonds, as shown in Scheme 1.8. Such an arrangement of molecules is able to place olefinic group at photoactive distance, in order to undergo photochemical cycloaddition reaction in solid state. UV irradiation of powdered crystalline sample of the co-crystal produced *rcctt*-tetrakis(4-pyridyl)cyclobutane in quantitative yield.



**Scheme 1.8.** Alignment of molecules of **bpe** in crystal structure of the co-crystals and product obtained upon UV irradiation.

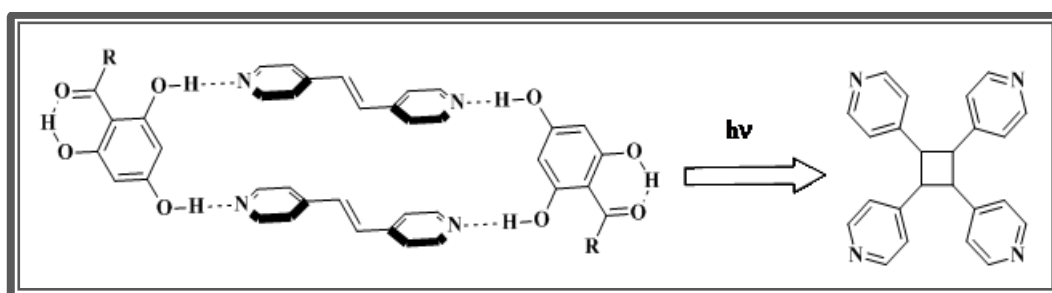
Wolf and co-workers demonstrated another template agent such as 4-[8-(4-pyridyl)-1-naphthyl]pyridine to carry out [2+2] cycloaddition between molecules of fumaric acid. Thus, co-crystallization of the template with the acid gave a discrete four-component molecular assembly through O–H···N hydrogen bonds, as in the above example, and UV irradiation of co-crystals gave cyclobutanetetracarboxylic acid (**CA**), in quantitative yield.<sup>35</sup> The four-component discrete unit and the product obtained are shown in Scheme 1.9.



**Scheme 1.9.** Schematic representation for the preparation of **CA**.

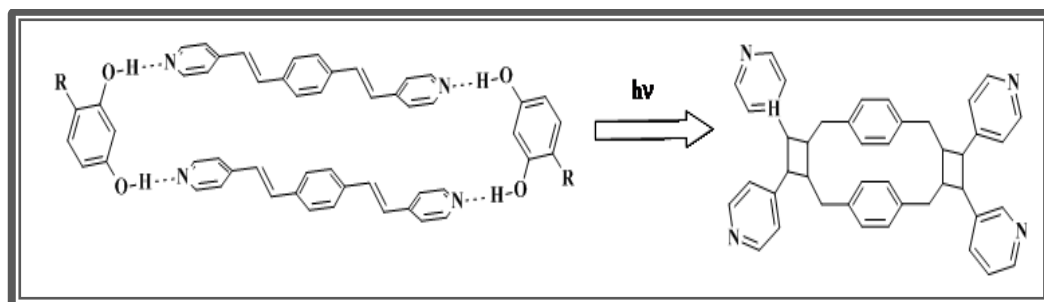
Apart from the synthesis of cyclobutane derivatives, co-crystallization approach, by the use of appropriate template as a co-former, has been utilized for the synthesis of molecules such as cyclophanes and ladderanes which are difficult

to synthesise by conventional organic synthesis methods. Co-crystallization approach for the synthesis of cyclophanes and ladderanes has arise from preliminary studies carried out by MacGillivray and co-workers for the synthesis of *rctt*-tetrakis(4-pyridyl)cyclobutane, by co-crystallization of derivatives resorcinol with *trans*-1,2-bis(4-pyridyl)ethylene,<sup>36</sup> as shown in Scheme 1.10.



**Scheme 1.10.** Shows four-component discrete unit which formed by resorcinol and **bpe** through hydrogen bonds, and product, *rctt*-tetrakis(4-pyridyl)cyclobutane which obtained from UV irradiation of the unit.

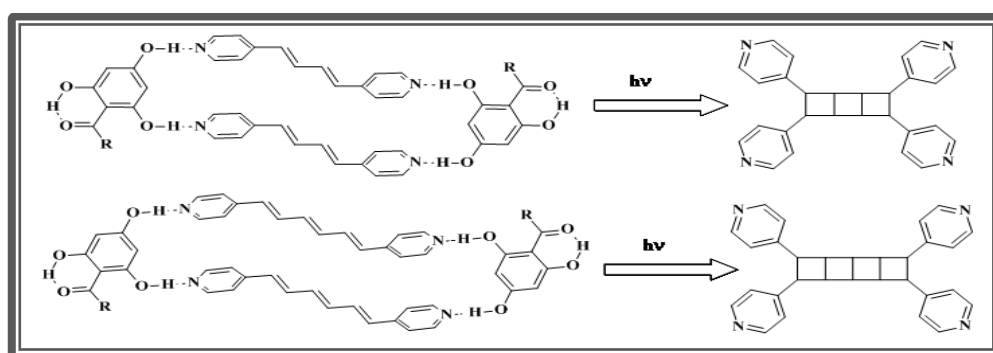
The cyclophane, product shown in Scheme 1.11, has been synthesised from the co-crystals, upon UV irradiation, which are obtained by co-crystallization of 1,4-bis[2-(4-pyridyl)ethenyl]benzene with resorcinol derivative.<sup>37</sup>



**Scheme 1.11.** Represent the synthesis of cyclophane from co-crystals of 1,4-bis[2-(4-pyridyl)ethenyl]benzene with resorcinol derivative.



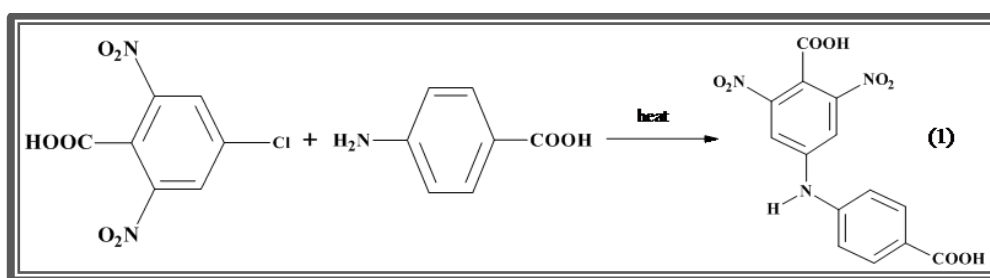
Similarly, co-crystallization of resorcinol derivative with diene/triene molecules gave cocrystals in which the molecules are aggregated in four-component discrete units through O–H···N hydrogen bonds.<sup>38</sup> UV irradiation of the co-crystals results into ladderanes, the products shown in Scheme 1.12. These examples show the elegance of co-crystallization approach toward the synthesis of synthetically challenging molecules.



**Scheme 1.12.** Representation of the synthesis of ladderanes through co-crystallization approach.

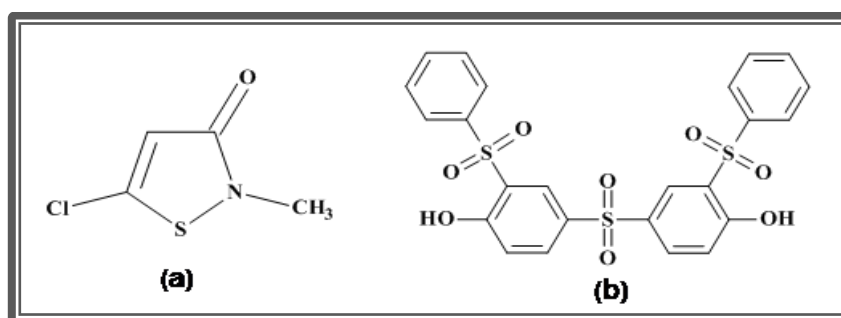
Apart from cycloaddition reactions, co-crystallization has been used to carry out some nucleophilic aromatic substitution reaction. Etter and co-workers reported a nucleophilic aromatic substitution reaction which apparently occurs because of the molecular orientation in the co-crystal. A co-crystal of 4-chloro-3,5-dinitrobenzoic acid with 4-aminobenzoic acid when subjected to heat gave a product, **1**, in quantitative yield, Scheme 1.13.<sup>39</sup> Progress of this reaction is monitored by adding a drop of aqueous silver nitrate solution over the sample of co-crystal (during heating) which developed a precipitate of silver chloride, showing that hydrochloric acid was being evolved. Although a crystal structure of

the co-crystal was not obtained, the suspicion is that a hetero acid dimer results in alternation of the components in the structure and that serendipitous proximity of the amino and C–Cl moieties leads to the solid-state reaction.



**Scheme 1.13.** Representing the components of the co-crystal and the product which is obtained upon heating the co-crystal.

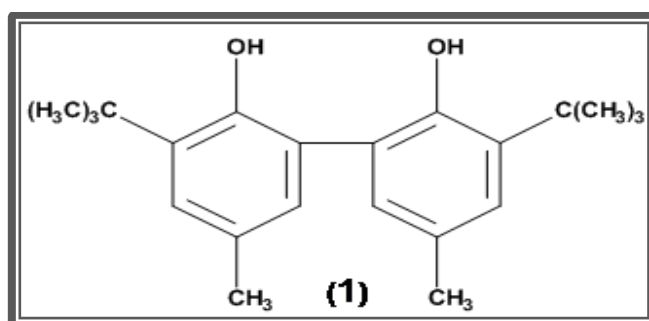
Co-crystallization approach has been applied to impart stability to compounds that are otherwise unstable at ambient condition. For example, Aoki and co-workers carried out co-crystallization of a disinfectant compound, **a**, which decomposed in liquid, forms co-crystals with compound **b**, which are thermally stable.<sup>40</sup> In fact, there are several reports of co-crystals of various disinfectants which were stable and less volatile as compared to disinfectants.



**Scheme 1.14.** a) Molecular structures of (a) 5-chloro-2-methyl-isothiazol-3-one and b) 2-(benzenesulfonyl)-4-[3-(benzenesulfonyl)-4-hydroxy-phenyl]sulfonyl-phenol.

Similarly, Fischer and co-workers reported stable acid chlorides through co-crystallization studies, which otherwise hydrolyze when exposed to the moisture. For example, co-crystals of acetyl chloride with 4-(phenylazo)phenol, which melts at 172 °C, were found to be stable even after exposure to atmosphere for several days.<sup>41</sup>

Purification and separation of valuable compounds also have been carried out through co-crystallization process. Magne and co-workers purified fatty acids of about 90% purity, by co-crystallization.<sup>42</sup> They cocrystallized commercially available fatty acids such as stearic, palmitic, myristic, and lauric with acetamide in organic solvent, and obtained co-crystals were separated by centrifuging mother liquor. From the separated co-crystals, purified fatty acids, free of homologues, could be obtained. Similarly, Bowman and co-workers recovered bis-phenols, as shown in Scheme 1.15, in pure form from crude reaction product mixtures by co-crystallization. Co-crystals of bi-phenols with amines such as hydrazine, alkylamines such as methylamine and ethylamine, aromatic amines such as pyridine and 2,6-lutidine, and hydroxyamines such as ethanolamine and triethanolamine have been prepared and isolated.<sup>43</sup>



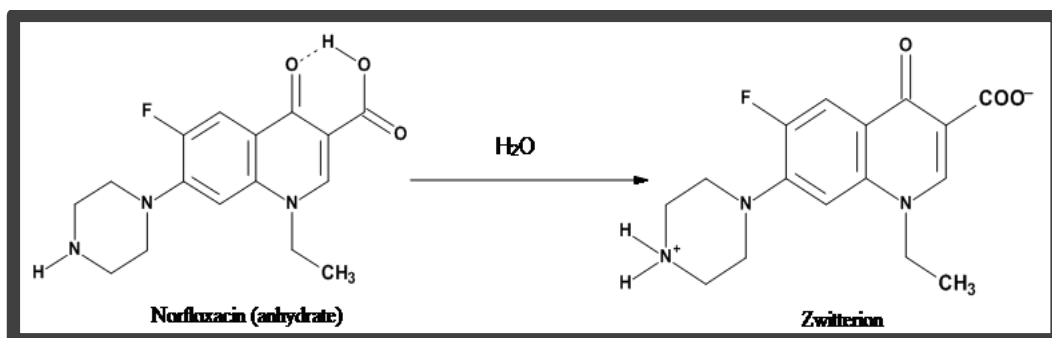
Scheme 1.15.

In very recent times, the efficacy of co-crystallization is extended into pharmaceuticals as the co-crystal of various active pharmaceutical ingredients (APIs) have shown varied properties over the pure forms. Co-crystallization of APIs has emerged as a frontier area of research in supramolecular chemistry. Since it (co-crystallization) is identified as one of the approaches for tailoring the properties of APIs, it is named as “Pharmaceutical Co-crystallization”.

### **1.5 Pharmaceutical Co-crystallization**

Pharmaceutical co-crystal is a crystalline solid which contains an API and co-former, which would be pharmaceutically accepted molecules (food additives) or a drug molecule. Incorporation of such co-former, in stoichiometric ratio, in a crystalline solid of API affects the intermolecular interactions that in turn affect the enthalpy of the API crystal. Thus, pharmaceutical co-crystal will have different physical and technical properties such as solubility, dissolution rate, stability, hygroscopicity, and compressibility without altering pharmacological behaviour of API.<sup>46</sup> Due to such pharmaceutical applications, in recent time, pharmaceutical co-crystallization gained enormous interest in research as well as in pharmaceutical industry, as illustrated in the recent literature.

Norfloxacin is a widely used fluoroquinolone antibacterial compound. In aqueous solution, norfloxacin exists in a zwitterionic form, owing to the acid/base interaction between the basic nitrogen of the piperazine and the carboxylic acid group (Scheme 1.16).

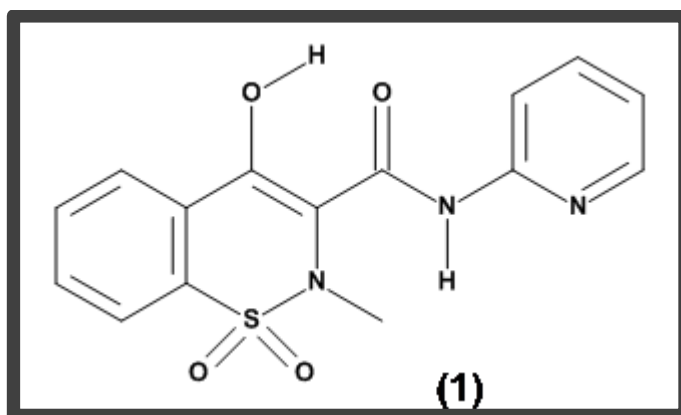


**Scheme 1.16.** Represents zwitterionic form of Norfloxacin in presence of water.

Therefore, the aqueous solubility of norfloxacin at a pH close to 7 (isoelectric point of the molecule) is low (0.28-0.40 mg/mL). This poses significant challenges in the formulation of conventional dosage forms, e.g. tablets, and impedes the design of liquid dosage forms, such as parenteral and ophthalmic solutions. Therefore, improving the aqueous solubility of norfloxacin through the preparation of co-crystals is of interest for the design of dosage forms. In this context, Velaga and co-workers prepared co-crystals of norfloxacin with carboxylic acids such as malonic, succinic, maleic acid, etc.<sup>49</sup> They have demonstrated that the solubility of the co-crystals is enhanced as compared to norfloxacin.

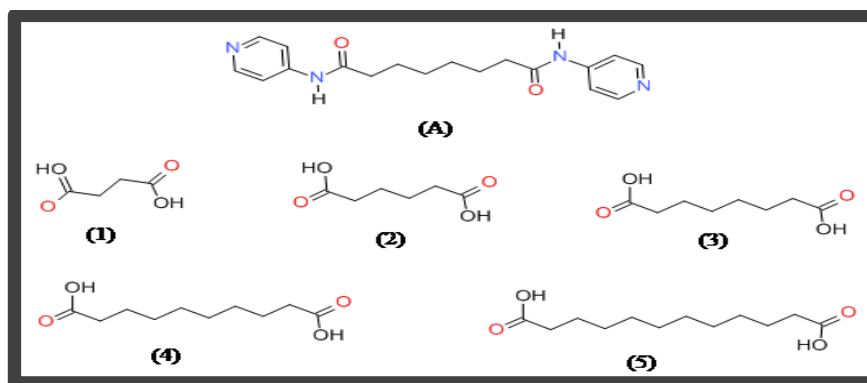
Piroxicam, **1**, (Scheme 1.17) is a nonsteroidal anti-inflammatory drug (NSAID). Piroxicam is an enolic acid used in the symptomatic relief of rheumatoid arthritis and osteoarthritis. Piroxicam has low solubility at physiological pH and is classified as a Class II API (low solubility and high permeability) based on the Biopharmaceutics Classification System (BCS). It takes more than 2 h for piroxicam to reach the maximum concentration after being administered orally. A more rapid onset and increased bioavailability is desirable for analgesics of this

type and formulation and delivery of piroxicam with improved bioavailability has been the goal of a number of research studies. In this context, Childs and co-workers prepared the co-crystals of piroxicam with various carboxylic acids. They have shown the improvement in bioavailability of piroxicam.<sup>50</sup>



**Scheme 1.17.** The molecular structure of piroxicam.

Aakeroy and co-workers prepared the co-crystals of hexamethylenebisacetamide, **A** (a compound that is capable of inhibiting the proliferation of lung cancer cells and is also being used in the treatment of myelodysplastic syndrome and resistant acute myelogenous leukemia) with aliphatic dicarboxylic acids (co-former) having even number of methylene groups, Scheme 1.18.<sup>51</sup> The main objectives of this study were (i) to synthesize a series of co-crystals with the desired structural consistency, (ii) to establish a correlation between melting point, solubility, etc. of the co-crystals and co-formers.

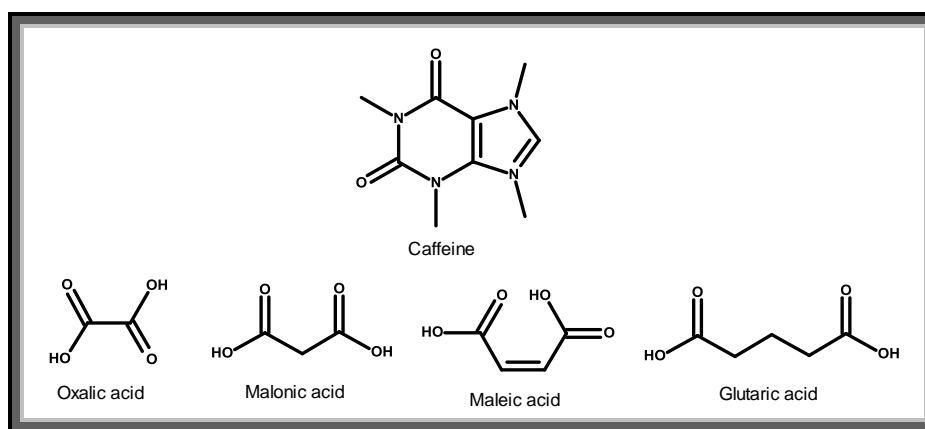


**Scheme 1.18.** Molecular structures of API and dicarboxylic acids (co-former)

It is observed that all the co-crystals are isostructural and having structural consistency. The melting points of these co-crystals are directly related to the melting points of the acids. The highest melting co-crystal contains the acid with the highest melting point, and the lowest melting acid produces the lowest melting co-crystal. This demonstrated that the melting behaviour of the co-crystals of the API can be modulated in a predictable manner over a considerable range 148-188 °C (the melting point of the API itself is 181-182 °C). Further, aqueous solubility determination of the co-crystals show that the solubility of **A** is improved by a factor of 2.5 without altering the molecular structure of the API itself.

Caffeine (1,3,7-trimethyl-2,6-purinedione), a central nervous system stimulant and a smooth muscle relaxant and commonly employed as a formulation additive to analgesic remedies is highly unstable with respect to humidity, with the formation of nonstoichiometric hydrate, etc. However, Jones and co-worker demonstrated that the co-crystal of caffeine with oxalic acid is stable at all relative humidities as compared to the caffeine.<sup>52</sup> They have further demonstrated that the co-crystal is stable even by slurrying in water for 2 days at ambient temperature.

They also prepared some other co-crystals of caffeine with aliphatic acids such as malonic, maleic and glutaric, Scheme 1.19. It is observed that in all the cases, the co-crystals are stable as compared to pure caffeine and among the co-crystals caffeine with oxalic acid found to be more stable than others. In continuum, the properties of some other APIs such as carbamazepine, itraconazole, sildenafil, etc. have been altered through co-crystallization approach.<sup>53</sup>

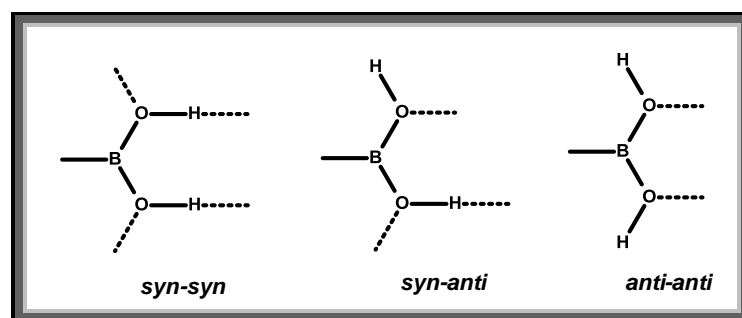


**Scheme 1.19.** Molecular Structures of caffeine and aliphatic dicarboxylic acids.

Further, in recent times, co-crystallization studies are directed towards identifying novel ligands capable of yielding exotic hydrogen bonding patterns. In this regards, new class of compounds such as boronic acids, phosphonic acid, sulphonic acid, etc., have been shown to form exotic co-crystals. In this context, Pedireddi and co-workers prepared co-crystals of phenylboronic acid or methoxyphenylboronic acid with aza compounds.<sup>55</sup> Co-crystallization of phenylboronic acid with 4,4'-bipyridine or *trans*-1,2-bis(4-pyridyl)ethane from methanol gave crystals which are characterized by single crystal X-ray diffraction method. The analysis shows that the molecules interact through O-H $\cdots$ N hydrogen

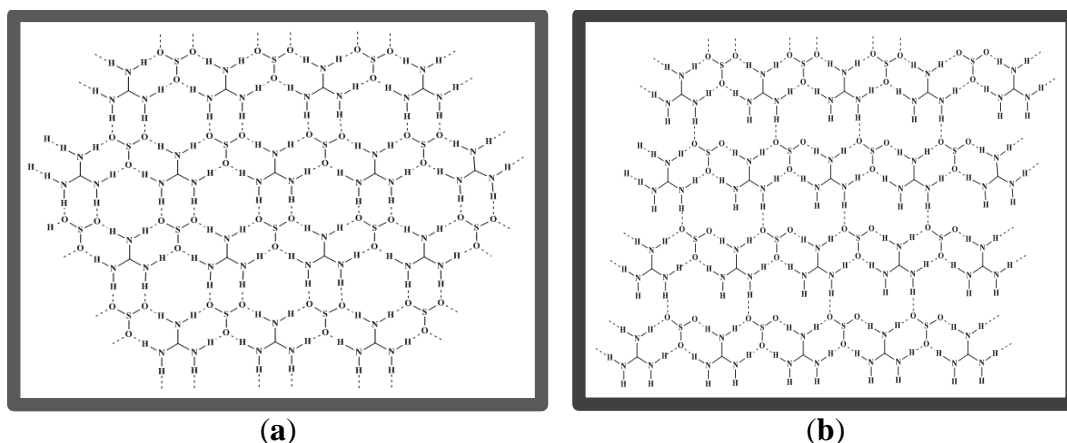


bonds, with boronic acid being in *syn-syn* conformation out of the three possible conformations of it, as shown Scheme 1.20.



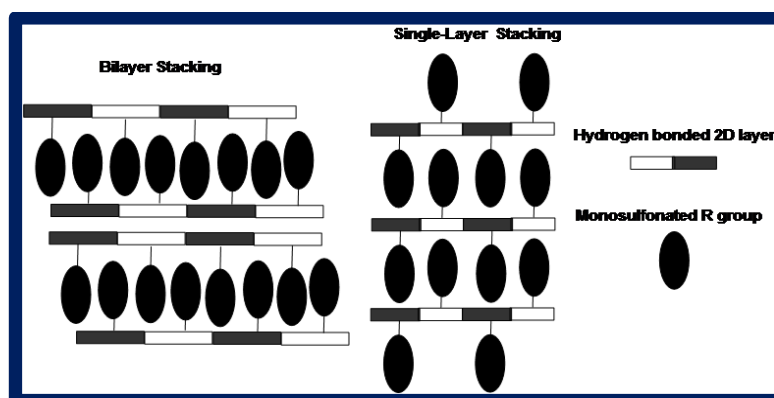
**Scheme 1.20.** Represents the three different conformations of hydroxyl groups in the boronic acids structures.

Ward and co-workers prepared co-crystals of sulfonic acids ( $R\text{-SO}_3\text{H}$ ,  $R$  is organic moiety such as Me, Ph,  $\text{OCH}_3$ , etc.) with guanidine.<sup>57</sup> In all the co-crystals sulfonate and guanidinium ions are assembled through, robust, charge assisted  $\text{N}^+\text{-H}\cdots\text{O}$  hydrogen bonds in two-dimensional sheet. In the 2D sheet, two kinds of arrangements were observed, quasihexagonal which is a favourable, and shifted ribbon motif, as shown in the Scheme 1.21. The shifted ribbon motif is resulted when there is steric demand from the  $R$  groups.



**Scheme 1.21.** (a) The quasihexagonal arrangement formed by  $\text{R-SO}_3^-$  and guanidinium ions in a 2D layer. R groups are not shown in figure for clarity. (b) The shifted ribbon motif in formed by  $\text{R-SO}_3^-$  and guanidinium ions in a 2D layer. R groups are not shown in figure for clarity.

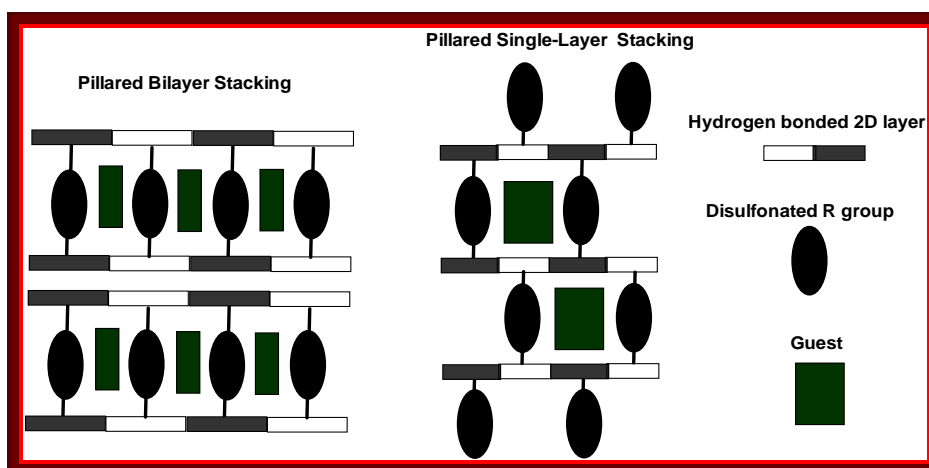
Further, such sheets are extended in three-dimensional arrangement either in interdigitated bilayer stacking in which all the R groups are oriented to one side of a given sheet or interdigitated single layer stacking in which R groups are oriented to both sides of a given hydrogen-bonded sheet, as shown in Scheme 1.22.



**Scheme 1.22**

Based on these network structures, Ward and co-workers realised that the replacement of monosulfonate by disulfonate compounds could result into pillared bilayer structures. Thus, they have carried out co-crystallization of various

disulfonic acids ( $\text{HO}_3\text{S-R-SO}_3\text{H}$ , where R is aliphatic and aromatic organic compounds) with guanidine. The obtained co-crystals were analysed by single crystal X-ray diffraction methods. The analyses revealed that sulfonate and guanidinium ions are assembled either quasi-hexagonal or shifted ribbon motif, based on steric demand of R group, as shown in the Scheme 1.22. Further, such layers are connected by other sulfonate groups of disulfonate compounds. Thus, in three-dimensional arrangement, structures showed pillared layer packing which lead to the formation voids. Such voids are filled by the guest molecules. However, such packing found to be depending upon the size of pillars and guest molecules. Sterically undemanding pillars and small guests favoured a pillared bilayer packing, whereas large guests favoured a continuous single-layer stacking motif, Scheme 1.23. Large pillars would favour only single-layer motifs with small guests or might even exclude guest molecules. In this context, they have demonstrated that solid-state motifs can be predictable if modules are used that can maintain their structural dimensionality and integrity with changes in ancillary functional groups.



Scheme 1.23.

## **1.6 Conclusions**

The above mentioned and several other examples from literature showed the significance of co-crystals towards the applications in pharmaceuticals, catalysis, separation process, optoelectronics, etc. Thus, co-crystallization approach became an important component in the contemporary research in supramolecular chemistry. In the ongoing research, in various laboratories, novel explorations in the directions such as prediction of structures of co-crystals, finding practical application of co-crystals, preparation of stable apohost for gas adsorption, preventing hydration of co-crystals, etc., have emerged as some of the central focussed themes. To address such concerns, through unexplored novel molecular assemblies, co-crystallization study of adamantanedicarboxylic acid has been consider as current focus theme of research. The results obtained by co-crystallization of 1,3-adamantanedicarboxylic acid (**adc**) with different co-formers, especially with aza-donor compounds are compiled in following Chapters.

## 1.7 References

1. (a) Lehn, J. M. *Angew. Chem., Int. Ed.* **1990**, *29*, 1304-1319; (b) Williams, D. H.; Davies, N. L.; Zerella, R.; Bardsley, B. *J. Am. Chem. Soc.* **2004**, *126*, 2042-2049; (c) Desiraju, G. R., *Crystal Engineering: The Design of Organic Solids*. Elsevier: Amsterdam: 1989; (d) Braga, D.; Grepioni, F. *Accounts Chem. Res.* **2000**, *33*, 601-608; (e) Metrangolo, P.; Meyer, F.; Pilati, T.; Resnati, G.; Terraneo, G. *Angew. Chem. Int. Ed.* **2008**, *47*, 6114-6127; (f) Motherwell, W. B.; Moise, J.; Aliev, A. E.; Nic, M.; Coles, S. J.; Horton, P. N.; Hursthouse, M. B.; Chessari, G.; Hunter, C. A.; Vinter, J. G. *Angew. Chem. Int. Ed.* **2007**, *46*, 7823-7826; (g) Hosseini, M. W. *Chem. Commun.* **2005**, 5825-5829; (h) Aakeroy, C. B.; Schultheiss, N.; Desper, J.; Moore, C. *Cryst. Growth. Des.* **2007**, *7*, 2324-2331; (i) Mathias, J. P.; Seto, C. T.; Simanek, E. E.; Whitesides, G. M. *J. Am. Chem. Soc.* **1994**, *116*, 1725-1736; (j) Aakeroy, C. B.; Fasulo, M.; Schultheiss, N.; Desper, J.; Moore, C. *J. Am. Chem. Soc.* **2007**, *129*, 13772-+; (k) Braga, D.; Grepioni, F.; Biradha, K.; Pedireddi, V. R.; Desiraju, G. R. *J. Am. Chem. Soc.* **1995**, *117*, 3156-3166; (l) Mann, S. *Nature* **1993**, *365*, 499-505; (m) Metrangolo, P.; Resnati, G. *Science* **2008**, *321*, 918-919; (n) Metrangolo, P.; Resnati, G.; Pilati, T.; Biella, S. *Struct. Bond.* **2008**, *126*, 105-136; (o) Archer, E. A.; Gong, H. G.; Krische, M. J. *Tetrahedron* **2001**, *57*, 1139-1159; (p) Williams, D. H.; Stephens, E.; O'Brien, D. P.; Zhou, M. *Angew. Chem. Int. Ed.* **2004**, *43*, 6596-6616.

2. (a) Desiraju, G. R.; Steiner, T., *The Weak Hydrogen Bond: In Structural Chemistry and Biology*. Oxford University Press, Oxford: 2001; (b) Whitesides, G. M.; Simanek, E. E.; Mathias, J. P.; Seto, C. T.; Chin, D. N.; Mammen, M.; Gordon, D. M. *Accounts Chem. Res.* **1995**, *28*, 37-44; (c) Prins, L. J.; Reinhoudt, D. N.; Timmerman, P. *Angew. Chem., Int. Ed.* **2001**, *40*, 2382-2426; (d) Steiner, T. *Angew. Chem., Int. Ed.* **2002**, *41*, 48-76.
3. (a) Richardson, J. S. *Adv. Protein Chem.* **1981**, *34*, 167; (b) Fairlie, D. P.; West, M. L.; Wong, A. K. *Curr. Med. Biol.* **1998**, *5*, 29; (c) Eaton, W. A.; Munoz, V.; Thompson, P. A.; Chan, C.-K.; Hofrichter, J. *Curr. Opin. Struct. Biol.* **1997**, *7*, 10; (d) Barlow, D. J.; Thornton, J. M. *Mol. Biol.* **1998**, *201*, 601; (e) Watson, J. D.; Crick, F. H. C. *Nature* **1953**, *171*, 964; (f) Salemme, F. R. *Prog. Biophys. Mol. Biol.* **1983**, *42*, 95; (g) Bryngelson, J. D.; Onuchic, J. N.; Socci, N. D.; Wolynes, P. G. *Proteins* **1995**, *21*, 167.
4. (a) Bernstein, J., *Polymorphism in Molecular Crystals*. Oxford University Press: Oxford: 2002; (b) Chen, J.; Sarma, B.; Evans, J. M. B.; Myerson, A. S. *Cryst. Growth. Des.* **2011**, *11*, 887-895; (c) Price, S. L. *Phys. Chem. Chem. Phys.* **2008**, *10*, 1996-2009; (d) Sarma, B.; Chen, J.; Hsi, H. Y.; Myerson, A. S. *Korean J Chem Eng* **2011**, *28*, 315-322; (e) Almarsson, O.; Hickey, M. B.; Peterson, M. L.; Morissette, S. L.; Soukasene, S.; McNulty, C.; Tawa, M.; MacPhee, J. M.; Remenar, J. F. *Cryst. Growth. Des.* **2003**, *3*, 927-933; (f) Bernstein, J.; Davey, R. J.; Henck, J. O. *Angew. Chem., Int. Ed.* **1999**, *38*, 3440-3461.

5. Pedersen, C. J. *Angew. Chem. Int. Ed.* **1988**, 27, 1021-1027.
6. Lehn, J. M. *Angew. Chem. Int. Ed.* **1988**, 27, 89-112.
7. Cram, D. J. *Angew. Chem. Int. Ed.* **1988**, 27, 1009-1020.
8. (a) Atwood, J. L.; Davies, J. E. D.; MacNicol, D. D.; Vögtle, F., *Comprehensive Supramolecular Chemistry*. Pergamon, Oxford: 1996; (b) Lehn, J. M., *Supramolecular Chemistry: Concepts and Perspectives*. VCH: Weinheim: 1995; (c) Chin, D. N.; Gordon, D. M.; Whitesides, G. M. *J. Am. Chem. Soc.* **1994**, 116, 12033-12044; (d) Desiraju, G. R. *Nature* **2001**, 412, 397-400; (e) Hollingsworth, M. D. *Science* **2002**, 295, 2410-2413; (f) Lehn, J. M. *Science* **2002**, 295, 2400-2403; (g) Siegel, J. S. *Science* **1996**, 271, 949-949.
9. Fischer, E. *Ber. Dtsch. Chem. Ges.* **1894**, 27, 2985.
10. Pauling, L.; Delbruck, M. *Science* **1940**, 92, 77.
11. (a) Dunitz, J. D.; Gavezzotti, A. *Angew. Chem. Int. Ed.* **2005**, 44, 1766-1787; (b) Fan, E.; Vicent, C.; Geib, S. J.; Hamilton, A. D. *Chem. Mater.* **1994**, 6, 1113-1117.
12. Ranganathan, A.; Pedireddi, V. R.; Rao, C. N. R. *J. Am. Chem. Soc.* **1999**, 121, 1752-1753.
13. (a) Zimmerman, S. C.; Murray, T. J. *Tetrahedron Lett.* **1994**, 35, 4077-4080; (b) Zerkowski, J. A.; Macdonald, J. C.; Whitesides, G. M. *Chem. Mater.* **1994**, 6, 1250-1257; (c) Murray, T. J.; Zimmerman, S. C. *J. Am. Chem. Soc.* **1992**, 114, 4010-4011; (d) Jorgensen, W. L.; Pranata, J. *J. Am. Chem.*

- Soc.* **1990**, *112*, 2008-2010; (e) Murray, T. J.; Zimmerman, S. C. *J. Am. Chem. Soc.* **1992**, *114*, 4010-4011.
14. Bernal, J. D.; Megaw, H. D. *Proc. R. Soc. London A* **1935**, *151*, 384.
15. Huggins, M. L. *J. Org. Chem.* **1936**, *1*, 407.
16. (a) Jeffrey, G. A.; Saenger, W., *Hydrogen Bonding in Biological Structures* Springer, Berlin: 1991; (b) Desiraju, G. R. *Angew. Chem., Int. Ed.* **1995**, *34*, 2311-2327; (c) Desiraju, G. R. *Cryst. Growth. Des.* **2011**, *11*, 896-898.
17. Jeffrey, G. A., *An Introduction to Hydrogen Bonding*. Oxford University Press, New York: 1997.
18. (a) Moulton, B.; Zaworotko, M. J. *Chem. Rev.* **2001**, *101*, 1629-1658; (b) Zaworotko, M. J. *Cryst. Growth. Des.* **2007**, *7*, 4-9; (c) Remenar, J. F.; Morissette, S. L.; Peterson, M. L.; Moulton, B.; MacPhee, J. M.; Guzman, H. R.; Almarsson, O. *J. Am. Chem. Soc.* **2003**, *125*, 8456-8457.
19. (a) Hamilton, W. C.; Ibers, J. A., *Hydrogen Bonding in Solids*. W. A. Benjamin, Inc. New York: 1968; p 19-21; (b) Wells, A. F., *Structural Inorganic Chemistry*. Clarendon Press: Oxford: 1962; p 294-315.
20. (a) Etter, M. C. *Accounts Chem. Res.* **1990**, *23*, 120-126; (b) Etter, M. C.; Macdonald, J. C.; Bernstein, J. *Acta Crystallogr. B* **1990**, *46*, 256-262; (c) Bernstein, J.; Davis, R. E.; Shimoni, L.; Chang, N. L. *Angew. Chem., Int. Ed.* **1995**, *34*, 1555-1573.
21. Bis, J. A.; Vishweshwar, P.; Weyna, D.; Zaworotko, M. J. *Mol. Pharm.* **2007**, *4*, 401-416.



22. Wohler, F. *Annalen Chem. Pharm.* **1844**, *51*, 145.
23. Anderson, J. S. *Nature* **1937**, *140*, 850.
24. Matsuda, H.; Osaki, K. *Nitta, I. Bull. Chem. Soc. Jpn.* **1958**, *31*, 611.
25. (a) Stahly, G. P. *Cryst. Growth. Des.* **2007**, *7*, 1007-1026; (b) Stahly, G. P. *Cryst. Growth. Des.* **2007**, *7*, 1007-1026; (c) Perumalla, S. R.; Suresh, E.; Pedireddi, V. R. *Angew. Chem., Int. Ed.* **2005**, *44*, 7752-7757; (d) Arora, K. K.; Pedireddi, V. R. *J. Org. Chem.* **2003**, *68*, 9177-9185; (e) Pedireddi, V. R.; Chatterjee, S.; Ranganathan, A.; Rao, C. N. R. *Tetrahedron* **1998**, *54*, 9457-9474.
26. (a) Cheney, M. L.; McManus, G. J.; Perman, J. A.; Wang, Z. Q.; Zaworotko, M. J. *Cryst. Growth. Des.* **2007**, *7*, 616-617; (b) Yan, D. P.; Delori, A.; Lloyd, G. O.; Friscic, T.; Day, G. M.; Jones, W.; Lu, J.; Wei, M.; Evans, D. G.; Duan, X. *Angew. Chem., Int. Ed.* **2011**, *50*, 12483-12486; (c) Sharma, C. V. K. *Cryst. Growth. Des.* **2002**, *2*, 465-474.
27. Pan, F.; Wong, M. S.; Gramlich, V.; Bosshard, C.; Gunter, P. *J. Am. Chem. Soc.* **1996**, *118*, 6315-6316.
28. Huang, K. S.; Britton, D.; Etter, M. C.; Byrn, S. R. *J. Mater. Chem.* **1997**, *7*, 713-720.
29. (a) Hulliger, J.; Konig, O.; Hoss, R. *Adv. Mater.* **1995**, *7*, 719-721; (b) Hulliger, J.; Konig, O.; Hoss, R. *Adv. Mater.* **1995**, *7*, 719-721.
30. Imai, Y.; Tajima, N.; Sato, T.; Kuroda, R. *Org. Lett.* **2006**, *8*, 2941-2944.
31. Roy, S.; Biradha, K. *Cryst. Growth. Des.* **2011**, *11*, 4120-4128.

32. Chatterjee, S.; Pedireddi, V. R.; Rao, C. N. R. *Tetrahedron Lett.* **1998**, *39*, 2843-2846.
33. Schimdt, G. M. J. *Pure. Appl. Chem.* **1971**, *27*, 647.
34. Papaefstathiou, G. S.; Kipp, A. J.; MacGillivray, L. R. *Chem. Commun.* **2001**, 2462-2463.
35. Mei, X. F.; Liu, S. L.; Wolf, C. *Org. Lett.* **2007**, *9*, 2729-2732.
36. Friscic, T.; Drab, D. M.; MacGillivray, L. R. *Org. Lett.* **2004**, *6*, 4647-4650.
37. Friscic, T.; Macgillivray, L. R. *Chem. Commun.* **2003**, 1306-1307.
38. Friscic, T.; MacGillivray, L. R. *Supramol. Chem.* **2005**, *17*, 47-51.
39. Etter, M. C.; Frankenbach, G. M.; Bernstein, J. *Tetrahedron Lett.* **1989**, *30*, 3617-3620.
40. Aoki, I.; Sato, T.; Masato, A.; Hiroshi, S. World Patent Application WO99/11609 A1.
41. Fischer, W. M.; Taurinsch, A. *Ber. Dtsch. Chem. Ges. B: Abhandlungen* **1931**, *64B*, 236.
42. Magne, F. C.; Mod, R. R.; Skau, E. L. *J. Am. Oil Chem. Soc.* **1957**, *34*, 127.
43. Bowman, R. S.; Dubbs, A. C.; Hedenburg, J. F. U.S. Patent 2,829,175. 1958.
44. Seddon, K. R.; Zaworotko, M. J., *Crystal Engineering: The Design and Application of Functional Solids*. NATO-ASI Series; Kluwer: Dordrecht, The Netherlands: 1999; Vol. 539.
45. Schultheiss, N.; Newman, A. *Cryst. Growth. Des.* **2009**, *9*, 2950-2967.

46. (a) Jones, W.; Motherwell, S.; Trask, A. V. *Mrs Bull* **2006**, *31*, 875-879; (b) Delori, A.; Friscic, T.; Jones, W. *Crystengcomm* **2012**, *14*, 2350-2362.
47. Bak, A.; Gore, A.; Yanez, E.; Stanton, M.; Tufekcic, S.; Syed, R.; Akrami, A.; Rose, M.; Surapaneni, S.; Bostick, T.; King, A.; Neervannan, S.; Ostovic, D.; Koparkar, A. *J. Pharm. Sci.* **2008**, *97*, 3942-3956.
48. Chemburkar, S. R.; Bauer, J.; Deming, K.; Spiwek, H.; Patel, K.; Morris, J.; Henry, R.; Spanton, S.; Dziki, W.; Porter, W.; Quick, J.; Bauer, P.; Donaubaue, J.; Narayanan, B. A.; Soldani, M.; Riley, D.; McFarland, K. *Org Process Res Dev* **2000**, *4*, 413-417.
49. Basavoju, S.; Bostrom, D.; Velaga, S. P. *Cryst. Growth. Des.* **2006**, *6*, 2699-2708.
50. Childs, S. L.; Hardcastle, K. I. *Cryst. Growth. Des.* **2007**, *7*, 1291-1304.
51. Aakeroy, C. B.; Forbes, S.; Desper, J. *J. Am. Chem. Soc.* **2009**, *131*, 17048.
52. Trask, A. V.; Motherwell, W. D. S.; Jones, W. *Cryst. Growth. Des.* **2005**, *5*, 1013-1021.
53. (a) Fleischman, S. G.; Kuduva, S. S.; McMahon, J. A.; Moulton, B.; Walsh, R. D. B.; Rodriguez-Hornedo, N.; Zaworotko, M. J. *Cryst. Growth. Des.* **2003**, *3*, 909-919; (b) Remenar, J. F.; Morissette, S. L.; Peterson, M. L.; Moulton, B.; MacPhee, J. M.; Guzman, H. R.; Almarsson, O. *J. Am. Chem. Soc.* **2003**, *125*, 8456-8457; (c) Murray, K. S.; James, A.; McGeady, J. B.; Reed, M. L.; Nangia, A. K.; Kuang, W. W. *Fertil Steril* **2011**, *96*, S9-S9.

54. (a) Arora, K. K.; Talwelkar, M. S.; Pedireddi, V. R. *New J Chem* **2009**, *33*, 57-63; (b) Cincic, D.; Friscic, T.; Jones, W. *Crystengcomm* **2011**, *13*, 3224-3231.
55. Pedireddi, V. R.; Seethalekshmi, N. *Tetrahedron Lett.* **2004**, *45*, 1903-1906.
56. Talwelkar, M.; Pedireddi, V. R. *Tetrahedron Lett.* **2010**, *51*, 6901-6905.
57. (a) Russell, V. A.; Evans, C. C.; Li, W. J.; Ward, M. D. *Science* **1997**, *276*, 575-579; (b) Swift, J. A.; Pivovar, A. M.; Reynolds, A. M.; Ward, M. D. *J. Am. Chem. Soc.* **1998**, *120*, 5887-5894.

## CHAPTER TWO

### Preparation and Analysis of Co-crystals Of

### 1,3-Adamantanedicarboxylic Acid with N-Oxide and Aza Compounds

## 2.1 Introduction

The design and synthesis of molecular materials, with desired properties, by systematic variation of functional moieties on molecular structure, is the central theme of supramolecular chemistry.<sup>1</sup> The constituent molecules within a material, thus, are the fundamental building blocks for the creation of self-assembled assemblies, like network structures, with a desired arrangement and dimensionality through non-covalent interactions, such as hydrogen bonds, coordinate bonds, halogen bonds, etc.<sup>2</sup> Several examples of extended hydrogen bonding assemblies are known in the literature, illustrating the importance and influence of such interactions to facilitate the organization of molecules into supramolecular assemblies.<sup>3</sup> Among these assemblies, structures with multicomponents are of special interest, as directed synthesis of assemblies of tailor-made properties is viable following simple synthetic routes.<sup>4</sup> Some of the notable and illustrative examples from the literature are discussed in the following sections.

Yang and co-workers reported the structure of co-crystals of 1,4-diazabicyclo[2.2.2]octane (DABCO) with terephthalic acid.<sup>4a</sup> In the structure, the molecules are alternatively linked by N-H $\cdots$ O hydrogen bonds in a linear one-dimensional tape, as shown in Figure 2.1. The linear geometry of the tapes may be accounted for the topology of the recognition sites (-COOH groups and -N atoms) which are positioned linearly on both ends of DABCO and terephthalic acid. However, with isophthalic acid, in which the two -COOH groups are positioned at

an angle of  $60^\circ$ , DABCO forms a zig-zag chains or tapes, as reported by Braga and co-workers.<sup>4b</sup> The arrangement is represented in Figure 2.2.

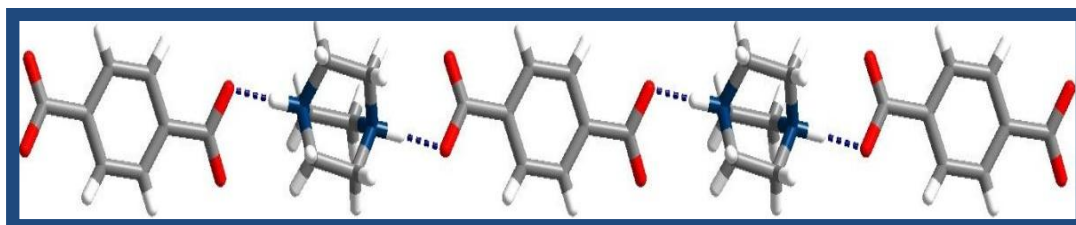


**Figure 2.1.** Representation of one-dimensional tapes formed through N-H...O hydrogen bonds, in the co-crystals of terephthalic acid and DABCO.

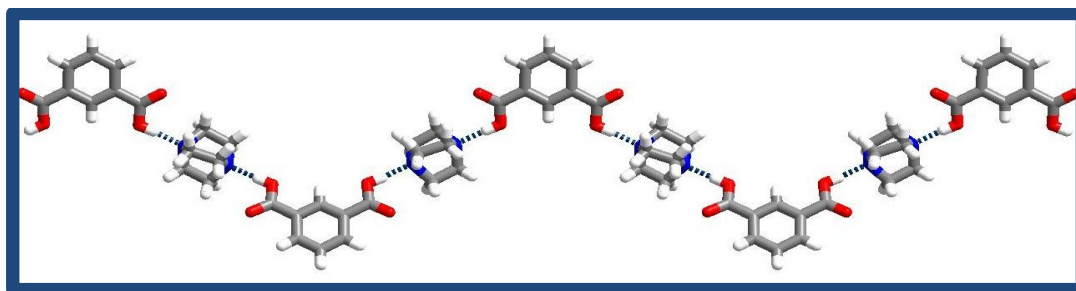


**Figure 2.2.** Zig-zag chains observed in the co-crystals of isophthalic acid and DABCO, through O-H...N hydrogen bonds.

Pedireddi and co-workers reported co-crystals of 1,2,4,5-benzenetetracarboxylic acid (**BTCA**) with 1,2-di-4-pyridylethylene/ethane.<sup>4c</sup> In these co-crystals, among the four -COOH groups on **BTCA**, two -COOH groups involved in intramolecular hydrogen bonding as shown in , Figures 2.3 and 2.4. Thus, the recognition sites (-COOH groups at 2 and 5 positions) are positioned linearly on opposite ends of **BTCA** like that of terephthalic acid. As a result, in the crystal structures of both the co-crystals, the two types of molecular components

are alternatively linked by N-H $\cdots$ O hydrogen bonds in linear one-dimensional tape, as shown in Figure 2.3 and 2.4.

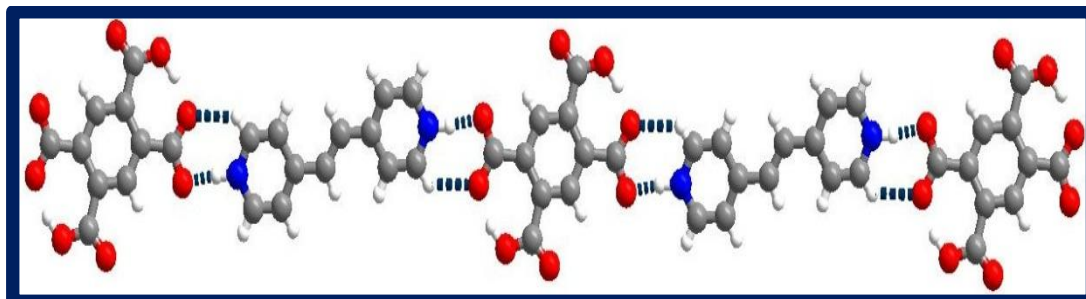


**Figure 2.3.** Representation of recognition pattern between molecules of **BTCA** and 1,2-di-4-pyridylethylene and a one-dimensional tape formed in the co-crystal.

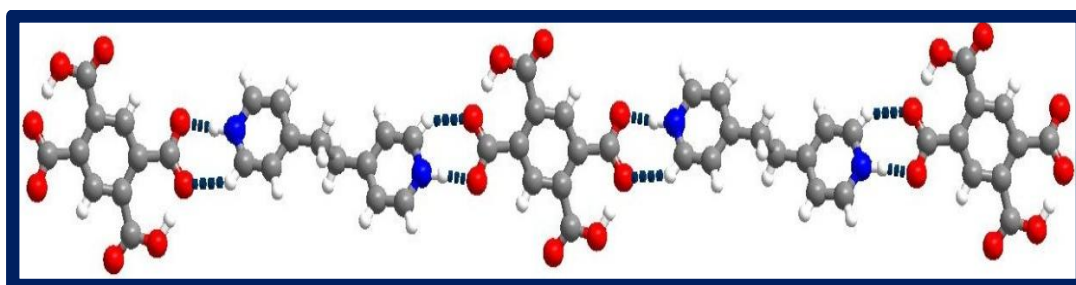


**Figure 2.4.** One-dimensional tape formed through N-H $\cdots$ O hydrogen bonds, in the co-crystals of **BTCA** and 1,2-di-4-pyridylethane.

However, molecules with  $C_3$  symmetry and functional groups capable of yielding hydrogen bonding such as carboxylic acid form networks in two-dimensional arrangement, with the crystal structure of trimesic acid and 2,4,6-tris(4-pyridyl)-1,3,5-triazine serving as a representative example, as reported by Coppens and co-workers.<sup>4d</sup> In the crystal lattice, the molecules are arranged in hexagonal network through O-H $\cdots$ N/C-H $\cdots$ O pair-wise hydrogen bonding pattern, as shown in Figure 2.5.



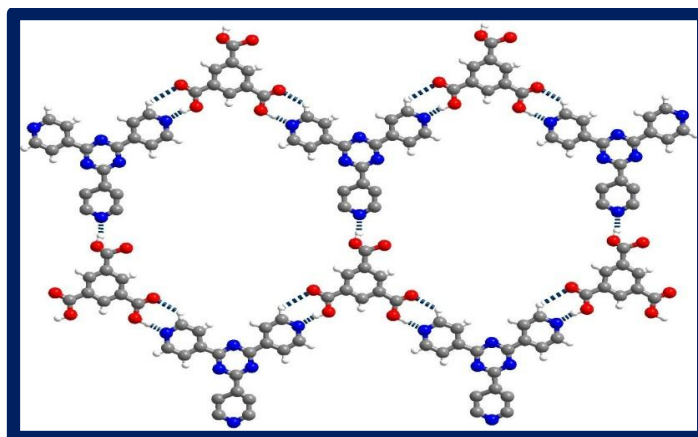


**Figure 2.5.** Hexagonal network formed by the aggregation of molecule of the components in the co-crystal of trimesic acid with 2,4,6-*tris*(4-pyridyl)-1,3,5-triazine.

In fact, formation of such a hexagonal network through self-assembly process is the propensity of trimesic acid, even in its pure form as reported by Duchamp and co-workers, which illustrates the significance of the position of the functional groups, Figure 2.6.<sup>4e</sup>

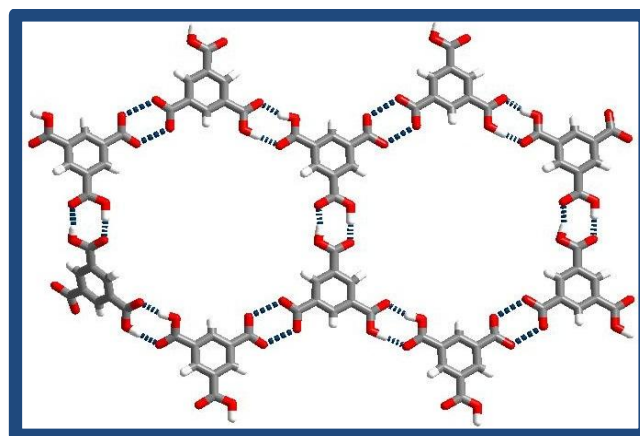


**Figure 2.6.** Hexagonal networks formed by molecules of trimesic acid in a two-dimensional layer.

Similarly, Men and co-workers reported co-crystal of 4-[tris(4-carboxyphenyl)methyl]benzoic acid with 4,4'-bipyridine.<sup>4f</sup> Molecules of the components are arranged in diamondoid network through O-H $\cdots$ N hydrogen bonds. The observed diamondoid network is due to the presence of recognition sites at tetrahedral position of 4-[tris(4-carboxyphenyl)methyl]benzoic acid, Figure 2.7.

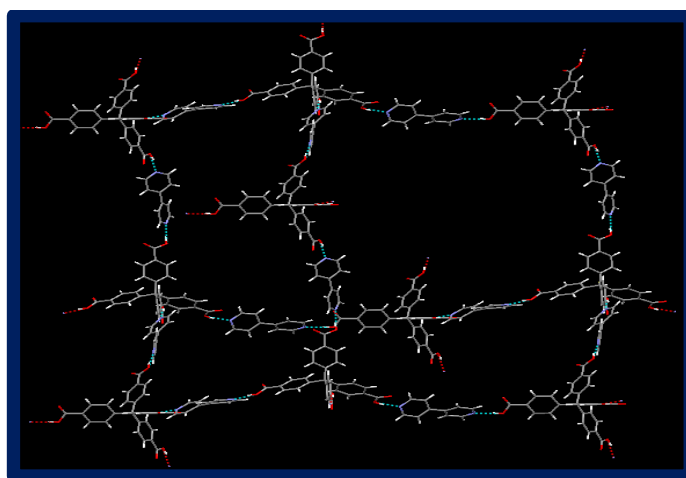


**Figure 2.7.** Diamondoid network observed in the co-crystal of 4-[tris(4-carboxyphenyl)methyl]benzoic acid with 4,4'-bipyridine.

As observed in trimesic acid, 1,3,5,7-adamantanetetracarboxylic acid, in which the  $\text{-COOH}$  groups are positioned at tetrahedral sites, indeed forms diamondoid network through O-H $\cdots$ O hydrogen bonds formed by  $\text{-COOH}$  groups in the form of dimeric units, demonstrate the elegance and efficacy of topology of functional moieties. The pattern of typical diamondoid topology is shown in Figure 2.8, as reported by Ermer in the year 1990.<sup>4g</sup>

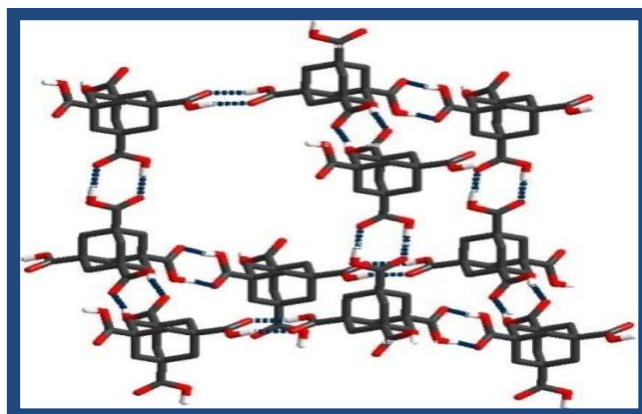


**Figure 2.8.** Three dimensional diamondoid network structure of 1,3,5,7-adamantanetetracarboxylic acid.

Thus, molecules with required topology and also possessing carboxylic acid groups are well utilized to obtain desired network structures, leading to the reports of a myriad of various aromatic and aliphatic carboxylic acids mediated supramolecular assemblies (particularly, utilizing O-H $\cdots$ N / C-H $\cdots$ O pair wise hydrogen bonding patterns, evolved due to the interaction of -COOH moieties with aza-donor compounds).<sup>5</sup> However, most of the compounds consider to be planar molecules despite a large number of organic molecules are three-dimensional in nature, like adamantanetetracarboxylic acid (**1**) as illustrated in Figure 2.8. Interestingly, supramolecular assemblies of even the acid (**1**) are not well known in the literature. Thus, preparation of supramolecular assemblies of adamantanedicarboxylic acid has been chosen to evaluate the structural features and its applications. For this purpose a few assemblies of acid **1** with various aza-donor and N-oxide compounds, as listed in chart 2.1, are prepared. However, it has been noted that, complexes of acid **1** with pyridyl ligands 4,4'-bipyridine, 1,2-di-4-

pyridylethylene / ethane<sup>6</sup> are reported in the recent literature. In these co-crystals, although the basic recognition between **1** and the aza-donor compounds is very much similar due to the topological similarity, the extended structures either in 2D and / or 3D are quite distinctly different, as shown in Figure 2.9, perhaps they are being influenced by various secondary interactions like C-H $\cdots$  $\pi$ ,  $\pi\cdots\pi$  etc.

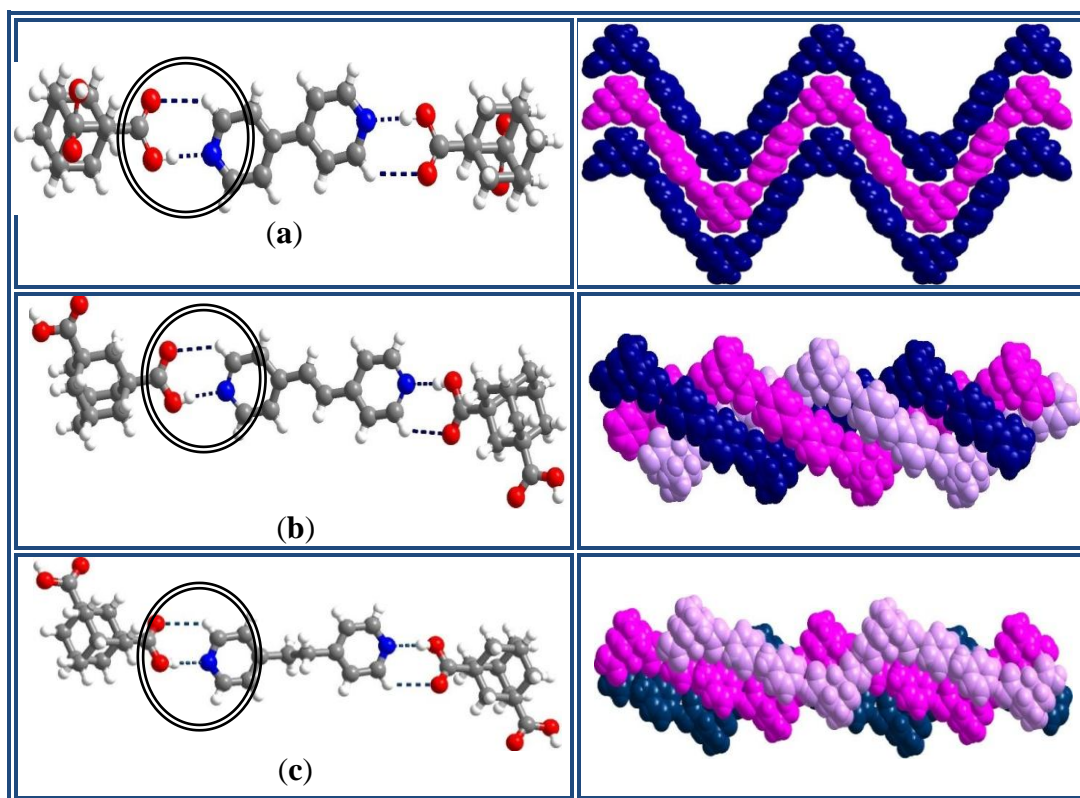
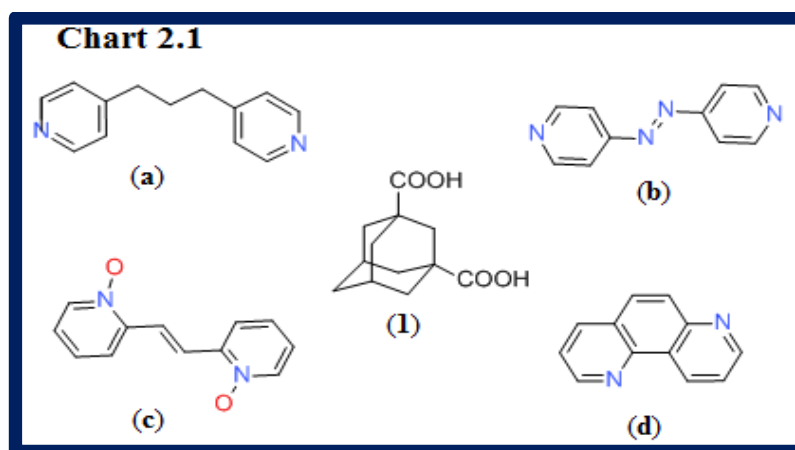


**Figure 2.9.** Distinct three dimensional arrangements in co-crystals of **1** with a) 4,4'-bipyridine, b) 1,2-di-4-pyridylethylene, c) 1,2-di-4-pyridylethane, despite possessing similar basic recognition patterns.

Hence, to explore such variations, being influenced by secondary interactions, in the assemblies mediated by 1,3-adamantanedicarboxylic acid, co-crystals of **1** with some other pyridyl based compounds with variable molecular

conformations, like 1,3-di(pyridin-4-yl)propane (**a**), *E*-1,2-di(pyridine-4yl)diazene (**b**), *E*-2,2'-(ethene-1,2-diyl)dipyridine 1-oxide (**c**) and 1,7-phenanthroline (**d**), as listed in chart 2.1, which are good hydrogen bond acceptors as well as show ability to form secondary interactions of appreciable characteristics. These assemblies have been characterized by single crystal X-ray diffraction method. The molecular ratios of the reactants, products and solvents used for the co-crystallization are given in Chart 2.2.



The analyses of the 3D structures reveal that, in all the co-crystals the basic interaction between the constituent molecules is established through a pair-wise hydrogen bonds ( $O-H\cdots N$  or  $O-H\cdots O / C-H\cdots O$ ), which is further extended in the crystal lattice by  $C-H\cdots O$  hydrogen bonds,  $C-H\cdots \pi$  and  $\pi\cdots\pi$  interactions.

<b>Chart 2.2</b>		
<b>Reactants (ratio)</b>	<b>Solvents</b>	<b>Products (ratio)</b>
<b>1 + a (1:1)</b>	Methanol + Water	<b>1a (1:1)</b>
<b>1 + b (1:1)</b>	Methanol	<b>1b (1:1)</b>
<b>1 + c (1:1)</b>	Methanol	<b>1c (1:1)</b>
<b>1 + d (1:1)</b>	Methanol + Dimethylsulfoxide	<b>1d &amp; 1d' (1:2)</b>

## 2.2 Structure of co-crystals of 1,3-adamantanedicarboxylic acid, **1**, with 1,3-di(pyridin-4-yl)propane (*a*), **1a**:

Co-crystallization of 1,3-adamantanedicarboxylic acid, **1** and 1,3-di(pyridin-4-yl)propane (*a*), by slow evaporation of a methanol / water solution, gave good quality single crystals. Structure determination by single crystal X-ray Diffraction method reveals that, in the asymmetric unit, co-crystal formers are present in a 1:1 ratio, as shown in Figure 2.10. For the convenience of discussion, these co-crystals are labeled as **1a**. The pertinent crystallographic data for **1a** is given in Table 2.1.

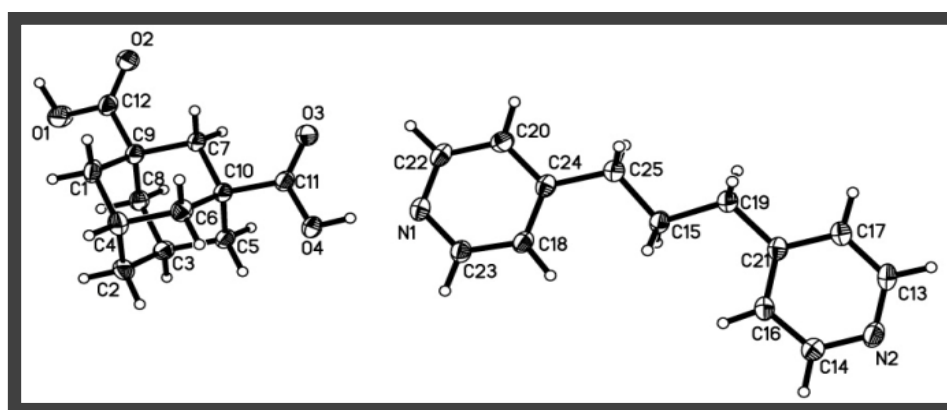


**Figure 2.10.** ORTEP of the contents in the asymmetric unit of **1a**.

Within the crystal lattice, each molecule of *a* is adhered to the acid molecules by two different types of hydrogen bonding patterns, though similar functional groups are involved in the recognition process. The recognition pattern between the co-crystal formers is shown in Figure 2.11. While one of the pattern is a typical O-H $\cdots$ N / C-H $\cdots$ O pair-wise hydrogen bonds<sup>7</sup> (H $\cdots$ N, 1.68 and 1.62 Å), other one is a single O-H $\cdots$ N hydrogen bond, (H $\cdots$ N, 1.66 Å), as shown in Figure 2.11. Complete characteristics of hydrogen bonds are listed in Table 2.2.

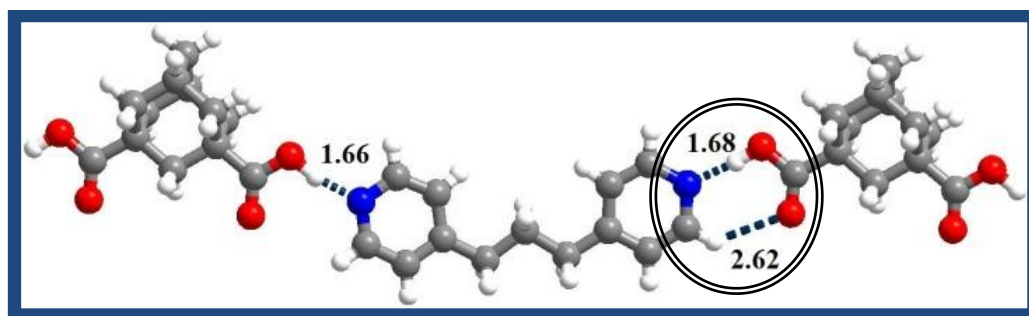


**Figure 2.11.** Interaction between the molecules of **1** and **a** through O-H...N and a pair-wise O-H...N and C-H...O hydrogen bonds.

These ensembles are further extended to form infinite tapes, which are connected to each other as binary units, by a series of C-H...O hydrogen bonds of H...O distance of 2.45 Å. Within each layer, such binary units are juxtaposed by hydrophobic interactions. A typical layer observed in crystal lattice is shown in Figure 2.12. The layers, in turn, are packed in three-dimensional array by C-H... $\pi$  and  $\pi$ ... $\pi$  interactions.

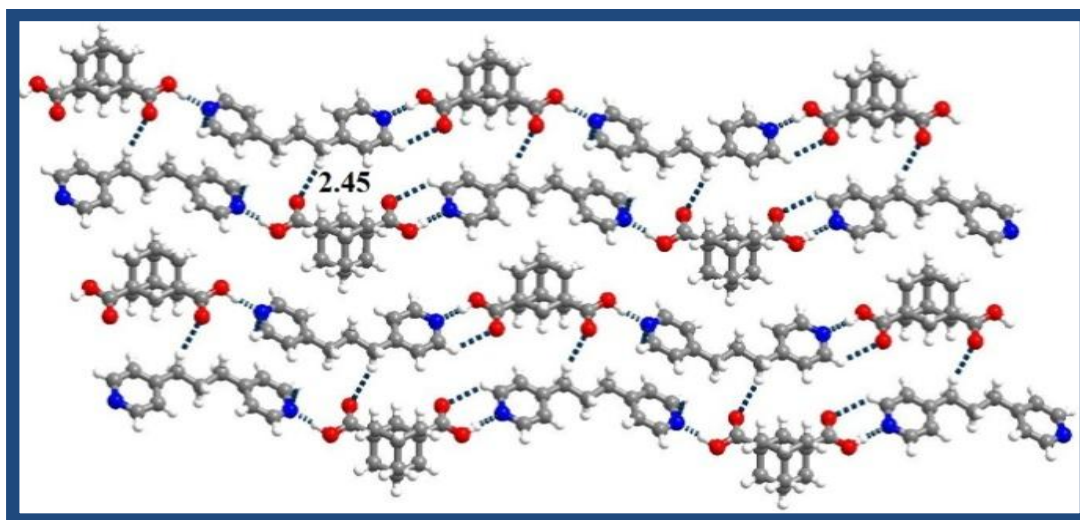


**Figure 2.12.** Representation of binary types, stabilized by C-H...O hydrogen bonds, in a layer structure held together by hydrophobic interactions.



It is apparent from the structural features of **1a** that the basic recognition is similar to the observed patterns in the other related examples in the literature. Three-dimensional arrangement has a close similarity with such a packing in the structure of **1** and 4,4'-bipyridine, unlike the variations noted in the co-crystals of **1** with 1,2-di-4-pyridylethane, an analogue of **a**. The observed similarity may be accounted for the molecular geometry of **a**, which is quite planar like 4,4'-bipyridine, whereas 1,2-di-4-pyridylethane is skewed.

Taken into account significance of molecular geometry towards the self-assembly process in the complex of acid **1**, as observed in **1a**, it is appreciable to study the structural variations by changing the functional moieties, maintaining the molecular geometry intact and vice versa. For this purpose, the co-crystals of the acid **1** with *E*-1,2-di(pyridine-4yl)diazene, **b**, have been prepared as the diazene is similar to *E*-1,2-di-4-pyridylethylene by geometrical feature, except for the replacement of olefinic bridge by -N=N- group.

### **2.3 Structure of co-crystal of 1,3-adamantanedicarboxylic acid, **1**, with *E*-1,2-di(pyridine-4yl)diazene (**b**), **1b**:**

Co-crystallization of the acid **1** and *E*-1,2-di(pyridine-4yl)diazene, **b**, from a MeOH solution, gave single crystals, **1b**, of good quality, by a slow evaporation process at ambient conditions. Structure determination by X-ray diffraction method reveals that, in the asymmetric unit, composition of the cocrystal formers is in a 1:1 ratio and an ORTEP drawing of the constituents is shown in Figure 2.13. Complete crystallographic parameters are given in Table 2.1.



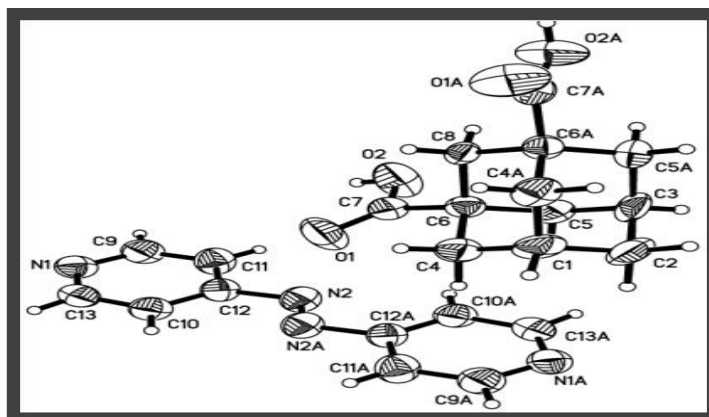


Figure 2.13. ORTEP of the asymmetric unit in the complex **1b**.

Analysis of the molecular arrangement within the crystal lattice reveals that the molecules **1** and **b** are held together by a pair-wise hydrogen bonding pattern (O-H $\cdots$ N and C-H $\cdots$ O), a well known pattern for the interaction between the -COOH and aza donor groups.<sup>7</sup> The topology of the network is shown in Figure 2.14, with the hydrogen bond distances of 1.80 and 2.53 Å for the corresponding O-H $\cdots$ N and C-H $\cdots$ O hydrogen bonds respectively, while the other characteristic parameters of the hydrogen bonds are listed in Table 2.2.

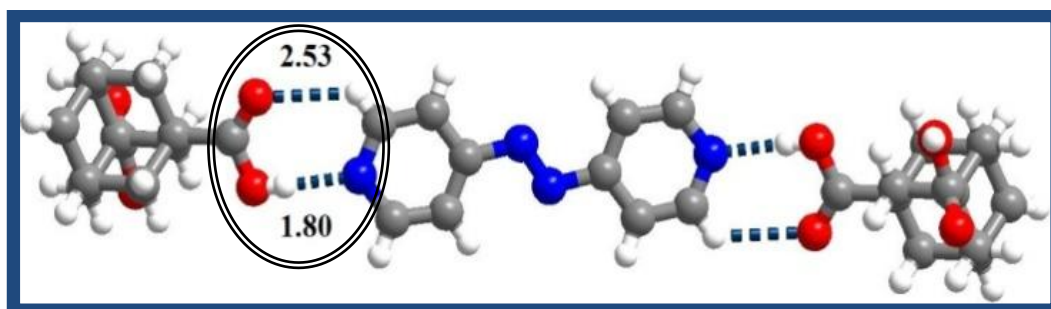
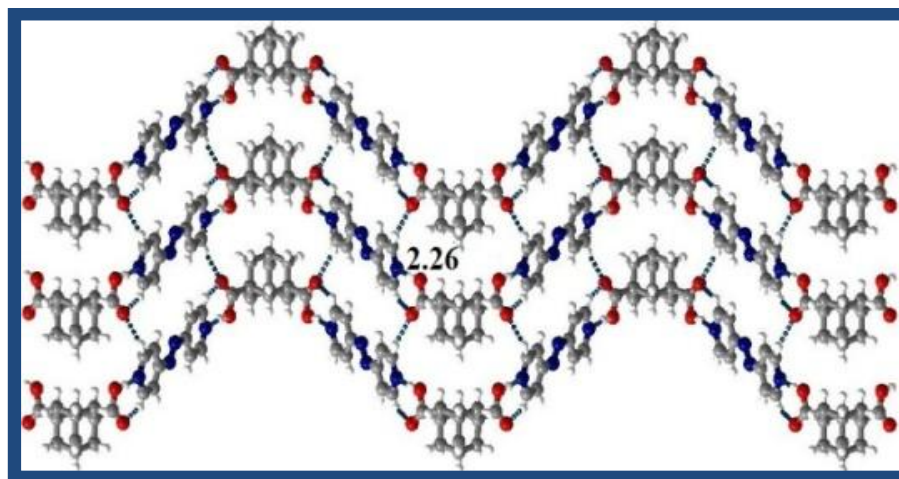


Figure 2.14. Recognition pattern between the co-crystal formers in the crystal structure of **1b**.

Such ensembles are further held together by C-H $\cdots$ O hydrogen bonds in two-dimensional arrangement, with H $\cdots$ O distance of 2.26 Å, Figure 2.15, in the

form of corrugate sheets. In the three dimensional packing, the sheets are stacked by C-H $\cdots$  $\pi$  interaction of 2.81 Å and  $\pi\cdots\pi$  interactions.



**Figure 2.15.** The arrangement of molecules in a typical layer in **1b**.

It is noteworthy to mention that although molecules of *E*-1,2-di(pyridine-4yl)diazene are similar to 1,2-di-4-pyridylethylene, except for the replacement of olefinic bridge by N=N (azo bridge), the three-dimensional packing in the resultant supramolecular assembly with **1** is entirely different, with former being a corrugated stacked sheets (Figure 2.15) while the later forms an helical assembly (Figure 2.9b). It may be understood in terms of the significance of the olefinic protons in the stabilization of secondary structure, which are not present in **b**. Furthermore, the structure of **1b** is reminiscent of the structure of the co-crystals of **1** and 4,4'-bipyridine (See Figure 2.9a) and **1a**. It is not so surprising, that in the absence of hydrogen bond directing olefinic moiety, the diazene molecule is more comparable to 4,4'-bipyridine in terms of conformational aspects, except for the length.

To further understand such structural variations, it may be noteworthy if the molecular conformational flexibility is coupled with functional moieties of varying acceptor / donor capabilities. Indeed, the co-crystals **1c**, formed by acid **1** with *E*-2,2'-(ethene-1,2-diyl)dipyridine-1-oxide (**c**), which is blended with both conformational flexibility as well as requisite functional moiety to form appreciable intermolecular interactions, gave entirely different structure than so far observed structures of co-crystals of **1** in literature or in **1a** and **1b**.

#### **2.4 Structure of co-crystal of 1,3-adamantanedicarboxylic acid, **1**, with *E*-2,2'-(ethene-1,2-diyl)dipyridine-1-oxide (**c**), **1c**:**

Co-crystallization of acid **1** and the N-oxide (**c**), in a 1:1 ratio, from a CH<sub>3</sub>OH solution, at ambient conditions, gave single crystals with an asymmetric unit of 1:1 co-crystal formers, as shown in Figure 2.16, obtained from the structure determined by X-ray diffraction methods. Complete details of structure determination and refinement parameters are given in Table 2.1.

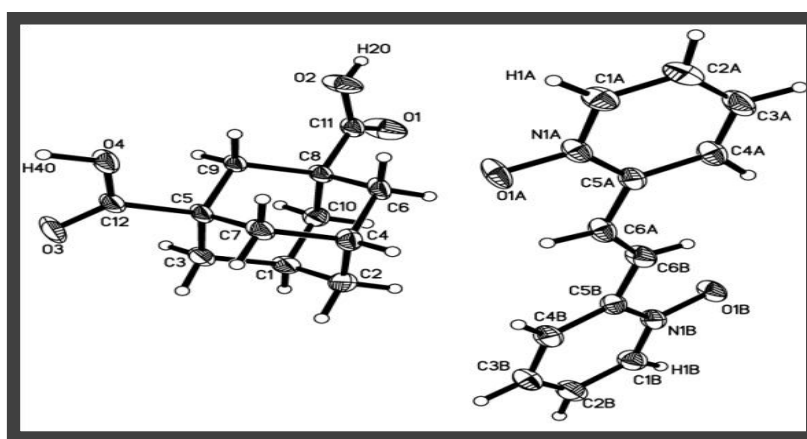


**Figure 2.16.** ORTEP of an asymmetric unit in **1c**.

In **1c**, basic recognition is established with the interaction of each acid molecule with two molecules of **c** or vice versa, through a pair-wise O-H $\cdots$ O (H $\cdots$ O, 1.64 Å) and C-H $\cdots$ O (H $\cdots$ O, 2.22 Å) hydrogen bonds. Other characteristics of these hydrogen bonds and also of other such bonds are given in Table 2.1. A pictorial representation of the recognition pattern is shown in Figure 2.17.

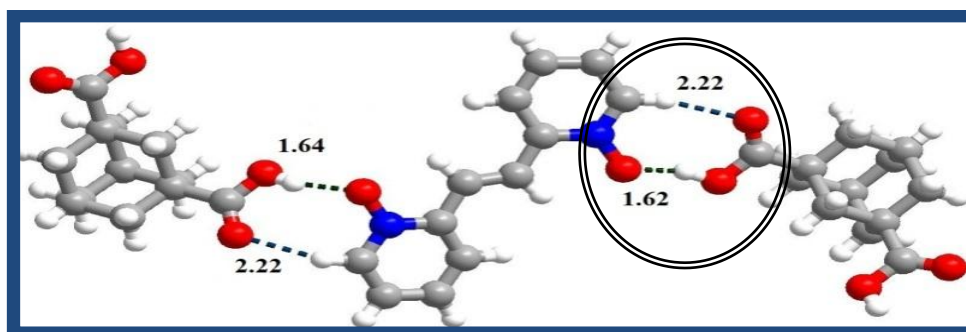


**Figure 2.17.** Molecular recognition pattern between the molecules of **1** and **c**.

Such adjacent ensembles are further held together by C-H $\cdots$ O (H $\cdots$ O, 2.33 and 2.44 Å) hydrogen bonds, as shown in Figure 2.18, creating voids of approximately 10 x 8 Å<sup>2</sup> in two-dimensional arrangement.

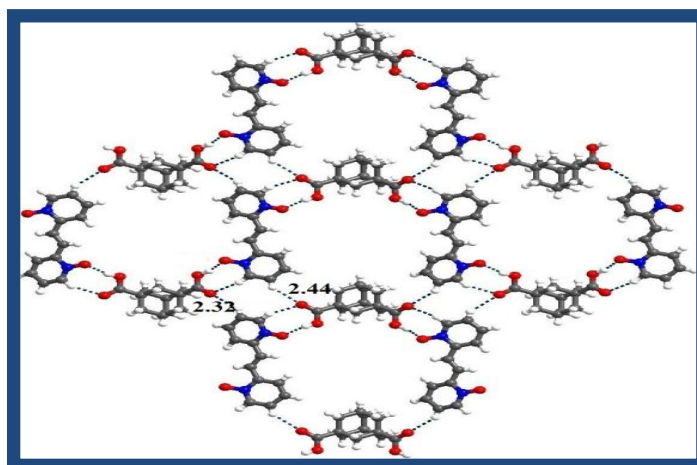


**Figure 2.18.** Arrangement of molecules in a typical layer within the crystal structure of **1c**, with void space.

However, these voids are not able to constitute channels in the three-dimensional arrangement, as the void space is effectively being masked by the electron density from molecules lying in the adjacent sheets along the stacking direction. Such a packing arrangement is shown in Figure 2.19.

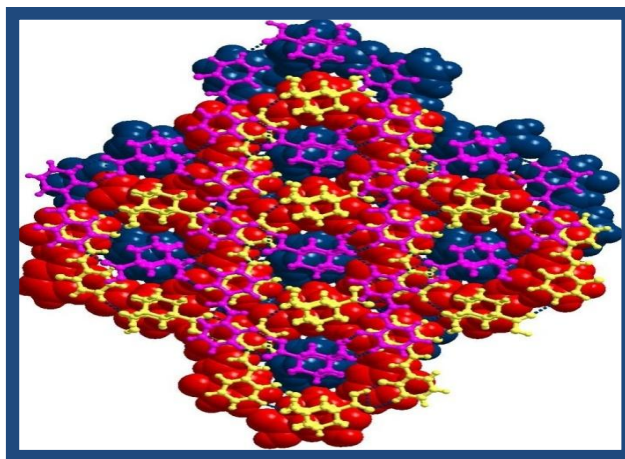


**Figure 2.19.** Stacking of layers in the three-dimensional arrangement, as observed in the crystal structure of **1c**.

In further studies to evaluate other possible structural variations, with the molecules in rigid conformation, co-crystals of acid **1** with 1,7-phenanthroline, (*d*) have been prepared. Interestingly, two different types of crystals were found in the reaction flask, upon slow evaporation of a MeOH / DMSO solution of mixture of the co-crystal formers, in a 1:1 ratio, which have been found to be concomitant polymorphs, as characterized by single crystal X-ray diffraction method. The pertinent crystallographic information is compiled in Table 2.1. In fact, co-crystal polymorphs are increasingly being seen in the recent literature.<sup>8</sup>

## 2.5 Structure of two polymorphs of co-crystal of 1,3-adamantanedicarboxylic acid, **1**, with 1,7-phenanthroline (*d*), **1d** and **1d'**:

The two forms are labeled as **1d** and **1d'**. Composition and conformation of the co-crystal formers in the asymmetric units of **1d** and **1d'** are shown in Figures 2.20 and 2.21 respectively.

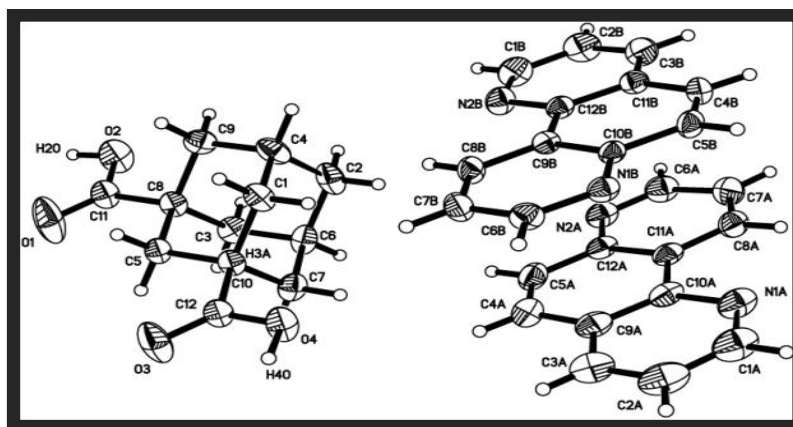


**Figure 2.20.** Molecular conformations of **1** and **d** in a 1:2 ratio, in an asymmetric unit of co-crystals of **1d**.

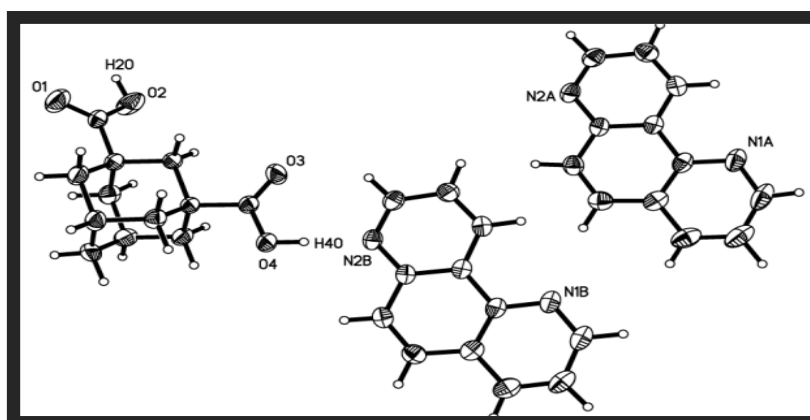


**Figure 2.21.** ORTEP of the co-crystal formers in the complex **1d'**.

It is apparent that while orientation of two  $-\text{COOH}$  groups is *cisoid* in **1d**, the same is *transoid* in **1d'** with respect to the position of proton on the  $-\text{COOH}$  group. Such transoid orientation of  $-\text{COOH}$  groups in **1** was observed in its two co-crystals, out of four systems<sup>6a,b</sup> as documented in the Cambridge Structural Database<sup>6c</sup> (version 5.32, ConQuest 1.13) with reference codes DIWGOG and TEFSIH. The remaining two co-crystals, in cisoid conformation are TEFSAZ and TEFSED.

In both **1d** and **1d'**, however the recognition between the acid **1** and phenanthroline, **d**, is through typical pair-wise hydrogen bonding patterns, comprising  $\text{O}-\text{H}\cdots\text{N}$  /  $\text{C}-\text{H}\cdots\text{O}$  hydrogen bonds. The recognition patterns are highlighted in Figures 2.22 and 2.23. The complete characteristics of hydrogen bonds are given in Table 2.2.

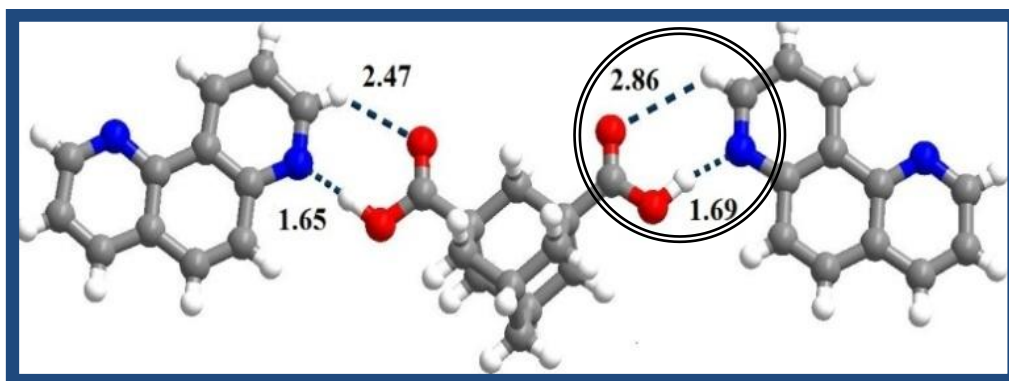


**Figure 2.22.** Recognition patterns observed between the molecules of **1** and **d** in the complex **1d**.



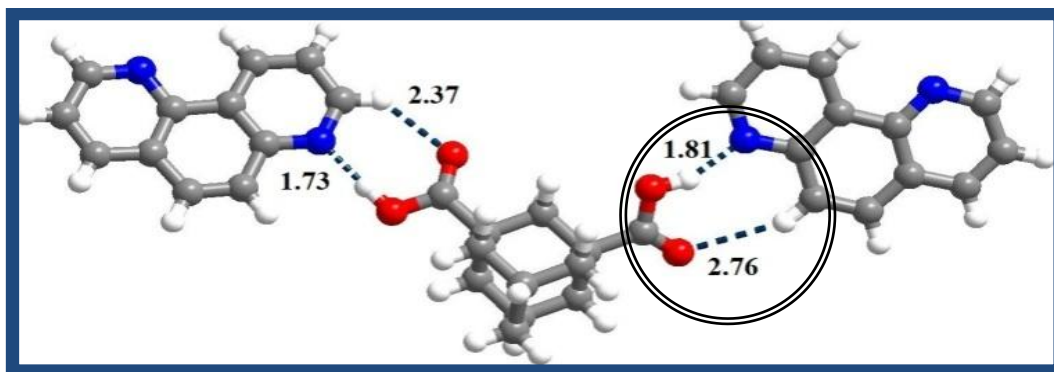


**Figure 2.23.** Basic recognition pattern between the acid **1** and **d** in the co-crystals of **1d'**.

These self-assembled supermolecules are further held together by a series of C-H $\cdots$ O and C-H $\cdots$ N hydrogen bonds in **1d**, whereas only by C-H $\cdots$ O hydrogen bonds in **1d'**, as shown in Figures 2.24 and 2.25. The ensembles are further packed in 2D, in the form of layers, by hydrophobic interactions (see Figures 2.24 and 2.25).

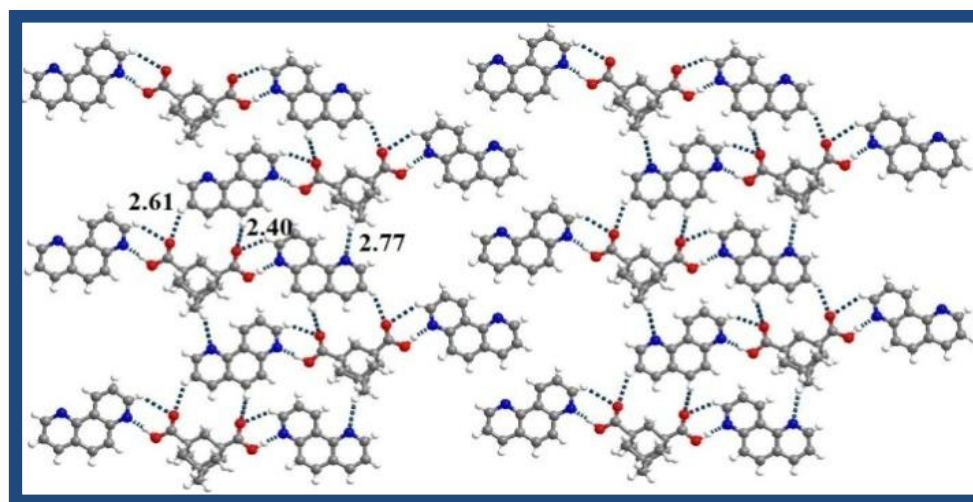


**Figure 2.24.** Packing of discrete supermolecules in 2D arrangement, through C-H $\cdots$ O and C-H $\cdots$ N hydrogen bonds, in the crystal lattice of **1d**.



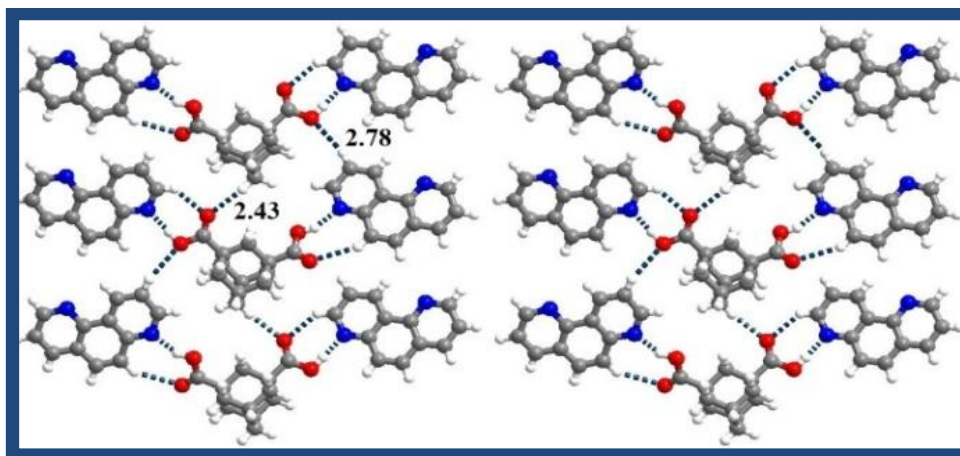


**Figure 2.25.** Arrangement of supermolecules, in the form of a layer, through C-H $\cdots$ O hydrogen bonds, in co-crystals **1d'**.

Such layers are however, stacked in 3D by a series of C-H $\cdots$ N hydrogen bonds and  $\pi\cdots\pi$  interactions. The packing is illustrated in Figures 2.26 and 2.27.

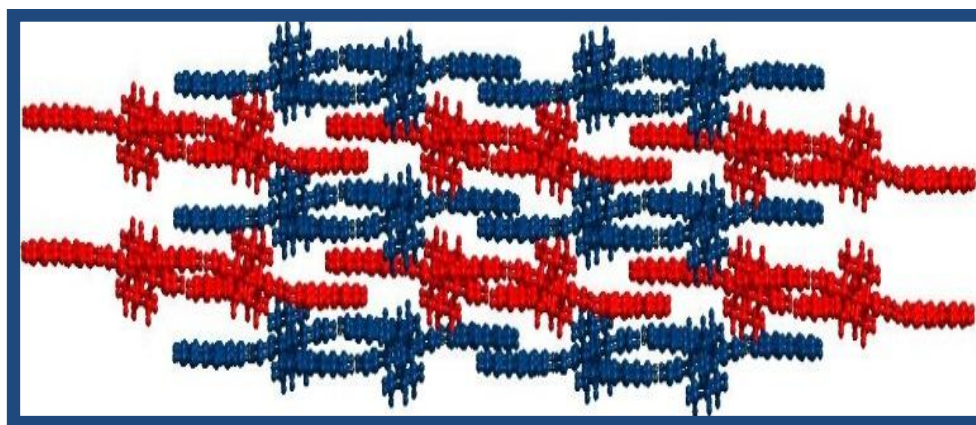


**Figure 2.26.** Stacking arrangement of 2D layers in three-dimensional arrangement, through  $\pi\cdots\pi$  interactions in **1d**.

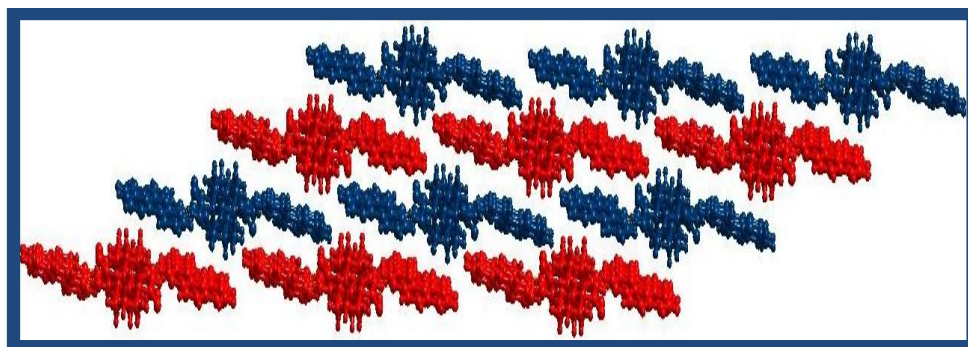


**Figure 2.27.** Packing of layers in three-dimension, with the aid of  $\pi\cdots\pi$  interactions, in the crystal lattice of **1d'**.

The pertinent C-H $\cdots$ N hydrogen bonds between the molecules in the polymorph **1d'**, along the stacking direction are shown in Figure 2.28. Thus, each acid molecule in both **1d** and **1d'** is connected to two molecules of **d**, but interestingly, only one of the pyridyl -N atom did participate in the basic recognition with the acid molecules, while second one is involved in the formation of only secondary interactions in the stabilization of three-dimensional packing. As a result, within a layer, the distinct zero-dimensional supermolecules of these compounds is formed, which are held together by C-H $\cdots$ O hydrogen bonds in a one-dimensional mode.

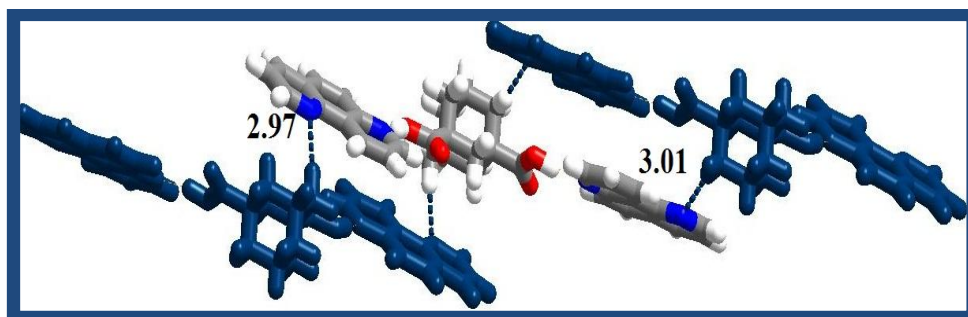


**Figure 2.28.** Packing of layers in 3D through C-H $\cdots$ N hydrogen bonds in the crystal lattice of **1d'**.

## 2.6 Conclusions

In summary, supramolecular assemblies of **1a**, **1b**, **1c**, **1d** and **1d'** formed by 1,3-adamantanedicarboxylic acid with an N-oxide and aza compounds **a-d**, as the case may be, have been prepared and analyzed for the structural features. These assemblies have been characterized by single crystal X-ray diffraction method. The analyses of 3D structures reveal that, in all the structures (**1a-1d** and **1d'**), the basic interaction between the co-crystal formers exist through a pair wise hydrogen bond (O-H $\cdots$ N / O-H $\cdots$ O, C-H $\cdots$ O). Such supermolecules are further extended in 2D through C-H $\cdots$ O hydrogen bonds. The observed 3-D structures, in turn, are found to be stabilized by both C-H $\cdots$  $\pi$  and  $\pi\cdots\pi$  interactions.

## 2.7 Experimental section

### 2.7.1 Preparation of molecular adducts **1a-1d** and **1d'**.

All chemicals used in this study were obtained from Sigma Aldrich Chemicals Private Limited and used as such without any further purification. The solvents employed for the co-crystallization purpose were of spectroscopy grade of highest available purity. Co-crystals of **1a-1d** and **1d'** have been prepared by slow evaporation of corresponding solutions of the co-crystal formers which are dissolved in the appropriate ratios, as listed in Chart 1. Single crystals of good quality were obtained over a period of 48 h which are suitable for characterization by X-ray diffraction method.

**2.7.2 X-ray Structure Determinations.** Good quality single crystals of **1a-1d** and **1d'** were carefully selected using Leica microscope and glued to a glass fiber using an adhesive (cyano acrylate). In all the cases, the crystals were smeared in the adhesive solution to prevent decay of crystals. The intensity data were collected on a Bruker single-crystal X-ray diffractometer, equipped with an APEX detector. Subsequently, the data were processed using the Bruker suite of programs (SAINT), and the convergence was found to be satisfactory with good  $R_{\text{ini}}$  parameters.<sup>9</sup> The details of the data collection and crystallographic information are given in Table 2.1. Absorption corrections were applied using SADABS package.<sup>9</sup> The structure determination by direct methods and refinements by least-squares methods on  $F^2$  were performed using the SHELXTL-PLUS package. The processes were smooth without any complications. All non-hydrogen atoms were refined anisotropically, while hydrogen atoms are treated isotropically. All the intermolecular interactions were computed using PLATON.<sup>10</sup> All packing diagrams are generated using Diamond software.<sup>11</sup>

**Table 2.1.** Crystallographic data and structure refinement parameters for the co-crystals, **1a** - **1d** and **1d'**

	<b>1a</b>	<b>1b</b>	<b>1c</b>	<b>1d</b>	<b>1d'</b>
formula	C <sub>12</sub> H <sub>16</sub> O <sub>4</sub> :C <sub>13</sub> H <sub>14</sub> N <sub>2</sub>	C <sub>12</sub> H <sub>16</sub> O <sub>4</sub> :C <sub>10</sub> H <sub>8</sub> N <sub>4</sub>	C <sub>12</sub> H <sub>16</sub> O <sub>4</sub> :C <sub>12</sub> H <sub>10</sub> N <sub>2</sub> O <sub>2</sub>	C <sub>12</sub> H <sub>16</sub> O <sub>4</sub> :2(C <sub>12</sub> H <sub>8</sub> N <sub>2</sub> )	C <sub>12</sub> H <sub>16</sub> O <sub>4</sub> :2(C <sub>12</sub> H <sub>8</sub> N <sub>2</sub> )
formula wt	422.51	408.45	438.47	584.66	584.66
crystal system	triclinic	monoclinic	monoclinic	Orthorhombic	monoclinic
space group	<i>P</i> $\bar{1}$	<i>P</i> 2 <sub>1</sub> / <i>m</i>	<i>C</i> 2/ <i>c</i>	<i>P</i> 2 <sub>1</sub> 2 <sub>1</sub>	<i>P</i> 2 <sub>1</sub> / <i>c</i>
<i>a</i> /Å	7.310(2)	6.378(1)	23.332(7)	6.812(1)	8.59(3)
<i>b</i> /Å	11.830(3)	25.714(5)	13.044(4)	13.329(2)	14.65(4)
<i>c</i> /Å	13.276(4)	6.565(1)	13.742(4)	32.622(5)	24.10(7)
$\alpha$ /°	83.31(4)	90	90	90	90
$\beta$ /°	77.62(4)	110.23(3)	95.88(5)	90	97.88(5)
$\gamma$ /°	76.43(4)	90	90	90	90
<i>V</i> /Å <sup>3</sup>	1087.4(5)	1010.2(4)	4160(2)	2962.1(8)	3004(2)
<i>Z</i>	2	2	8	4	4
<i>D<sub>c</sub></i> /g cm <sup>-3</sup>	1.290	1.340	1.400	1.311	1.293
$\mu$ /mm <sup>-1</sup>	0.087	0.094	0.101	0.087	0.086
2 $\theta$ range[°]	50.60	50.04	50.74	49.98	50.42
<i>T</i> /K	100	293	297	293	293
<i>F</i> (000)	452	430	1856	1232	1232
$\lambda$ /Å	0.71073	0.71073	0.71073	0.71073	0.71073
$\Delta\rho_{\text{min,max}}$ /e Å <sup>-3</sup>	-0.176, 0.263	-0.162, 0.567	-0.313, 0.316	-0.209, 0.312	-0.329, 0.316
total reflections	10522	7356	14153	14909	14464
unique reflections	3937	1833	3787	2997	5344
reflections used	3518	956	2860	2294	4025
no. of parameters	400	143	390	405	517
<i>R</i> <sub>1</sub> , <i>I</i> > 2 $\sigma$ ( <i>I</i> )	0.0396	0.0766	0.0670	0.0484	0.0655
<i>wR</i> <sub>2</sub> , <i>I</i> > 2 $\sigma$ ( <i>I</i> )	0.1003	0.1857	0.1595	0.1057	0.1712
GOF on <i>F</i> <sup>2</sup>	1.060	1.022	1.112	1.145	1.238
CCDC no.	828066	828065	828069	828067	828068

**Table 2.2.** Characteristics of hydrogen bond distances and angles observed in the co-crystals **1a**, **1b**, **1c**, **1d** and **1d'**.<sup>\$</sup>

H-Bond	1a			1b			1c			1d			1d'											
O-H $\cdots$ N	1.66	2.63	168	1.80	2.72	154				1.65	2.63	174	1.73	2.72	179									
	1.68	2.66	174							1.69	2.66	168				1.81	2.73	154						
O-H $\cdots$ O							1.62	2.57	162															
							1.64	2.59	162															
C-H $\cdots$ O	2.45	3.48	159	2.26	3.28	156	2.22	3.26	162	2.40	3.35	145	2.37	3.22	134									
	2.53	3.60	169							2.53	3.27	125				2.22	3.19	147	2.47	3.23	126	2.43	3.46	160
	2.56	3.26	121							2.32	3.24	142				2.61	3.46	135	2.76	3.77	155			
	2.62	3.37	126							2.44	3.36	142				2.86	3.55	122	2.78	3.71	144			
C-H $\cdots$ N										2.77	3.59	132	2.97	3.99	156									
										3.01	4.08	169												

<sup>\$</sup>In each row for each interaction, the three numbers correspond to H $\cdots$ N / H $\cdots$ O, O $\cdots$ N / O $\cdots$ O / C $\cdots$ O / C $\cdots$ N distances in Å and angles O-H $\cdots$ N/ O-H $\cdots$ O / C-H $\cdots$ O / C-H $\cdots$ N ( $^{\circ}$ ), respectively.

## 2.8 References

- (1) (a) Lehn, J. -M. *Angew. Chem., Int. Ed.* **1990**, 29, 1304. (b) Yan, Y.; Deng, K.; Yu, J.; Wei, Z. *Angew. Chem., Int. Ed.* **2009**, 48, 2003. (c) Hollingsworth, M. D. *Science* **2002**, 295, 2410. (d) Custelcean, R.; Gorbunova, M. G. *J. Am. Chem. Soc.* **2005**, 127, 16362. (e) Hosseini, M. W. *Chem. Commun.* **2005**, 5825. (f) Lehn, J. -M. *Science* **2002**, 295, 2400. (g) Ziegler, M.; Miranda, J. J.; Andersen, U. N.; Johnson, D. W.; Leary, J. A.; Raymond, K. N. *Angew. Chem., Int. Ed.* **2001**, 40, 733. (h) Desiraju, G. R. *Crystal Engineering: The Design of Organic Solids*; Elsevier: Amsterdam, 1989. (i) Lehn, J. M. *Supramolecular Chemistry: Concepts and Perspectives*; VCH: Weinheim, 1995. (j) Atwood J. L.; Davies J. E. D.; MacNicol D. D.; Vögtle F. *Comprehensive Supramolecular Chemistry*, Pergamon, Oxford, 1996. (k) Zaworotko, M. J. *Chem. Commun.* **2001**, 1. (l) Zaworotko, M. J. *Cryst. Growth Des.* **2007**, 7, 4. (m) Atwood, J. L.; Barbour, R. J.; Jerga, A. *Angew. Chem., Int. Ed.* **2004**, 43, 2948. (n) Braga, D.; Giaffreda, S. L.; Grepioni, F.; Maini, L.; Polito, M. *Coord. Chem. Rev.* **2006**, 250, 1267. (o) Mahata, G.; Roy, S.; Biradha, K. *Chem. Commun.* **2011**, 6614. (p) Barnett, S. A.; Champness, N. R.; *Coord. Chem. Rev.* **2003**, 246, 145.
- (2) (a) Steiner, T. *Angew. Chem., Int. Ed.* **2002**, 41, 48. (b) Prins, L. J.; Reinhoudt, D. N.; Timmerman, P. *Angew. Chem., Int. Ed.* **2001**, 40, 2382. (c) Desiraju, G. R. *Angew. Chem., Int. Ed.* **1995**, 34, 2311. (d) Espallargas, G. M.; Zordan, F.; Marín, L. A.; Adams, H.; Shankland, K.; Streek, J. V.; Brammer, L. *Chem.*

- Eur. J.* **2009**, *15*, 7554. (e) Zordan, F.; Brammer, L.; Sherwood, P. *J. Am. Chem. Soc.* **2005**, *127*, 5979. (f) Metrangolo, P.; Meyer, F.; Pilati, T.; Resnati, G.; Terraneo, G. *Angew. Chem., Int. Ed.* **2008**, *47*, 6114. (g) Jeffrey, G. A.; Saenger, W. *Hydrogen Bonding in Biological Structures*, Springer, Berlin, 1991. (h) Jeffrey, G. A. *An Introduction to Hydrogen Bonding*, Oxford University Press, New York, 1997. (i) MacDonald, J. C.; Whitesides, G. M. *Chem. Rev.* **1994**, *94*, 2383. (j) Numerous examples are given in a Special Issue of *Chemistry of Materials: Structure and Chemistry of the Organic Solid State*, *Chem. Mater.* **1994**, *6* (No. 8). (k) Chang, Y. L.; West, M. A.; Fowler, F. W.; Lauher, J. W. *J. Am. Chem.Soc.* **1993**, *115*, 5991. (l) Paul, A. K.; Madras, G.; Natarajan, S. *CrystEngComm* **2009**, *11*, 55.
- (3) (a) Perumalla, S. R.; Suresh, E.; Pedireddi, V. R. *Angew. Chem., Int. Ed.* **2005**, *44*, 7752. (b) Varughese, S.; Desiraju, G. R. *Cryst. Growth Des.* **2010**, *10*, 4184. (c) Ahn, S.; PrakashaReddy, J.; Kariuki, B. M.; Chatterjee, S.; Ranganathan, A.; Pedireddi, V. R.; Rao, C. N. R.; Harris, K. D. M. *Chem. Eur. J.* **2005**, *11*, 2433. (d) Zimmerman, S. C.; Zeng, F.; Reichert, D. C. C.; Kolotuchin, S. V. *Science* **1996**, *271*, 1095. (e) Applegarth, L.; Goetra, A. E.; Steed, J. W. *Chem. Commun.* **2005**, 2405. (f) Talwelkar, M.; Pedireddi V. R. *Tetrahedron Lett.* **2010**, *51*, 6901. (g) Aakeroy, C. B.; Forbes, S.; Desper, J. *J. Am. Chem.Soc.* **2009**, *131*, 17048. (h) Remenar, J. F.; Morissette, S. L.; Peterson, M. L.; Moulton, B. *J. Am. Chem. Soc.* **2003**, *125*, 8456. (i) Aakeroy, C. B.; Fasulo, M.; Schultheiss, N.; Forbes, S.; Desper, J.; Moore, C. *J. Am.*



- Chem.Soc.* **2007**, *129*, 13772. (j) Braga, D.; Grepioni, F. *Chem. Commun.* **2005**, 3635. (k) Biradha, K.; Su, C.; Vittal, J. *Cryst. Growth Des.* **2011**, *11*, 875.
- (4) (a) Yang, E.; Song, X.; Zhu, J. *Acta Crystallogr., Sect. E.* **2008**, *64*, o1764. (b) Marivel, S.; Braga, D.; Grepioni, F.; Lampronti, G. *CrystEngComm* **2010**, *12*, 2107. (c) Arora, K. K.; Pedireddi, V. R. *J. Org. Chem.* **2003**, *68*, 9177. (d) Ma, B. Q.; Coppens, P. *Chem. Commun.* **2003**, 2290. (e) Duchamp, C. J.; Marsh, R. E. *Acta Crystallogr.* **1969**, *B25*, 5. (f) Men, Y. B.; Sun, J. L.; Huang, Z. T.; Zheng, Q. Y. *Crystengcomm* **2009**, *11*, 978. (g) Ermer, O. *J. Am. Chem. Soc.* **2011**, *110*, 3141. (h) Swift, J. A.; Pivovar, A. M.; Reynolds, A. M.; Ward, M. D. *J. Am. Chem. Soc.* **1998**, *120*, 5887. (i) Guo, F.; Cheung, E. Y.; Harris, K. D. M.; Pedireddi, V. R. *Cryst. Growth Des.* **2006**, *6*, 846. (j) Ranganathan, A.; Pedireddi, V. R.; Chatterjee, S.; Rao, C. N. R. *J. Mater. Chem.* **1999**, *9*, 2407. (k) Wuest, J. D.; *Chem. Commun.* **2005**, 5830. (i) Aakeroy, C. B.; Chopade, P. *Org. Lett.* **2011**, *13*, 1. (l) Goldberg, I.; Bernstein, J. *Chem. Commun.* **2007**, 132.
- (5) (a) Chatterjee, S.; Pedireddi, V. R.; Rao, C. N. R. *Tetrahedron Lett.* **1998**, *39*, 2843.
- (b) Pedireddi, V. R.; Ranganathan, A.; Chatterjee, S. *Tetrahedron Lett.* **1998**, *39*, 9831. (c) Shan, N.; Batchelor, E.; Jones, W. *Tetrahedron Lett.* **2002**, *43*, 8721. (d) Bowers, J. R.; Hopkins, G. W.; Yap, G. P. A.; Wheeler, K. A. *Cryst. Growth Des.* **2005**, *5*, 727. (e) Duchamp, D. J.; Marsh, R. E. *Acta Crystallogr.*

- 1969, B25, 5. (f) Ermer, O.; Lindenberg, L. *Chem. Ber.* **1990**, 123, 1111. (g) Kuppers, H. *Cryst. Struct. Commun.* **1981**, 10, 989. (h) Holy, P.; Zavada, J.; Cisarova, I.; Podlaha, J. *Angew. Chem., Int. Ed.* **1999**, 38, 381. (i) Vishweshwar, P.; Nangia, A.; Lynch, V. M. *J. Org. Chem.* **2002**, 67, 556. (j) Batchelor, E.; Klinowski, J.; Jones, W. *J. Mater. Chem.* **2000**, 10, 839. (k) Fournier, J.; Maris, T.; Wuest, J. D.; Guo, W.; Galoppini, E. *J. Am. Chem. Soc.* **2003**, 125, 1002.
- (6) (a) Zeng, Q.; Wu, D.; Ma, H.; Shu, C.; Wang, C. *CrystEngComm* **2006**, 8, 189. (b) Pan Y.; Li K.; Bi W.; Li J. *Acta Crystallogr., Sect. C.* **2008**, 64, o41. (c) Allen, F. H.; Kennard, O. *Chem. Des. Automate. News* **1993**, 8, 31-37.
- (7) (a) Pedireddi, V. R.; Chatterjee, S.; Ranganathan, A.; Rao, C. N. R. *J. Am. Chem. Soc.* **1997**, 119, 10867. (b) Varughese, S.; Pedireddi, V. R. *Chem. Eur. J.* **2006**, 12, 1597. (c) Varughese, S.; Pedireddi, V. R. *Chem. Commun.* **2005**, 1824. (d) Sharma, C. V. K.; Zaworotko, M. J. *Chem. Commun.* **1996**, 2655. (e) Friscic, T.; MacGillivray, L. R. *Chem. Commun.* **2005**, 5748. (f) Bhogala, B. R.; Basavoju, S.; Nangia, A. *Cryst. Growth Des.* **2005**, 5, 1683. (g) Pedireddi, V. R.; Shimpi, M. R.; Yakhmi, J. V. *Macromol. Symp.* **2006**, 241, 83. (h) Walsh, R. D.; Bradner, M. W.; Fleischman, S.; Morales, L. A.; Moulton, B.; Rodríguez-Hornedo, N.; Zaworotko, M. J. *Chem. Commun.* **2003**, 186. (i) Arora, K. K.; Pedireddi, V. R. *J. Org. Chem.* **2003**, 68, 9177.
- (8) (a) Braga, D.; Palladino, G.; Polito, M.; Rubini, K.; Grepioni, F.; Chierotti, M. R.; Gobetto, R. *Chem. Eur. J.* **2008**, 14, 10149. (b) Sokolov, A. N.; Swenson,

- D. C.; MacGillivray, L. R. *Proc. Natl. Acad. Sci.* **2008**, *105*, 1794. (c) Babu, N. J.; Reddy, L. S.; Aitipamula, S.; Nangia, A. *Chem. Asian. J.* **2008**, *3*, 112. (d) Porter, W. W.; Elie, S. C.; Matzger, A, J. *Cryst. Growth Des.* **2008**, *8*, 14.
- (9) (a) Siemens, SMART System, Siemens Analytical X-ray Instruments Inc., Madison, WI, 1995. (b) G. M. Sheldrick, SHELXTL-PLUS Program for Crystal Structure Solution and Refinement, University of Gottingen, Gottingen, Germany.
- (10) Spek, A. L. *PLATON*, Molecular Geometry Program; University of Utrecht: The Netherlands, 1995.
- (11) Diamond—Crystal and Molecular Structure Visualization, Version 3.1f, Crystal Impact, Brandenburg & Putz, Bonn, 2008.

## **CHAPTER THREE**

### **Host-Guest Assemblies of** **1,3-Adamantanedicarboxylic Acid in the Presence of Various** **Hydrogen Bond Donor and Acceptor Compounds**

### 3.1 Introduction

Host-guest assemblies,<sup>1</sup> popularly represented by a class of compounds known as zeolites, which are essentially microporous crystalline solids of aluminosilicates with guest species ranging from simple water molecules to different alkali cations, etc.<sup>2</sup> The interaction between the host and guest, in general, is formulated through noncovalent interactions such as hydrogen bonds, van der Waals, etc., which are relatively weaker than conventional ionic, covalent, coordinate bonds, etc. Because of such weak nature of these interactions prevail between the host and guest, several new avenues are opened up, through the evaluation of zeolites in the fields such as catalysis, separation process, gas adsorption, etc.

The host-guest chemistry not only restricted to the zeolites, but also extended to the hosts made up of covalent networks such as cyclodextrins, calixarenes, cucurbiturils, crown ethers, cryptands, spherands and cryptophanes, etc. The cyclodextrins are long being known since 1891, which is first synthesized from starch by A. Villiers.<sup>3</sup> Typical cyclodextrins contain a number of glucose monomers ranging from six to eight units in a ring, creating a cone shape. The cyclodextrins with six, seven and eight membered sugar ring molecule is known as  $\alpha$ ,  $\beta$  and  $\gamma$ -cyclodextrin, respectively.<sup>4</sup> The  $\alpha$ -cyclodextrin is shown in Figure 3.1.

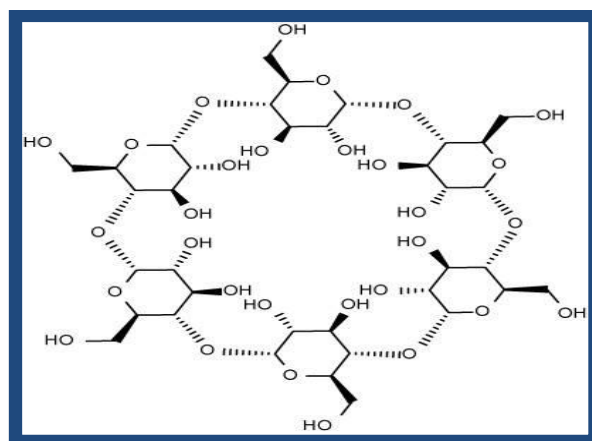


**Figure 3.1.** The  $\alpha$ -cyclodextrin molecule.

The calixarene, as shown in Figure 3.2, is another class of host compounds which is prepared by condensation of a phenol and an aldehyde. The calixarenes are macrocyclic hosts containing hydrophobic cavities which can be occupied by small molecules or ions.<sup>5</sup> The nomenclature of calixarenes is calix[ $n$ ]arene, where  $n$  represents the repeating units in a macrocycle.

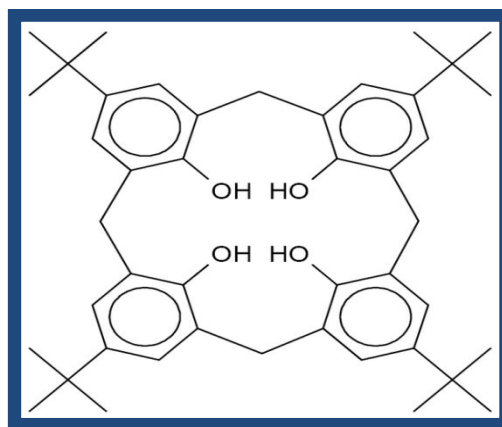


**Figure 3.2.** The molecular structure of calyx[4]arene.

The Cucurbiturils contain glycouril monomers which are linked through methylene groups.<sup>6</sup> The glycouril monomer is obtained from urea and dialdehyde, and such monomers are further condensed with formaldehyde. The condensation

results in to cucurbiturils of various sizes. However, the cucurbiturils which are made up of six glycouril monomers are stable. The cucurbiturils are commonly denoted as cucurbit[ $n$ ]uril, where  $n$  is the number of glycoluril units. The cucurbit[7]uril is shown in Figure 3.3.

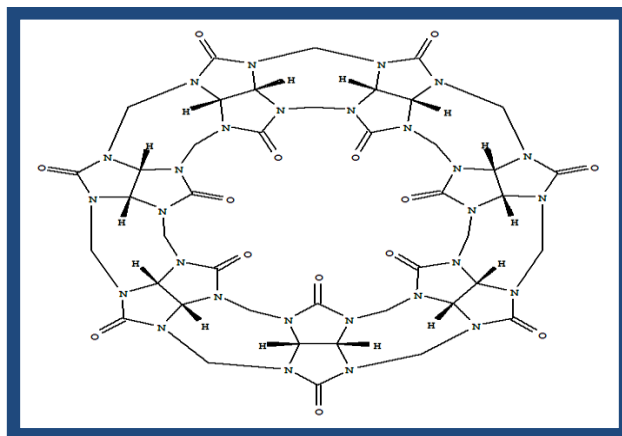


**Figure 3.3.** The molecular structure of the cucurbit[7]uril.

The crown ethers (cyclic ethers) are known since the discovery of dibenzo-18-crown-6, as depicted in Figure 3.4, by Charles Pedersen in 1967.<sup>7</sup> Crown ethers are well known class of host compounds with extended application in the field of organic synthesis, phase transfer catalysis, etc.<sup>8</sup> Crown ethers are named as [x]-crown-[y] where x denotes the total number of atoms in the cyclic backbone and y denotes the number of oxygen atoms.

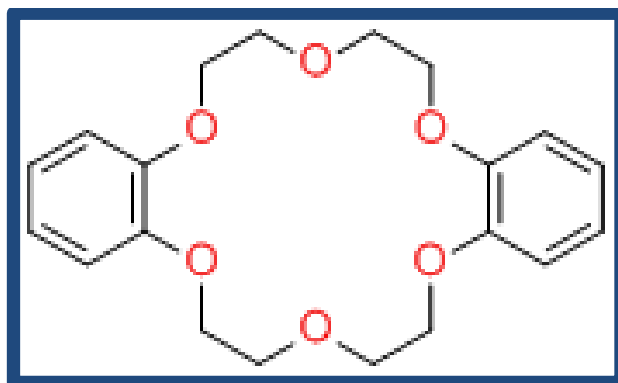


**Figure 3.4.** The molecular structure of dibenzo-18-crown-6.

In 1969, Jean-Marie Lehn prepared another class of macrocyclic ether with three-dimensional cavity, which captivates guest molecule(s).<sup>9</sup> This class of compounds is named as cryptands and the compounds with the guest are named as cryptates.<sup>10</sup> One of the cryptands is shown in Figure 3.5.

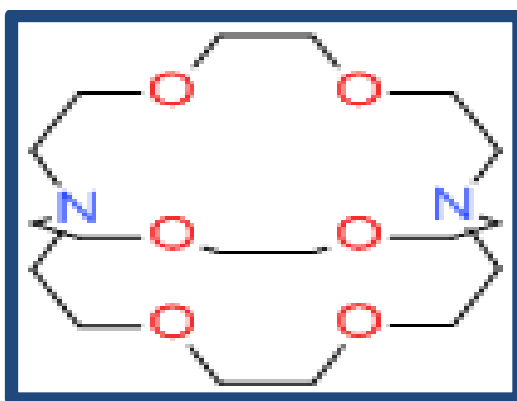


**Figure 3.5.** The molecular structure of [2.2.2]cryptand (the numbers indicate the number of oxygen atoms in each of the three bridges between the amine nitrogen atoms).

In 1970, Donald J. Cram prepared another class of compounds, named as spherands, which are cyclic in nature with pre-organized cavities for the incorporation of guest entities.<sup>1c</sup> The pre-organized cavity is due to the rigidity in spherand which does not allow its parts to rotate to fill the cavity.<sup>11</sup> The cavity is ordinarily too small to be filled with either solvent or parts of solvent. Thus, the cavity is empty and relatively unsolvated. The molecular structure of a spherand is given in Figure 3.6.



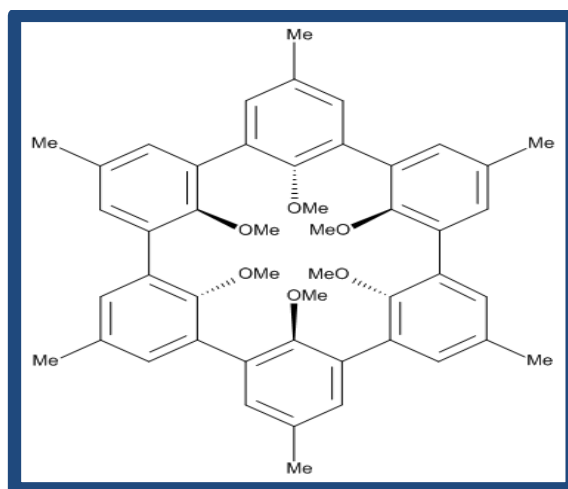


**Figure 3.6.** The molecular structure of the spherand.

The hosts mentioned in above context are obtained by the use of traditional covalent synthesis. However, hosts are also obtained by the aggregation of molecules through noncovalent interactions such as hydrogen bonds,<sup>12</sup> halogen bonds,<sup>13</sup> co-ordinate covalent bonds,<sup>14</sup> van der Waals,<sup>15</sup> etc. Such approach is extensively used for the synthesis of large number of different host-guest complexes. Toda and co-workers reported that 1,1,6,6-tetraphenylhexa-2,4-diyne-1,6-diol (see Figure 3.7) forms numbers of host-guest complexes with various polar and nonpolar small molecules such as ketones, aldehydes, esters, ethers, amides, amines, nitriles, sulfoxides, sulphides, arenes, alkenes, alkynes and haloalkanes.<sup>16</sup> The host-guest complexes are formed because of hydrogen bonding with the -OH groups, the linear nature of the acetylenic bond, and  $\pi \cdots \pi$  interactions with the aryl rings. A typical structure of the host-guest complex formed by the molecules of 1,1,6,6-tetraphenylhexa-2,4-diyne-1,6-diol, with acetone, guest molecules, is shown in Figure 3.8.



**Figure 3.7.** The molecular structure of diacetylenic diol.

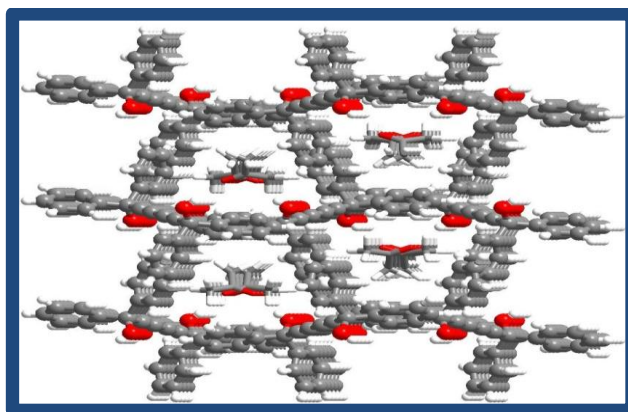


**Figure 3.8.** Host-guest complex of diacetylenic diol (host) and acetone (guest).

Further, Hart and co-workers prepared host-guest complexes by using the compound 1,1,6,6,6-pentakis-phenylhexa-2,4-diynylbenzene (Figure 3.9).<sup>17</sup> The compound is obtained by the replacement of hydroxyl groups of 1,1,6,6-tetraphenylhexa-2,4-diyne-1,6-diol by the phenyl groups. Such hosts are so efficient to captivate the guest molecules such as *p*-xylene, benzene, toluene, *o*-xylene, chlorobenzene, etc.



**Figure 3.9.** Molecular structure of 1,1,6,6,6-pentakis-phenylhexa-2,4-diynylbenzene.

Weber and co-workers reported several substituted derivatives of anthracene, as shown in Figure 3.10, such as 1,5-*bis*[(diphenylhydroxymethyl)ethynyl]anthracene (**1**), 1,5-*bis*[(9-hydroxyfluoren-9-yl)ethynyl]anthracene (**2**), 1,8-*bis*[(diphenylhydroxymethyl)ethynyl]anthracene (**3**), etc., as efficient entities for clathrates formation, by incorporating various solvents such as *n*-propylamine, *n*-butylamine, triethylamine, dimethylsulfoxide, dimethylformamide, and tetrahydrofuran.<sup>18</sup>

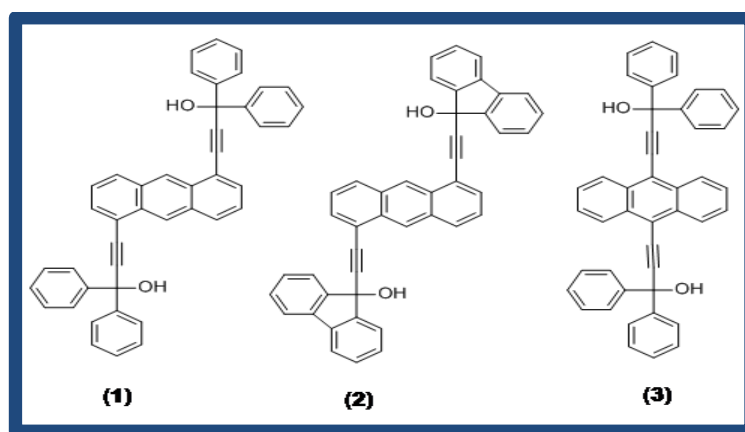


**Figure 3.10.** Molecular structures of compounds **1**, **2** and **3**.

Wuest and co-workers showed molecular tectons approach for the synthesis of host structures. Strong directional interactions in the tectons usually dominate, leading to the formation of open networks with a significant capacity for inclusion. Porous networks derived from tectons are molecular analogues of zeolites, but they are held together by hydrogen bonds and other interactions. Guests located in these channels can often be exchanged without loss of crystallinity, simply by exposing single crystals to new guests. In crystals of spirofluorene, **4**, which incorporates four sticky aminotriazene groups, 75% of the volume is accessible to guests and the hydrogen bonded network formed by tecton **4** is the most porous ever built from

small molecules, (Figure 3.11). Also, the crystallization of trigonal tecton **5** was directed reliably by hydrogen bonding of pyridinone groups to form porous corrugated sheets, which then stack in a translational symmetry to yield pores as shown in Figure 3.12. Thus, molecular tectonics offer a very powerful tool and will continue to be a prolific source of new crystalline materials with predictable structural features and properties.<sup>19</sup>

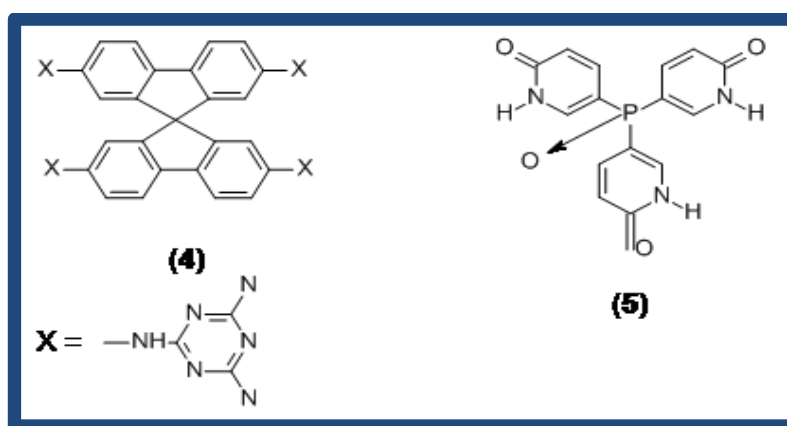


**Figure 3.11.** The molecular structures of the compounds **4** and **5**.

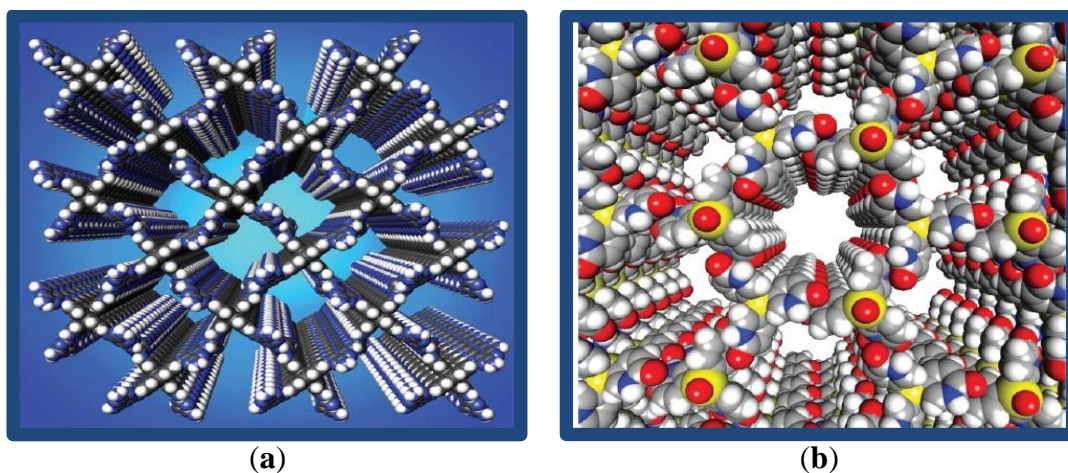


**Figure 3.12.** (a) The porous network constructed by crystallizing **4**. (b) The porous network constructed by crystallizing trigonal tecton **5**. In both the networks guests are omitted for clarity purpose.

Moorthy and co-workers have shown the significance of the position of functional groups, such as hydroxyl and carboxylic groups, on a given substrate such as 3,3',5,5'-tetraphenylbimesityl towards the formation of host-guest complex. The crystallization of tetrakis(4-hydroxyphenyl)bimesityl (Figure 3.13) from solution of ethanol gives a complex, in which the molecules are self-assembled through O-H...O hydrogen bonds to produce a hydrogen bonded “pseudo helical spine”.<sup>20</sup>

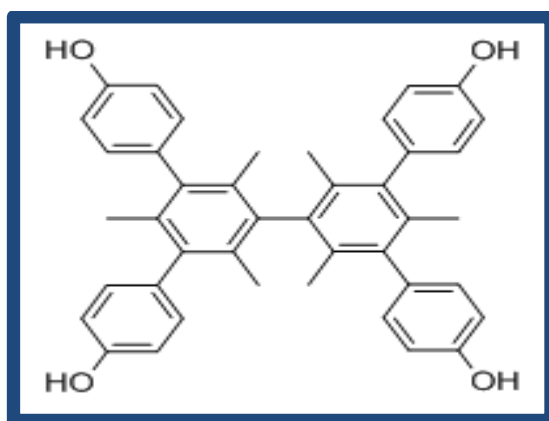


**Figure 3.13.** The molecular structure of tetrakis(4-hydroxyphenyl)bimesityl.

Further such parallel helices are interconnected through C-H...O hydrogen bonds to form porous channels, Figure 3.14. The channels thus obtained are occupied by ethanol molecules, (Figure 3.15).

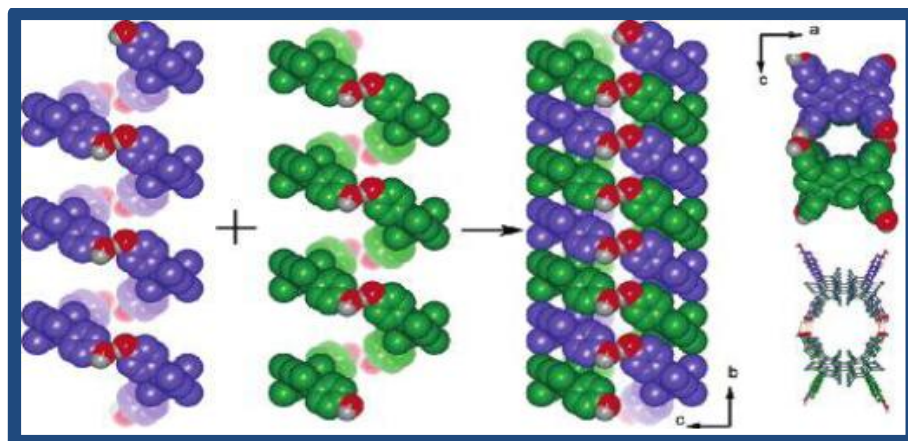


**Figure 3.14.** Formation of a porous channel from two parallel helices generated each by the self-assembly of the given molecules via O-H $\cdots$ O hydrogen bonds.

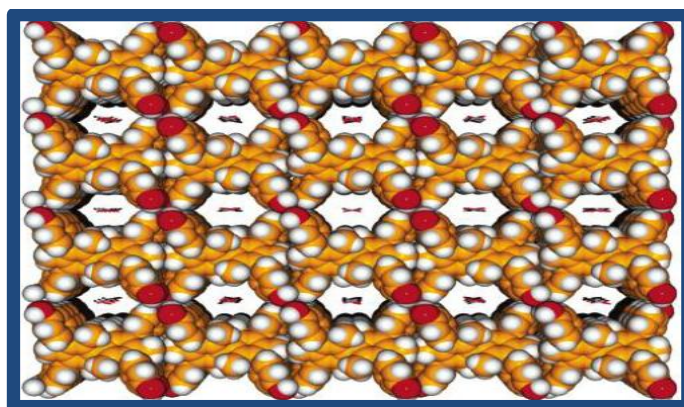


**Figure 3.15.** The channels formed by the aggregation of helices, which are occupied by molecules of ethanol.

Harris and co-workers have shown the capacity of host formed by urea or thiourea for the inclusion of guest, such as hexadecane or 1-bromoadamantane.<sup>21</sup> The channels obtained by the self aggregation of molecules of thiourea are large than those formed by molecules of urea. Thus, the urea and thiourea hosts tend to incorporate different types of guest molecules, Figures 3.16 and 3.17. It is noted



that the urea host is stable only when the channels are occupied by dense molecules.

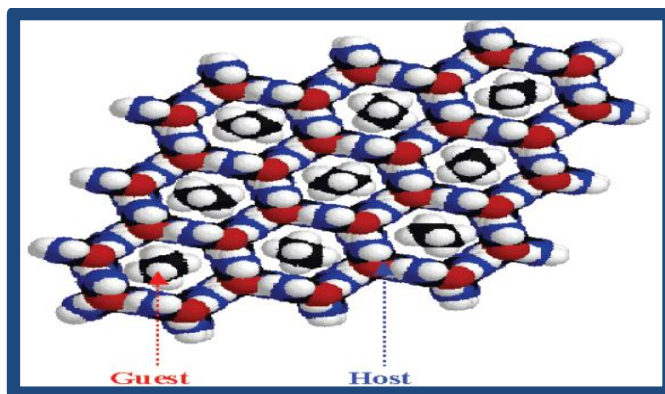


**Figure 3.16.** Structure of host-guest complex formed by molecules of urea (host) and hexadecane (guest).

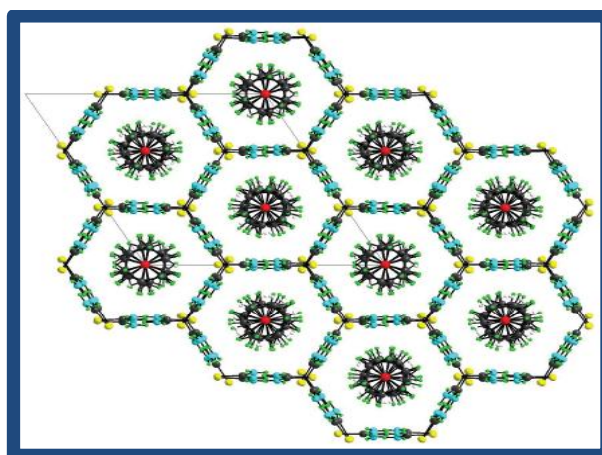


**Figure 3.17.** The structure of host-guest complex formed by inclusion of molecules of 1-bromoadamantane into host which is formed by molecules of urea.

The host networks discussed in the above examples are formed by the aggregation of molecules of one component. However, there are also several hosts which are formed by molecules of two or more components. In this regard, Jones and co-workers demonstrated that the host formed by the molecules of caffeine and

succinic acid (Figure 3.18) is capable to include eighteen different guests such as 1,4-dioxane, 1,4-thioxane, tetrahydropyran, 3,4-dihydropyran, 1,4-dithiane, norbornane, norbornylene, etc.<sup>22</sup>

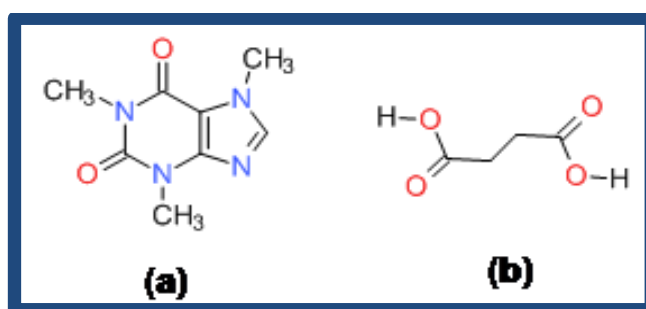


**Figure 3.18.** Molecular structures of components of host (a) caffeine, (b) succinic acid.

Further, they demonstrated the importance of solid state grinding over the solution evaporation method for the preparation of the host-guest complexes and is concluded that, only four host-guest complexes have been obtained by solution evaporation method out of eighteen host guest complexes, which are obtained by solid state grinding of the components.

Similarly, Pedireddi *et al* demonstrated the inclusion ability of host which is obtained from molecules of trithiocyanuric acid and 4,4'-bipyridine (Figure 3.19) towards different guests such as benzene, toluene, *p*-xylene, anthracene, etc..<sup>23</sup> The host networkers are stacked in the crystals through  $\pi \cdots \pi$  interaction. Such stacking results into channels which are occupied by the guest molecules. The guest molecules are removed from the channels by thermal treatment and the apohost is found to be thermally stable, which shows selective inclusion of *p*-xylene as guest out of its mixture with *m*-, *o*-xylene and mesitylene.



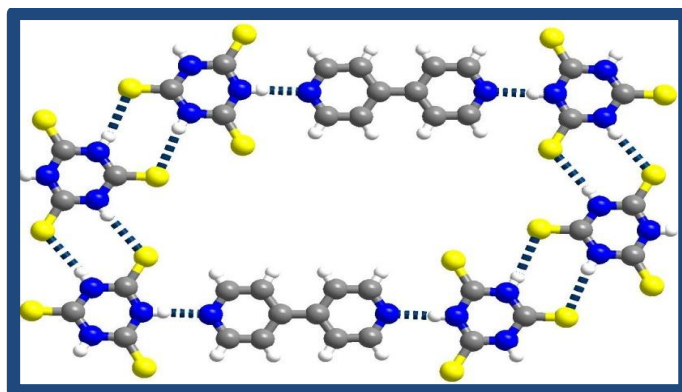


**Figure 3.19.** The host formed by aggregation of trithiocyanuric acid and 4,4'-bipyridine through N-H...N and N-H...S hydrogen bonds. Guest moieties are removed for clarity purpose.

Further, Pedireddi and co-workers reported numbers of host guest complex through co-crystallization of 2,4-diamino-6-methyl-1,3,5-triazine (**DMT**) with different carboxylic acids such as oxalic, malonic, succinic, fumaric, acetylene dicarboxylic, glutaric, thiodiglycolic, diglycolic and adipic acid.<sup>24</sup> These complexes showed two types of host guest networks. The different types of host-guest networks appear to be resulted from differences in the acidity of the dicarboxylic acids. The acids with  $pK_a$  less than 3.0 give host networks that consist of only **DMT**, and the host is occupied by the acids as guests, (Figure 3.20a). But the acids having  $pK_a$  more than 3.0, host is being constituted by both **DMT** and the acid molecules, (Figure 3.20b). The host is occupied by molecules of solvent of crystallization.

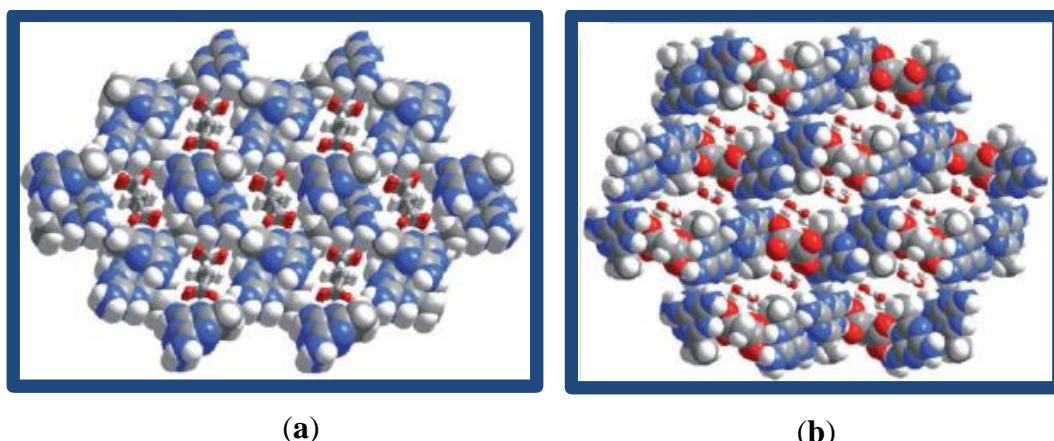


**Figure 3.20.** (a) Host guest network observed in complex **DMT**-succinic acid, with the host is being formed by the molecules of **DMT**, and succinic acid molecules occupies these host networks. (b) Host guest network observed in complex **DMT**-malonic acid, with the host networks are being filled by water molecules.

Thus, host-guest structures with host itself being mediated by noncovalent interactions, in particularly through hydrogen bonds, formed between multiple components, emerged as novel and frontier area of research in the studies of organic materials. To explore further through exotic and novel examples and at the same time, keeping the focus towards evaluation of adamantanedicarboxylic acids mediated assemblies, studies are directed to prepare co-crystals of 1,3-adamantanedicarboxylic acid with rigid aza-donor compounds. Hence, co-crystallization of acid **1** with 4,7-phenanthroline has been carried out.

### 3.2 Structure of 1,3-adamantanedicarboxylic acid and 4,7-phenanthroline with water:

1,3-adamantanedicarboxylic acid (**1**) and 4,7-phenanthroline (**phen**) upon co-crystallization from MeOH/H<sub>2</sub>O solution gave co-crystals in a 1:1 ratio of the co-formers along with water molecules. The asymmetric unit, in the form of an ORTEP, is shown in Figure 3.21. The pertinent crystallographic details are given in Table 3.1.

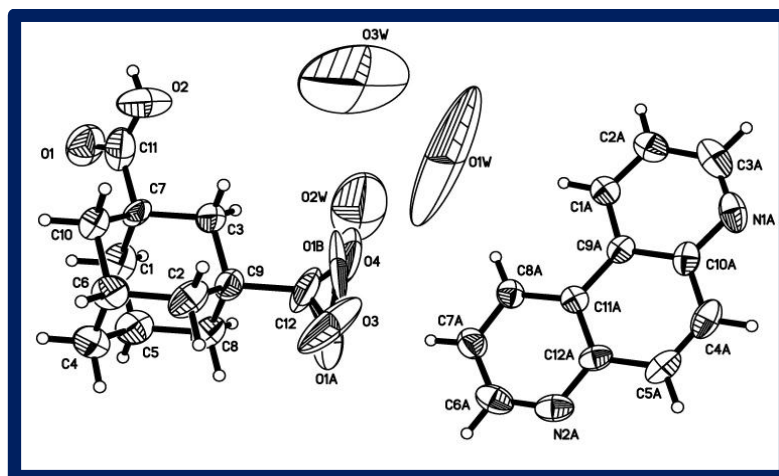


**Figure 3.21.** ORTEP of the components in the asymmetric unit of the co-crystals.

The co-crystal components interact with each other such that two of each of acid **1** and phenanthroline form a quartet molecular assembly, through a pair-wise hydrogen bonding pattern, comprising of O-H $\cdots$ N/C-H $\cdots$ O hydrogen bonds. The arrangement is shown in Figure 3.22. Thus, a void space of dimension 7 x 8 Å<sup>2</sup> is realized in two-dimensional geometry. The ensembles however are stacked along a crystallographic axis such that the voids are aligned to constitute channels, which are being occupied by water molecules. Such channel structure is depicted in Figure 3.23.

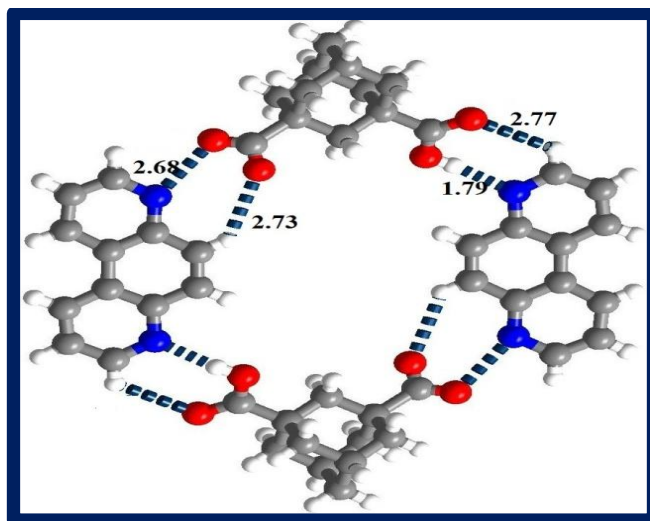


**Figure 3.22.** An ensemble of quartet molecules obtained by the aggregation of two of each molecule of **1** and **phen** through a pair-wise hydrogen bonding patterns, in the crystals.

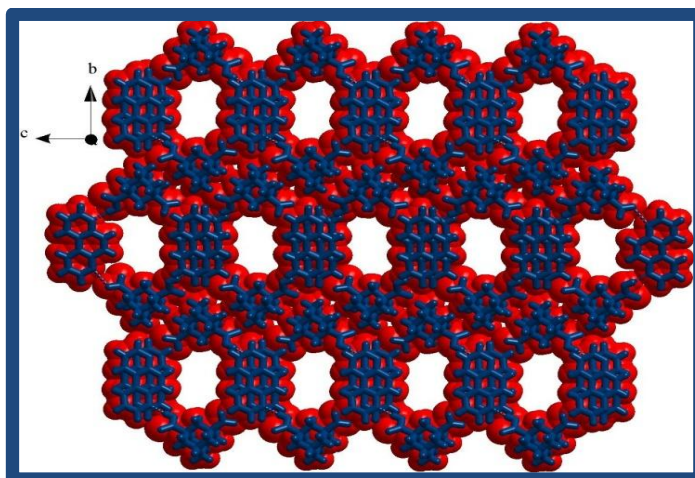
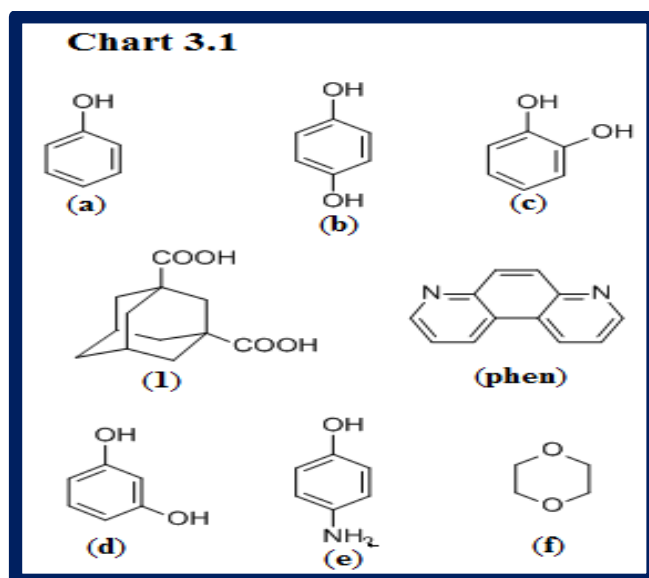


**Figure 3.23.** Packing of molecules in three-dimensional arrangement, with channels being occupied by water molecules, in the structure of co-crystals. The guest molecules are removed for clarity.

Indeed, such structures are in general capable of exchanging of guest species within the channels, provided the guest species are capable of establishing

appropriate intermolecular interactions with the host ensembles and also match with the cavity dimension. To explore the feasibility of incorporating other guest molecules within the host, co-crystallization of 1,3-adamantanedicarboxylic acid (**1**) and 4,7-phenanthroline (**phen**) in the presence of various hydrogen bond donor and acceptor compounds such as phenol (**a**), 1,4-dihydroxybenzene (**b**), 1,2-dihydroxybenzene (**c**), 1,3-dihydroxybenzene (**d**), 4-aminophenol (**e**) and 1,4-dioxane (**f**), have been carried out, Chart 3.1.



### 3.3 Host Guest Complex of 1,3-Adamantanedicarboxylic Acid and 4,7-Phenanthroline with Phenol:

Co-crystallization of 1,3-adamantanedicarboxylic acid (**1**) and 4,7-phenanthroline (**phen**) in presence of phenol (**a**), gave good quality single crystals from a solution of dimethylsulfoxide (**DMSO**). The obtained crystals are characterized by X-ray diffraction methods. The structural analysis by single crystal X-ray diffraction method reveals that, the crystal is composed of molecules of 1,3-adamantanedicarboxylic acid, 4,7-phenanthroline and a phenol in disordered orientation, with the constituents in the asymmetric unit in a 1:1:0.5 ratio, respectively. The co-crystals are labeled as **1a**, for the ease of further discussion. The ORTEP diagram is shown in Figure 3.24. The complete crystallographic details are given in Table 3.1.

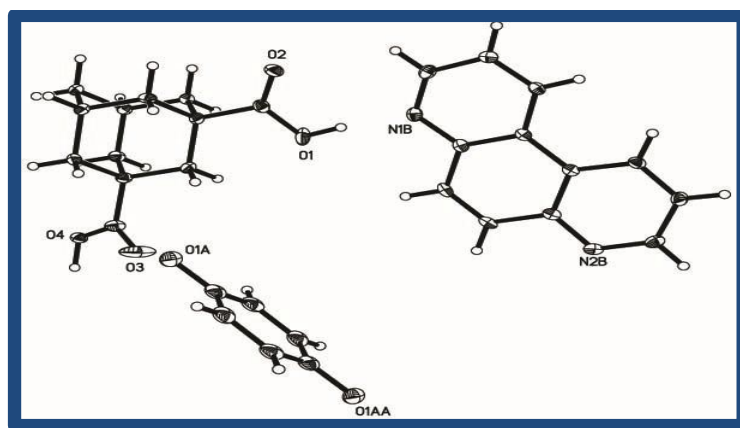


**Figure 3.24.** ORTEP drawing of the constituents in the asymmetric unit of the complex **1a**.

Structural analysis of **1a** shows that two of each molecules of **1** and **phen** are assembled through a pair-wise  $R_2^2(7)$  and  $R_2^2(8)$  hydrogen bonding patterns in a

cyclic four-membered network yielding void, as anticipated, with the network being as similar as found for the complex of **1** and **phen** with water, such arrangement is shown in Figure 3.25. Complete characteristics of hydrogen bonds for these patterns are listed in Table 3.3.

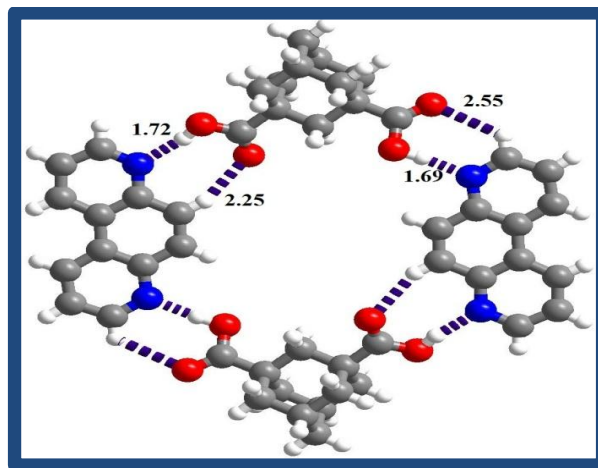


**Figure 3.25.** Host network formed by **1** and **phen**, in the presence of phenol in the complex **1a**.

Such networks are stacked along a crystallographic direction through  $\pi \cdots \pi$  interactions in the crystal lattice of **1a**. In such an arrangement, due to the alignment of voids present within the two-dimensional arrangement, one-dimensional channels are realized in the three-dimensional packing of molecules in the crystal lattice of **1a** resembling the observation made in the previous structure with water. The packing is shown in Figure 3.26a. Within these channels, phenol molecules are embedded, as shown in Figure 3.26b.



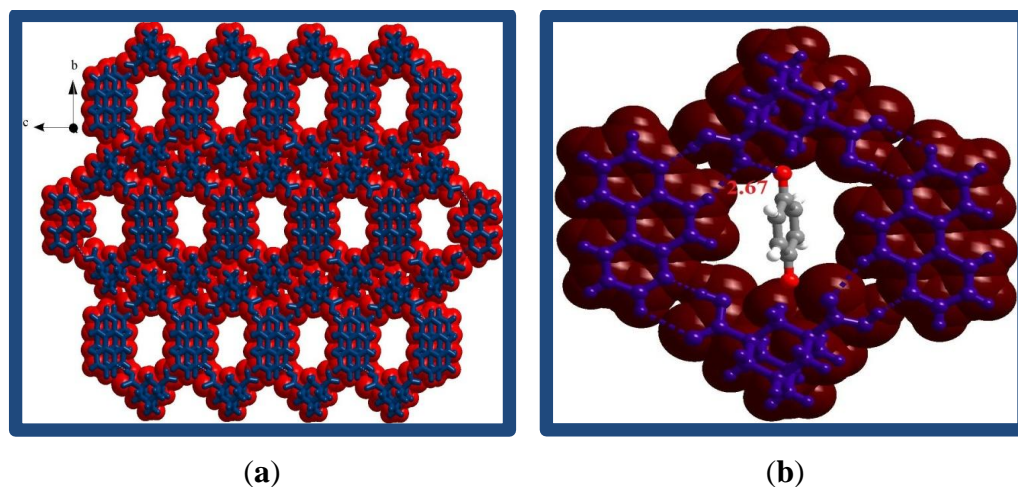


**Figure 3.26.** (a) Channels observed in crystal lattice of **1a**. (b) Presentation of guest species in the channels formed in **1a**.

Taken into account the disorder nature of phenol, in the crystal lattice, hydroquinone (1,4-dihydroxybenzene), perhaps may also able to form a host-guest complex as noted in **1a**.

### 3.4 Host Guest Complex of 1,3-Adamantanedicarboxylic Acid and 4,7-Phenanthroline with Hydroquinone (1,4-Dihydroxybenzene):

Co-crystallization of 1,3-adamantanedicarboxylic acid (**1**) and 4,7-phenanthroline (**phen**) with 1,4-dihydroxybenzene (**b**) from solution of dimethylsulfoxide (**DMSO**) gave good quality single crystals, which are characterized by X-ray diffraction methods. The structural analysis reveals that, the crystal is composed of molecules of **1**, **phen** and **b**, with the constituents in the asymmetric unit in a 1:1:0.5 ratio, respectively. The ORTEP diagram is shown in Figure 3.27. The complete crystallographic details are given in Table 3.1.



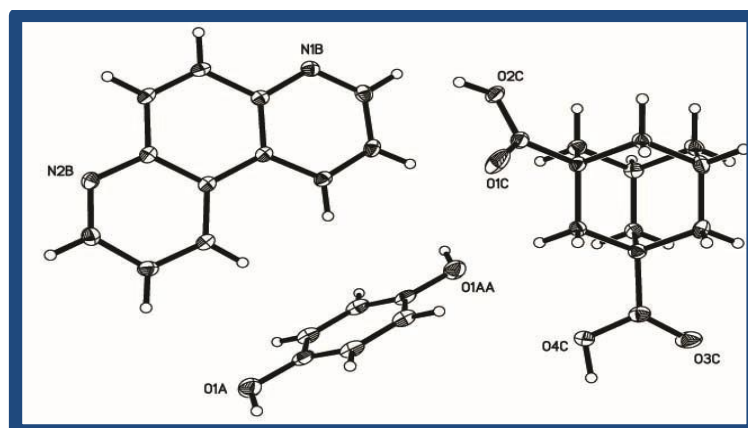


**Figure 3.27.** ORTEP of the constituents in the asymmetric unit of the complex **1b**.

Packing analysis of **1b** confirmed that, in this structure also two of each molecules of **1** and **phen** are assembled through a pair-wise  $R_2^2(7)$  and  $R_2^2(8)$  hydrogen bonding patterns in a cyclic four-membered network, like in **1a**, except for the hydrogen bond distances. The arrangement is shown in Figure 3.28. Complete characteristics of hydrogen bonds for these patterns are listed in Table 3.3.

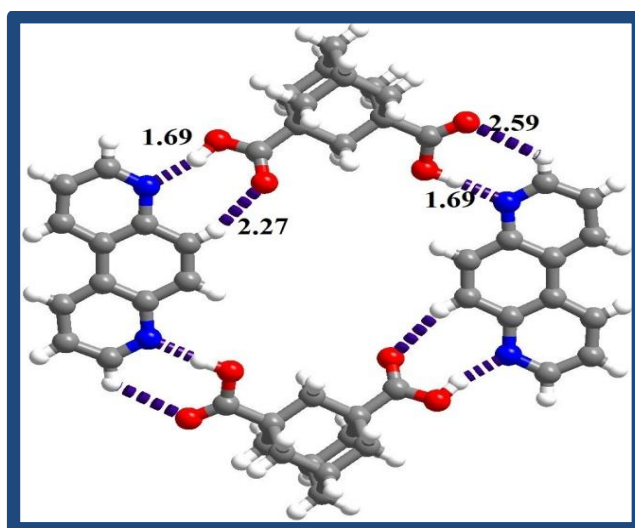


**Figure 3.28.** Host network formed by the aggregation of molecules of **1** and **phen**.

As expected, the ensembles are stacked, creating channels (Figure 3.29a) in which, hydroquinone molecules are embedded as guest species. In contrast to the nature of guest, phenol, in **1a**, hydroquinone is fully ordered in the structure of **1b**. In fact, due to such ordered nature, the interaction of hydroquinone with host network through O-H $\cdots$ O hydrogen bonding could be well resolved as shown in Figure 3.29b.

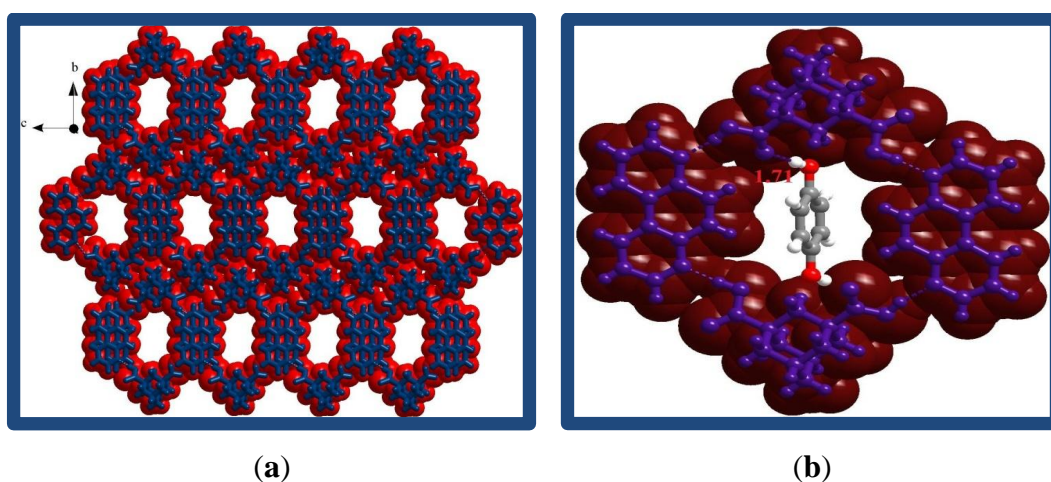


**Figure 3.29.** (a) Channels in the crystal lattice of **1b**. (b) Representation of guest species in the channels observed in the crystal structure of **1b**. [Notice the hydrogen bonding between the host and guest species.]

To study further, varying the value of the guest substrate for the evaluation of selective binding properties, co-crystallization of **1** and **phen** is carried out with catechol and resorcinol, the isomers of hydroquinone.

### 3.5 Host Guest Complex of 1,3-Adamantanedicarboxylic Acid and 4,7-Phenanthroline with Catechol (1,2-Dihydroxybenzene):

1,3-adamantanedicarboxylic acid (**1**) and 4,7-phenanthroline (**phen**) with catechol (**c**) gave good quality single crystals from a solution of dimethylsulfoxide (**DMSO**). The obtained crystals are characterized by X-ray diffraction methods. The crystals are composed of molecules of 1,3-adamantanedicarboxylic acid, 4,7-phenanthroline and 1,2-dihydroxybenzene in a 2:2:1 ratio, respectively. The ORTEP of the asymmetric unit is shown in Figure 3.30. The complete crystallographic details are given in Table 3.1.

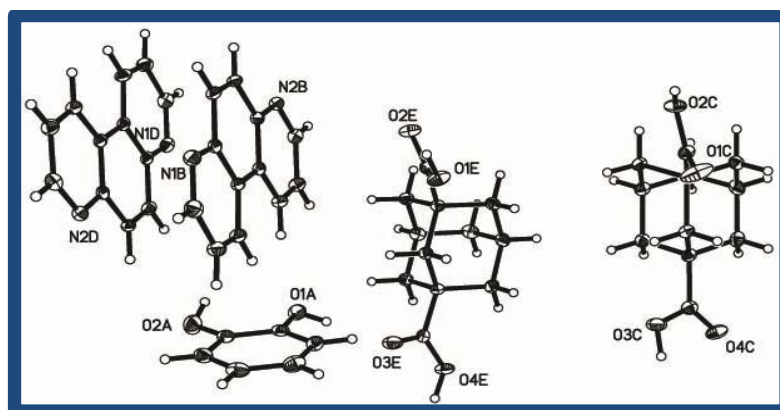


**Figure 3.30.** Asymmetric unit observed in the crystal structure of **1c**.

In the structure of **1c** also, as observed in **1a** and **1b**, two of each molecules of **1** and **phen** are assembled through a pair-wise  $R_2^2(7)$  and  $R_2^2(8)$  hydrogen bonding patterns. The network is depicted in Figure 3.31. Complete characteristics of hydrogen bonds for these patterns are listed in Table 3.3.

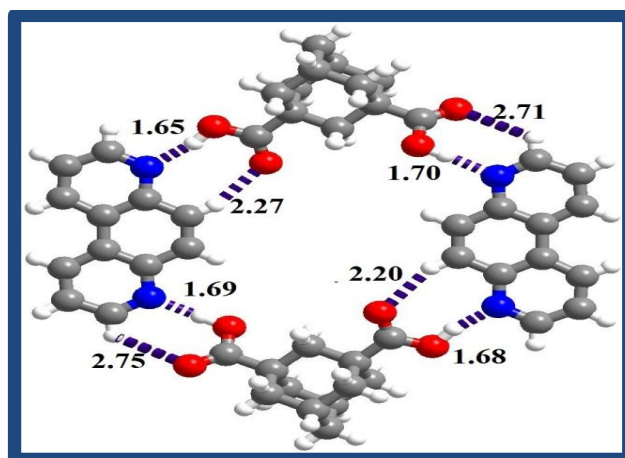


**Figure 3.31.** Host network formed by the aggregation of molecules of **1** and **phen**.

Without any deviation as observed in **1a** and **1b**, the ensembles are stacked, yielding channels in three-dimensional arrangement, as shown in Figure 3.32(a). Catechol molecules, as guest species, occupied the channels as represented in Figure 3.32(b), interacting with the host lattice by O-H $\cdots$ O hydrogen bonding.

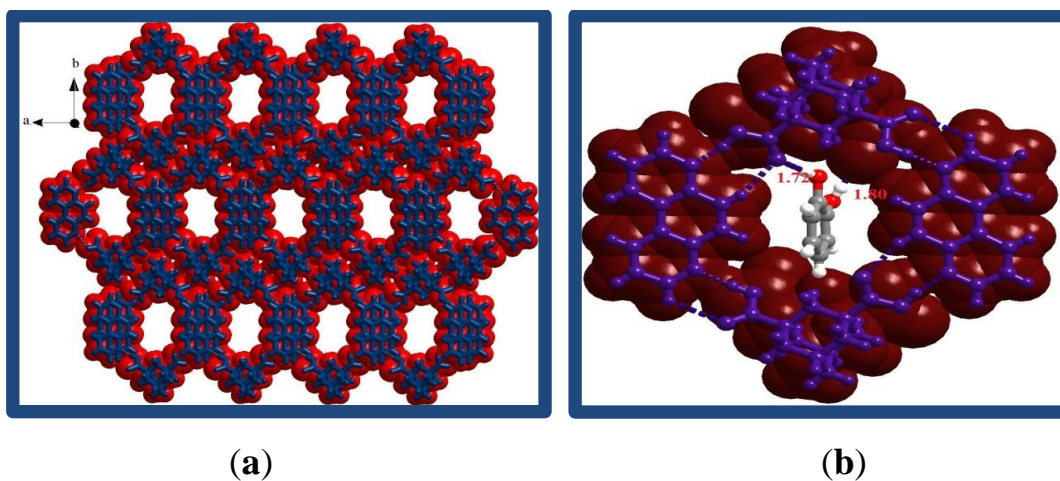


**Figure 3.32.** (a) Channels observed in crystal lattice of **1c**. (b) Presentation of guest species in the channels formed in **1c**.

Thus, it may be concluded that selectivity between the isomers catechol and hydroquinone could not be established by the host lattice. Also further experiment with resorcinol is proved to be the same.

### 3.6 Host Guest Complex of 1,3-Adamantanedicarboxylic Acid and 4,7-Phenanthroline with Resorcinol (1,3-Dihydroxybenzene), **1d**:

Acid **1** and 4,7-phenanthroline with 1,3-dihydroxybenzene (**d**), from DMSO solution gave good quality single crystals, suitable for structural determination by single crystal X-ray diffraction method. The characterization reveals that, the crystals are of 2:2:1 ratio of molecules of acid **1**, phenanthroline and resorcinol, respectively. An asymmetric unit of crystals of **1d** is shown in Figure 3.33. The complete crystallographic details are given in Table 3.2.

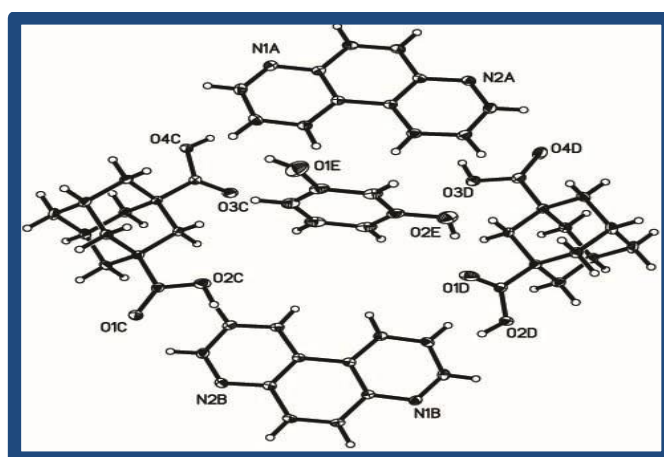


**Figure 3.32.** ORTEP of the components of crystals of **1d**.

Structural analysis reveals that, packing of molecules in **1d** is as same as observed in **1b-1d**, without any appreciable deviations. Thus, molecules of **1** and phenanthroline form a quartet molecular cyclic network, a pair-wise hydrogen bonding patterns, as depicted in Figure 3.33. Complete characteristics of hydrogen bonds for these patterns are listed in Table 3.3.

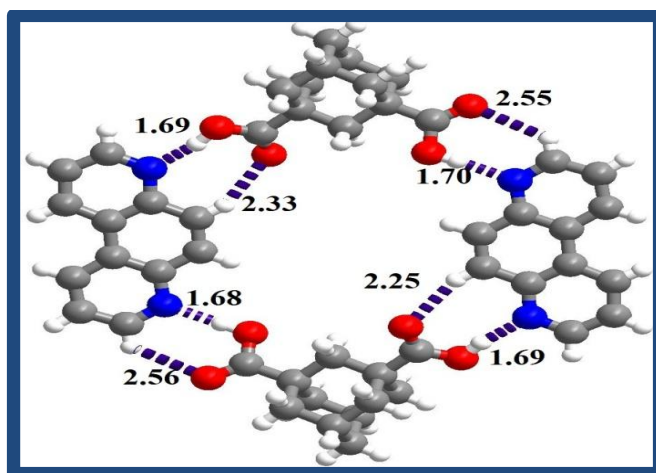


**Figure 3.33.** Cyclic network formed by acid **1** and phenanthroline in the complex **1d**.

Such ensembles are aligned along a crystallographic direction yielding channels, as represented in Figure 3.34(a). The channels are filled up by guest species, resorcinol, establishing O-H $\cdots$ O hydrogen bonds with host networks, (see Figure 3.34(b)).

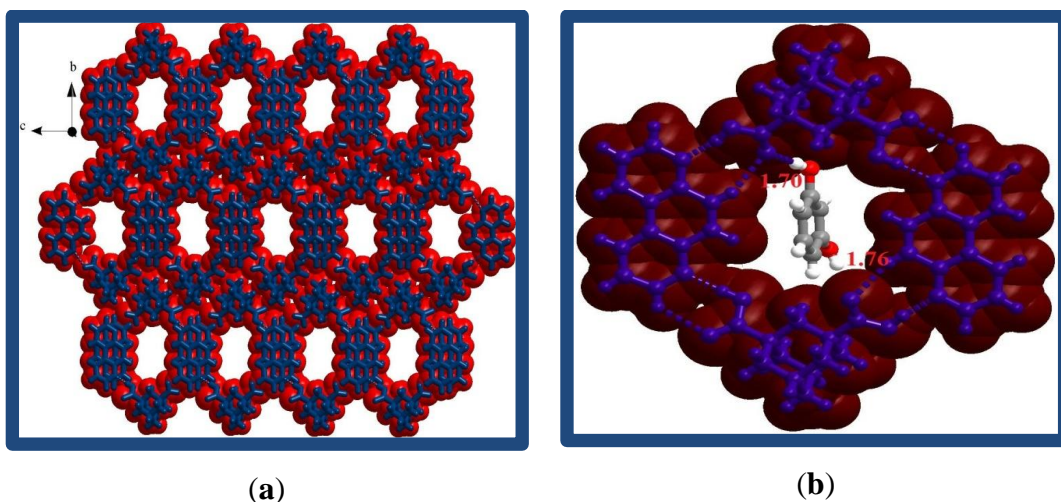


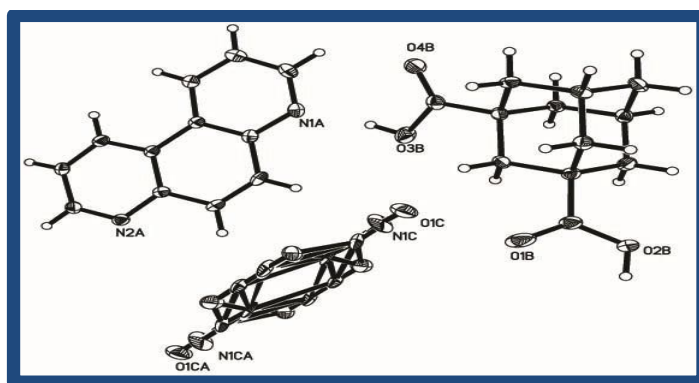
**Figure 3.34.** (a) Channels in the structure of **1e**. (b) A typical channel with guest species, resorcinol.



As selectivity of guest is not being established for isomers of dihydroxybenzene, experiments are further directed towards guest species of multifunctional moieties to understand the rigidity of the host network observed in the earlier structures. Thus, co-crystallization of **1** and phenanthroline has been carried out with 4-aminophenol (**e**).

### 3.7 Host Guest Complex of 1,3-Adamantanedicarboxylic Acid and 4,7-Phenanthroline with 4-Aminophenol, **1e**:

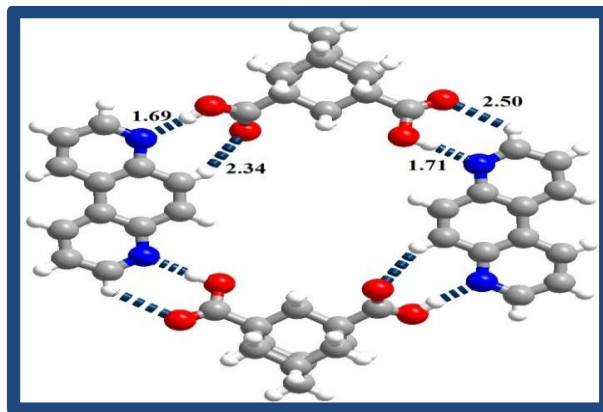
Crystals obtained from a solution of DMSO have been characterized by X-ray diffraction methods. The analysis reveals that, the crystals are composed of molecules of **1**, phenanthroline and 4-aminophenol in a 1:1:0.5 ratio, respectively. The ORTEP diagram of an asymmetric unit is shown in Figure 3.35. The complete crystallographic details are given in Table 3.2.



**Figure 3.35.** An asymmetric unit of the complex **1e**.

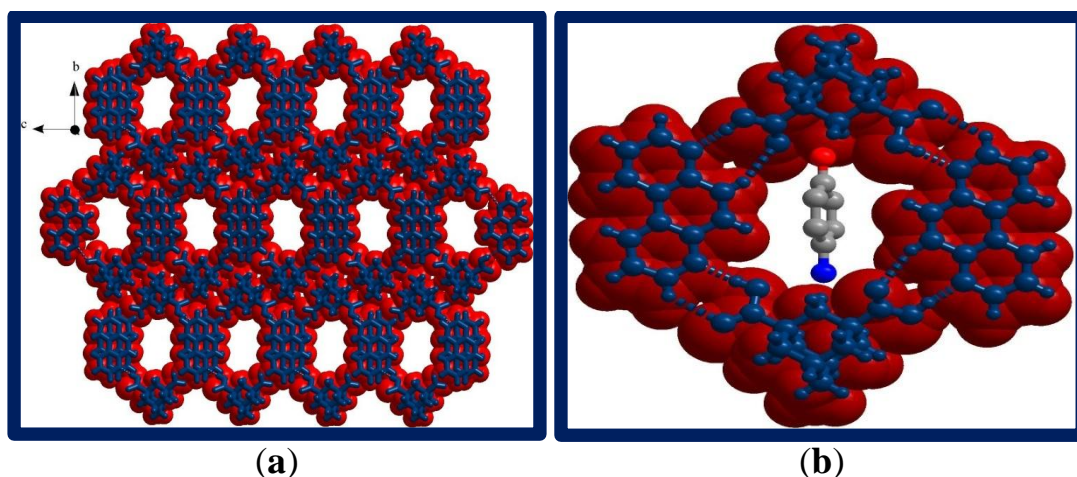
Further structural analysis of **1e** shows that, even in presence of multifunctional guest species, two of each molecules of **1** and phenanthroline are assembled through a pair-wise  $R_2^2(7)$  and  $R_2^2(8)$  hydrogen bonding patterns, in a cyclic four-membered network, like in **1a-1d**. The observed network is shown in

Figure 3.36. Complete characteristics of hydrogen bonds for these patterns are listed in Table 3.3.



**Figure 3.36.** The four-membered cyclic network formed by the aggregation of molecules of **1** and phenanthroline, crystal lattice of **1e**.

In addition, along a crystallographic direction, stacking of the ensembles, is also followed the same observation found **1a-1d**. However, channels as shown in Figure 3.37(a) are occupied by molecules of 4-aminophenol. Guest occupied typical channel is shown in Figure 3.37(b).



**Figure 3.37.** (a) Three-dimensional arrangement in the crystal structure of **1e** with channels. (b) The interaction of guest molecules with the host network.



In the above examples discussed so far, the guest species possesses hydrogen bond donor functional groups, and found to be yielding the channel structures irrespective of strength of hydrogen bond and dimensionality of guest molecules. In order to extend the study by changing the nature of the guest with only hydrogen bond acceptor, co-crystallization experiment in presence of 1,4-dioxane have been carried out.

### 3.8 Host Guest Complex of 1,3-Adamantanedicarboxylic Acid and 4,7-Phenanthroline with 1,4-Dioxane, **1f**:

The co-crystals obtained from 1,4-dioxane solution of **1** and phenanthroline are analysed by single crystal X-ray diffraction method. The analysis reveals that, the crystals are composed of molecules of **1** and phenanthroline in a 1:1 ratio along with 1,4-dioxane. An asymmetric unit in the form of ORTEP is shown in Figure 3.38. Complete crystallographic details are given in Table 3.3.

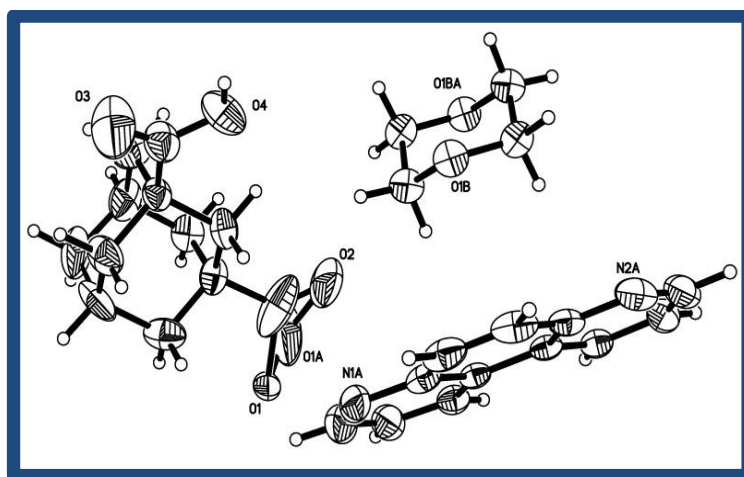
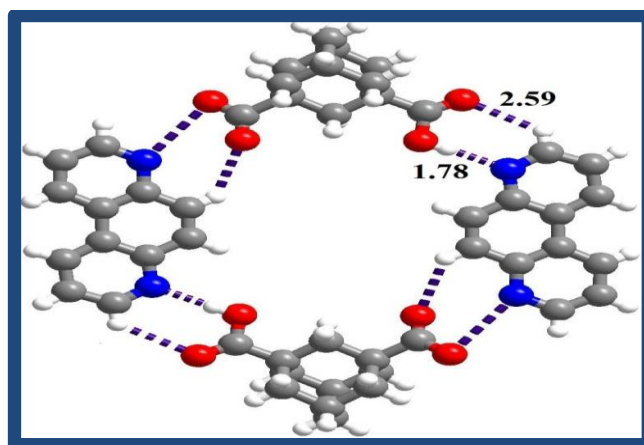


Figure 3.38. ORTEP of an asymmetric unit in the complex **1f**.

Crystal structure analysis shows that two of each molecules of **1** and phenanthroline are assembled through a pair-wise  $R_2^2(7)$  and  $R_2^2(8)$  hydrogen bonding patterns in a cyclic four-membered network with a void space of dimension  $7 \times 8 \text{ \AA}^2$  like in **1a-1f**, as depicted in Figure 3.39. Complete characteristics of hydrogen bonds for these patterns are listed in Table 3.3.



**Figure 3.39.** Host network in complex **1f**.

The void space in the obtained network is occupied by a molecule of guest (**f**) which exactly fits in to it. This arrangement is not observed in the complexes **1a-1e** as the guest is present in between consecutive networks. Further, such host networks, however, extend in three-dimensional arrangement stabilized by  $\pi \cdots \pi$  interactions, as shown Figure 3.40(a). Thus, in **1f**, the ensembles are stacked by sliding of the voids being occupied by 1,4-dioxane molecules. Such an arrangement is shown in Figure 3.40(b).

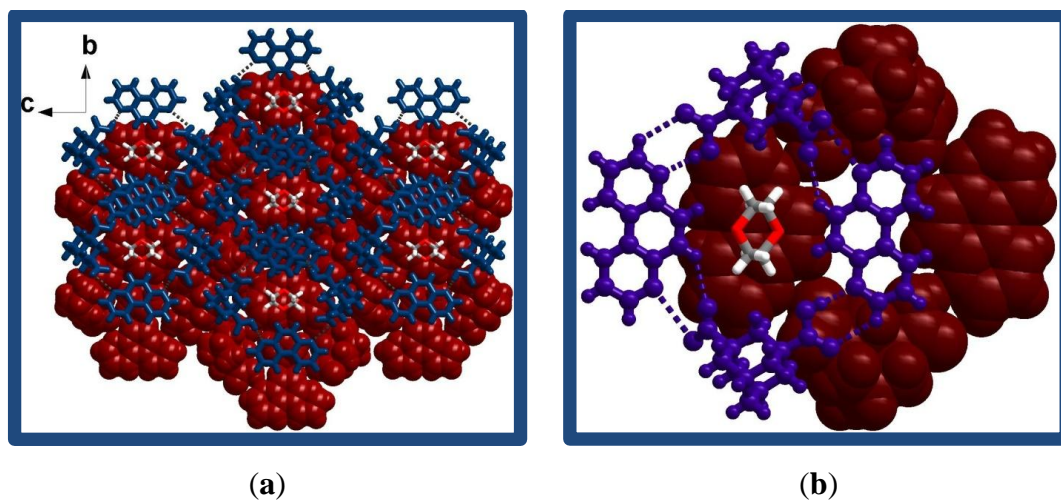


**Figure 3.40.** (a) Packing of layers in crystal lattice of **1f**. (b) Typical interaction of guest with the adjacent layer.

Thus, in the structure of **1f**, although the voids are embedded with guest species, in the ultimate three dimensional packing, the structure adopts, simply a layered packing.

### 3.9 Conclusions

In conclusion, host-guest complexes of 1,3-adamantanedicarboxylic acid, **1**, and 4,7-phenanthroline as a host have been prepared by co-crystallization of the acid **1** and phenanthroline in the presence of various guest species of variable acceptor and donor property like phenol, hydroquinone, catechol, resorcinol, 4-aminophenol and dioxane. In all the complexes, the molecules of **1** and phenanthroline formed a four-membered cyclic network through hydrogen bonds, with voids, which are aligned in three-dimensional packing, thus, creating channels, which are being occupied by the guest species in the structure of **1a-1f**. However, in the structure **1f**, the voids, although being filled by guest species, in the three-dimensional arrangement, due to sliding of layers along the stacking

direction, the guest species are obscured from other molecules from the adjacent layers leading to the formation of channels. Thus, structure of **1f** remains simply as a layered structure.

### 3.10 Experimental Section

#### 3.10.1 Synthesis of Co-crystals of water adduct and **1a-1f**

All chemicals used in this study were obtained from Sigma Aldrich and used as such without any further purification. The solvents employed for the co-crystallization purpose were of spectroscopy grade of highest available purity. Co-crystals of have been prepared by slow evaporation of DMSO solutions of 1,3-adamantanedicarboxylic acid (**1**), 4,7-phenanthroline and corresponding guest species in 1:1:1 ratio. However, crystals of **1a** and **1f** are prepared from MeOH/H<sub>2</sub>O and 1,4-dioxane solution of **1** and phenanthroline in 1:1 ratio, respectively. Single crystals of good quality were obtained over a period of 12 h, which are used for characterization by single crystal X-ray diffraction method.

#### 3.10.2 X-ray Structure Determination

Good quality single crystals of water hydrate and **1a-1f** are carefully selected using Leica microscope and glued to a glass fibre using an adhesive (cyanoacrylate). In all the cases, the crystals were smeared in the adhesive solution to prevent decomposition of crystals. The intensity data were collected on a Bruker single-crystal X-ray diffractometer, equipped with an APEX detector. Subsequently, the data were processed using the Bruker suite of programs (SAINT),

and the convergence was found to be satisfactory with good  $R_{\text{ini}}$  parameters.<sup>25</sup> The details of the data collection and crystallographic information are given in Table 1. Absorption corrections were applied using SADABS package.<sup>25</sup> The structure determination by direct methods and refinements by least-squares methods on  $F^2$  were performed using the SHELXTL-PLUS package. The processes were smooth without any complications. All non-hydrogen atoms were refined anisotropically, while hydrogen atoms are treated isotropically. All the intermolecular interactions were computed using PLATON.<sup>26</sup> All packing diagrams are generated using Diamond software.<sup>27</sup>

**Table 3.1.** Crystallographic data and structure refinement parameters for the co-crystals **1a-1d**.

	1.phen.H <sub>2</sub> O	1a	1b	1c
formula	C <sub>12</sub> H <sub>15</sub> O <sub>4</sub> :C <sub>12</sub> H <sub>8</sub> N <sub>2</sub> :3H <sub>2</sub> O	C <sub>12</sub> H <sub>16</sub> O <sub>4</sub> :C <sub>12</sub> H <sub>8</sub> N <sub>2</sub> :0.5(C <sub>6</sub> H <sub>4</sub> O)	C <sub>12</sub> H <sub>16</sub> O <sub>4</sub> :C <sub>12</sub> H <sub>8</sub> N <sub>2</sub> :0.5(C <sub>6</sub> H <sub>6</sub> O <sub>2</sub> )	C <sub>12</sub> H <sub>16</sub> O <sub>4</sub> :C <sub>12</sub> H <sub>8</sub> N <sub>2</sub> :C <sub>6</sub> H <sub>6</sub> O <sub>2</sub>
formula wt	451.44	450.50	459.51	919.01
crystal system	monoclinic	triclinic	triclinic	monoclinic
space group	<i>P</i> 2 <sub>1</sub> / <i>c</i>	<i>P</i> $\bar{1}$	<i>P</i> $\bar{1}$	<i>P</i> 2 <sub>1</sub> / <i>c</i>
<i>a</i> /Å	6.899(1)	6.603(5)	6.632(3)	11.081(5)
<i>b</i> /Å	30.620(5)	11.176(3)	11.162(6)	29.945(1)
<i>c</i> /Å	12.598(2)	15.867(4)	15.860(8)	13.34(5)
<i>α</i> <sup>o</sup>	90	107.52(3)	107.18(7)	90
<i>β</i> <sup>o</sup>	119.82(6)	97.80(4)	97.52(7)	95.50(7)
<i>γ</i> <sup>o</sup>	90	95.45(4)	95.98(7)	90
<i>V</i> /Å <sup>3</sup>	2309.2(6)	1094.8(4)	1099.4(1)	4406(3)
<i>Z</i>	4	2	2	4
<i>D</i> <sub>c</sub> /g cm <sup>-3</sup>	1.160	1.367	1.388	1.385
<i>μ</i> /mm <sup>-1</sup>	0.080	0.094	0.096	0.096
2θ range[°]	50.06	50.58	50.58	50.70
<i>T</i> /K	120	120	120	120
<i>F</i> (000)	852	476	486	1944
<i>λ</i> /Å	0.71073	0.71073	0.71073	0.71073
$\Delta\rho_{\min.\max}/e \text{ \AA}^{-3}$	-0.287, 0.314	-0.466, 0.804	-0.287, 0.393	-0.395, 0.400
total reflections	16563	10729	10695	22282
unique reflections	4071	3970	3974	7985
reflections used	1438	3553	3553	6873
no. of parameters	290	315	323	613
<i>R</i> <sub>1</sub> , <i>I</i> > 2σ( <i>I</i> )	0.0962	0.0440	0.0401	0.0751
<i>wR</i> <sub>2</sub> , <i>I</i> > 2σ( <i>I</i> )	0.2203	0.1156	0.1088	0.2008

**Table 3.2.** Crystallographic data and structure refinement parameters for the co-crystals **1e–1g**.

	<b>1d</b>	<b>1e</b>	<b>1f</b>
formula	$C_{12}H_{16}O_4:C_{12}H_8N_2$ :C <sub>6</sub> H <sub>6</sub> O <sub>2</sub>	$C_{12}H_{16}O_4:C_{12}H_8N_2$ :0.5(C <sub>6</sub> H <sub>7</sub> ON)	$C_{12}H_{16}O_4:C_{12}H_8N_2$ :0.5(C <sub>4</sub> H <sub>8</sub> O <sub>2</sub> )
formula wt	919.01	455.49	447
crystal system	triclinic	triclinic	orthorhombic
space group	<i>P</i> $\bar{1}$	<i>P</i> $\bar{1}$	<i>Pbca</i>
<i>a</i> /Å	6.682(2)	6.671(1)	12.095(2)
<i>b</i> /Å	16.442(6)	11.104(2)	11.374(2)
<i>c</i> /Å	22.078(8)	16.027(3)	32.606(6)
<i>α</i> <sup>o</sup>	68.80(5)	107.93(3)	90
<i>β</i> <sup>o</sup>	87.00(6)	98.30(3)	90
<i>γ</i> <sup>o</sup>	78.68(5)	95.49(3)	90
<i>V</i> /Å <sup>3</sup>	2216.8(1)	1105.2(3)	4485.6(1)
<i>Z</i>	2	2	8
<i>D</i> <sub>c</sub> /g cm <sup>-3</sup>	1.377	1.369	1.325
<i>μ</i> /mm <sup>-1</sup>	0.095	0.094	0.092
2 <i>θ</i> range[°]	50.46	50.66	50.06
<i>T</i> /K	120	120	293
<i>F</i> (000)	972	479	1896
<i>λ</i> /Å	0.71073	0.71073	0.71073
$\Delta\rho_{\min.\max}/e \text{ \AA}^{-3}$	-0.334, 0.845	0.456, -0.395	-0.255, 0.428
total reflections	21308	10969	21078
unique reflections	7953	3993	3961
reflections used	6544	2946	2621
no. of parameters	629	352	311
<i>R</i> <sub>1</sub> , <i>I</i> > 2σ( <i>I</i> )	0.0615	0.0565	0.0830
<i>wR</i> <sub>2</sub> , <i>I</i> > 2σ( <i>I</i> )	0.1724	0.1572	0.2317

**Table 3.3.** Characteristics of hydrogen bond distances (Å) and angles (°) observed in the co-crystals **1a–1f**.

Complexes	O–H $\cdots$ N			C–H $\cdots$ O			O–H $\cdots$ O		
	H $\cdots$ N	O $\cdots$ N	O–H $\cdots$ N	H $\cdots$ O	C $\cdots$ O	C–H $\cdots$ O	H $\cdots$ O	O $\cdots$ O	O–H $\cdots$ O
<b>1.phen.H<sub>2</sub>O</b>	1.79	2.77	172	2.73	3.61	138			
				2.77	3.40	117			
<b>1a</b>	1.69	2.67	171	2.25	3.25	154			
	1.72	2.68	164	2.55	3.28	124			
<b>1b</b>	1.69	2.66	166	2.27	3.26	152	1.71	2.69	177
	1.69	2.67	175	2.59	3.30	122			
<b>1c</b>	1.65	2.62	165	2.20	3.23	158	1.72	2.71	180
	1.68	2.67	180	2.27	3.28	155	1.80	2.72	155
	1.69	2.67	177	2.71	3.36	118			
	1.70	2.66	166	2.75	3.38	117			
<b>1d</b>	1.69	2.66	168	2.25	3.25	153	1.70	2.68	178
	1.69	2.66	168	2.33	3.36	148	1.76	2.74	1.78
	1.68	2.66	176	2.55	3.28	124			
	1.70	2.68	176	2.56	3.26	121			
<b>1e</b>	1.69	2.66	173	2.34	3.31	148			
	1.71	2.69	173	2.50	3.23	124			
<b>1f</b>	1.78	2.76	177	2.39	3.35	147			
				2.59	3.31	124			
				2.66	3.64	151			



### 3.11 References

1. (a) Yoshizawa, M.; Klosterman, J. K.; Fujita, M. *Angew. Chem., Int. Ed.* 2009, *48*, 3418-3438; (b) Vogtle, F.; Lohr, H. G.; Franke, J.; Worsch, D. *Angew. Chem., Int. Ed.* 1985, *24*, 727-742; (c) Cram, D. J. *Science* 1988, *240*, 760-767.
2. Barthomeuf, D. *Catal. Rev.* 1996, *38*, 521-612.
3. Villiers, A. *Compt. Rend.* 1891, *112*, 536.
4. (a) Szejtli, J. *Chem. Rev.* 1998, *98*, 1743-1753; (b) Douhal, A. *Chem. Rev.* 2004, *104*, 1955-1976; (c) Chankvetadze, B.; Endresz, G.; Blaschke, G. *Chem. Soc. Rev.* 1996, *25*, 141-&.
5. (a) Dondoni, A.; Marra, A. *Chem. Rev.* 2010, *110*, 4949-4977; (b) Atwood, J. L.; Barbour, L. J.; Jerga, A. *Angew. Chem., Int. Ed.* 2004, *43*, 2948-2950.
6. Kim, K.; Selvapalam, N.; Ko, Y. H.; Park, K. M.; Kim, D.; Kim, J. *Chem. Soc. Rev.* 2007, *36*, 267-279.
7. (a) Pedersen, C. J. *J. Am. Chem. Soc.* 1967, *89*, 2495-&; (b) Pedersen, C. J. *J. Am. Chem. Soc.* 1967, *89*, 7017-&.
8. Pedersen, C. J. *Angew. Chem. Int. Ed.* 1988, *27*, 1021-1027.
9. (a) Dietrich, B.; Lehn, J. M.; Sauvage, J. P. *Tetrahedron Lett.* 1969, 2885-&; (b) Dietrich, B.; Lehn, J. M.; Sauvage, J. P. *Tetrahedron Lett.* 1969, 2889-&.
10. Lehn, J. M. *Angew. Chem. Int. Ed.* 1988, *27*, 89-112.
11. Cram, D. J. *Angew. Chem. Int. Ed.* 1988, *27*, 1009-1020.

12. (a) Desiraju, G. R.; Steiner, T., *The Weak Hydrogen Bond: In Structural Chemistry and Biology*. Oxford University Press, Oxford: 2001; (b) Jeffrey, G. A., *An Introduction to Hydrogen Bonding*. Oxford University Press, New York: 1997; (c) Steiner, T. *Angew. Chem., Int. Ed.* 2002, *41*, 48-76.
13. (a) Metrangolo, P.; Meyer, F.; Pilati, T.; Resnati, G.; Terraneo, G. *Angew. Chem. Int. Ed.* 2008, *47*, 6114-6127; (b) Derossi, S.; Brammer, L.; Hunter, C. A.; Ward, M. D. *Inorg. Chem.* 2009, *48*, 1666-1677.
14. Yoshizawa, M.; Klosterman, J. K.; Fujita, M. *Angew. Chem., Int. Ed.* 2009, *48*, 3418-3438.
15. Sozzani, P.; Bracco, S.; Comotti, A.; Ferretti, L.; Simonutti, R. *Angew. Chem., Int. Ed.* 2005, *44*, 1816-1820.
16. Toda, F.; Akagi, K. *Tetrahedron Lett.* 1968, 3695-&.
17. Hart, H.; Lin, L. T. W.; Ward, D. L. *J. Am. Chem. Soc.* 1984, *106*, 4043-4045.
18. Weber, E.; Hens, T.; Brehmer, T.; Csoregh, I. *J. Chem. Soc., Perkin Trans 2* 2000, 235-241.
19. Wuest, J. D. *Chem. Commun.* 2005, 5830-5837.
20. Moorthy, J. N.; Natarajan, R.; Venugopalan, P. *J. Org. Chem.* 2005, *70*, 8568-8571.
21. Harris, K. D. M. *Supramol. Chem.* 2007, *19*, 47-53.
22. Friscic, T.; Trask, A. V.; Jones, W.; Motherwell, W. D. S. *Angew. Chem., Int. Ed.* 2006, *45*, 7546-7550.

23. Ranganathan, A.; Pedireddi, V. R.; Chatterjee, S.; Rao, C. N. R. *J. Mater. Chem.* 1999, 9, 2407-2411.
24. Delori, A.; Suresh, E.; Pedireddi, V. R. *Chem.-Eur. J.* 2008, 14, 6967-6977.
25. (a) G. M. Sheldrick, *SHELXTL-PLUS*, Program for Crystal Structure Solution and Refinement, University of Gottingen, Gottingen, Germany. (b) Siemens, *SMART* System, Siemens Analytical X-ray Instruments Inc., Madison, WI, 1995.
26. Spek, A. L. *PLATON*, Molecular Geometry Program; University of Utrecht: The Netherlands, 1995.
27. Diamond—Crystal and Molecular Structure Visualization, Version 3.1f, Crystal Impact, Brandenburg & Putz, Bonn, 2008.

## **CHAPTER FOUR**

### **Preparation and Analysis of Anhydrous and Hydrated Forms of 1,3-Adamantanedicarboxylic Acid with Different Aza Compounds**

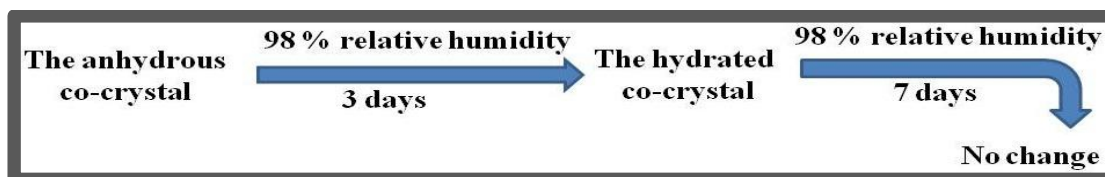
## 4.1 Introduction

Co-crystal which is generally being described as a crystalline material contains two or more components which are solids, under ambient conditions, when they are in their pure forms.<sup>1</sup> The co-crystals are long being known in the literature. The first co-crystal<sup>2</sup> is reported by Wohler in 1844 during the studies on quinine and since then numerous co-crystals were reported in the literature,<sup>3</sup> but in recent years due to unprecedented demand of novel assemblies/materials for tailor made properties, the studies on co-crystals synthesis, characterisation and evaluation gained a greater momentum.<sup>4</sup> Among various notable examples, co-crystals of active pharmaceutical ingredients (APIs),<sup>5</sup> explosives,<sup>6</sup> optical active materials,<sup>7</sup> etc., represent and illustrate the wide range of application of co-crystals.

Co-crystals are prepared by various methods such as solution evaporation,<sup>8</sup> solid state grinding (neat and solvent assisted),<sup>9</sup> solvothermal,<sup>10</sup> slurry crystallization,<sup>5e</sup> sublimation,<sup>11</sup> melt crystallization,<sup>12</sup> etc. Among these methods, solution evaporation and solvothermal methods have been extensively used for the preparation of co-crystals. Co-crystals often crystallize with solvent of crystallization also. Among solvated crystals, water mediated crystals popularly known as hydrates, are large in number over the other common organic solvents.<sup>13</sup>

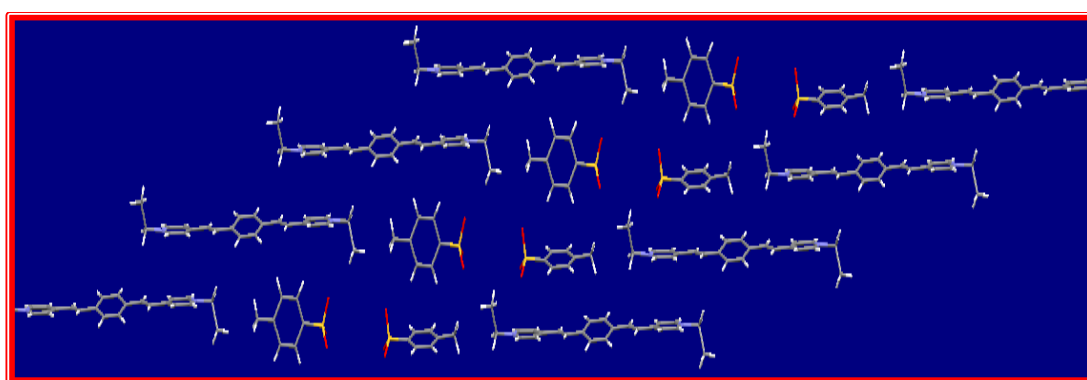
In general, such incorporation of water in the lattices of the co-crystal influences the internal energy, enthalpy, entropy, etc., that in turn affect the physical properties such as solubility, dissolution rate, stability, hygroscopicity, etc. of the crystals.<sup>14</sup> Such difference may be accounted for the formation of strong hydrogen

bonds by the water molecules with the substrate. For example, Jones and co-workers demonstrated that the hydrated co-crystal of theophylline with citric acid has been found to be more stable than the corresponding anhydrous co-crystal upon evaluation at 98% humidity as in Scheme 4.1.<sup>15</sup>

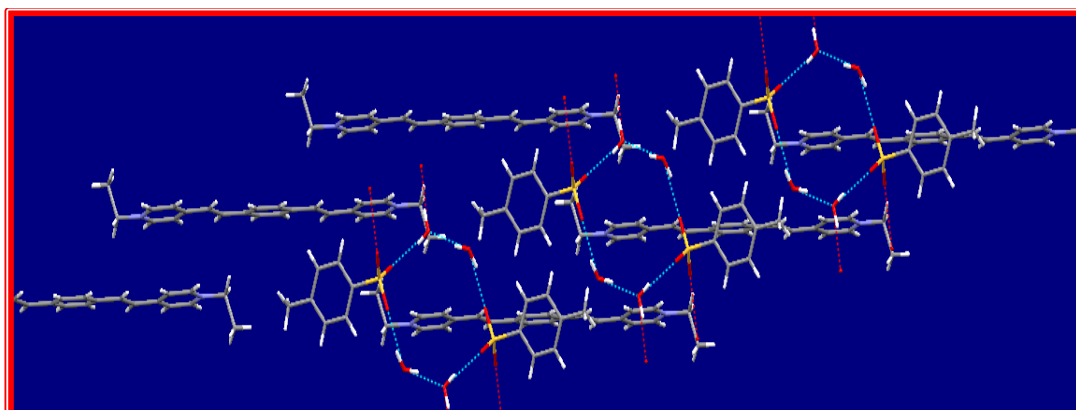


**Scheme 4.1.** Demonstration of stability of hydrated co-crystal towards 98 % relative humidity.

Similarly, Gutov and coworkers have reported crystal structures and luminescence property of hydrated and anhydrous forms of co-crystal of viologen analogue, *bis*[2-(1-ethyl-pyridinium-4-yl)vinyl]benzene with *p*-toluenesulfonate. This study demonstrated that, luminescence intensity is reduced by a factor greater than 10 in the hydrated co-crystal, as the included water prevent the  $\pi \cdots \pi$  interactions between the components of co-crystal, Figure 4.1.<sup>4a</sup>



**(a)**



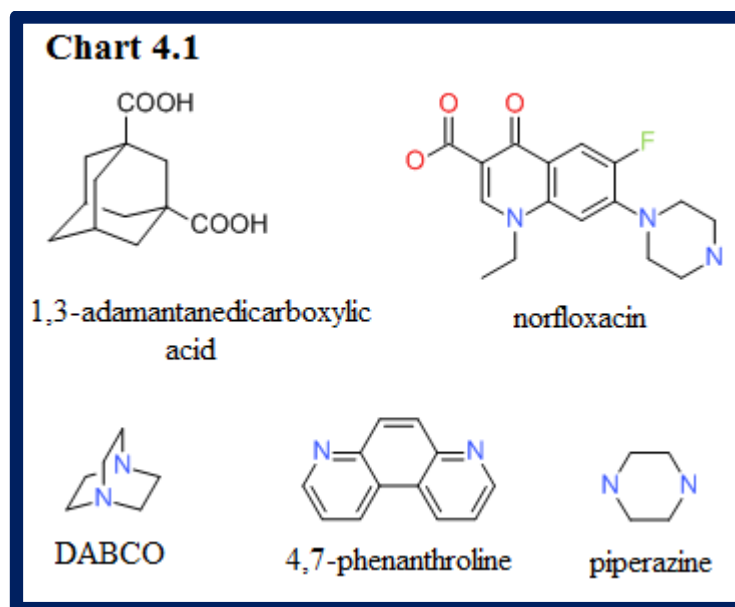
(b)

**Figure 4.1.** Packing of constituents molecules in the co-crystals of *bis*[2-(1-ethylpyridinium-4-yl)vinyl]benzene with *p*-toluenesulfonate (a) anhydrous (b) hydrated.

In fact analysis of Cambridge Structural Database (CSD, version 5.33, November 2011) shows that, 1933 of known hydrated co-crystals only for 141 crystals, corresponding anhydrous forms are available.<sup>16</sup> However, to establish any structural correlation, the known examples are all unique without any common basis in terms of either functionality or intermolecular interactions etc., thus, targeted preparation of crystal structure of the both anhydrous and hydrated co-crystal forms with specific organic entity is attempted.

In general, one of the cheaply available processes to obtain an anhydrous form is dehydration of a hydrated form by thermal treatment, as illustrated for the transformation of hydrated co-crystal of *D*-dibenzoyl tartaric acid and 3-toluidine to the corresponding anhydrous form, by heating at 74° C.<sup>17</sup> However, structural characterization of anhydrous forms, obtained by thermal treatment, is often a difficult process due to the formation of microcrystalline or amorphous materials, which could not be characterized by single crystal X-ray diffraction method, also taken into

account the practical difficulties associated with other methods such as powder X-ray diffraction to determine the structures of the compounds.<sup>18</sup> Hence, novel strategic crystallization conditions are necessitates for the preparation of anhydrous forms in the form of single crystals for elucidation of structural features by single crystal X-ray diffraction method. Thus, co-crystallization of 1,3-adamantedicarboxylic acid (**1**) with complementary ligands, as shown in Chart 4.1, was carried out from various solvents. The obtained single crystals were characterized by single crystal X-ray diffraction method and compared the structural features of the respective forms as illustrated in the following sections.



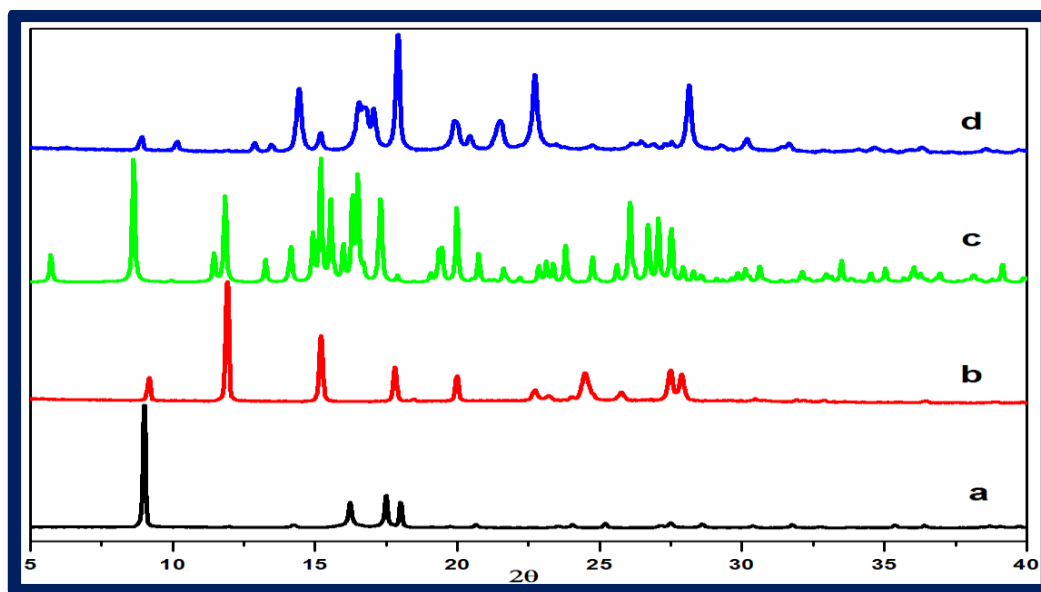


## **4.2 Co-crystals of Hydrated and Anhydrous Forms 1,3-Adamantanedicarboxylic Acid, **1**, and 4,7-Phenanthroline:**

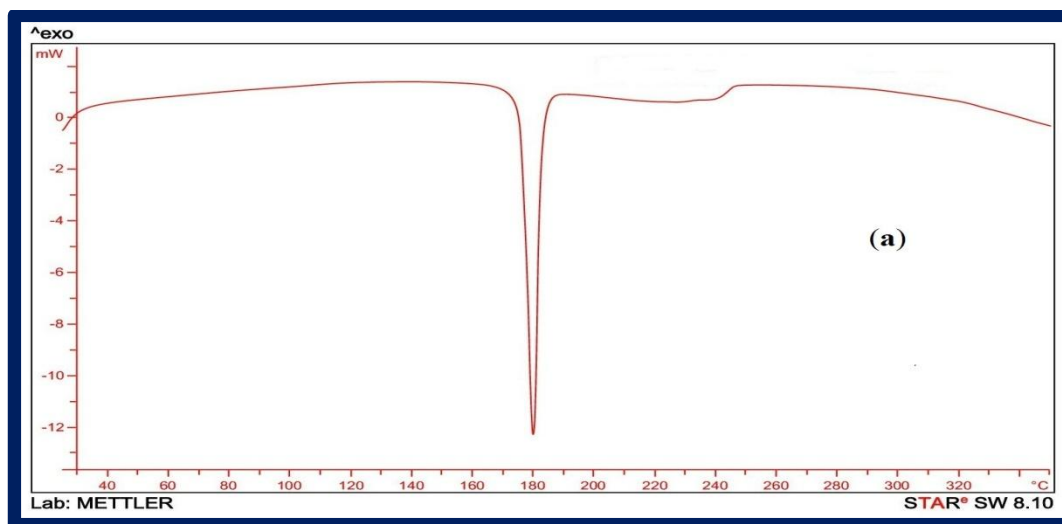
Co-crystallization of 1,3-adamantanedicarboxylic Acid (**1**) and 4,7-Phenanthroline (**a**) by slow evaporation of a solution of MeOH/H<sub>2</sub>O gave co-crystals, as illustrated in Chapter III, in the form of channels structure which are being occupied by water molecules, (see Figure 3.23). For the purpose of discussion, structure is labeled as **1a**.

It is noteworthy to mention that the crystals of **1a** upon exposure to the atmosphere at ambient temperature, the single crystals were found to be decomposed over a period of time and result into a microcrystalline material. In general, such material would be either a mixture of the co-crystal components, if the powder pattern match with the mixture of the pattern of the pure forms, or may be an amorphous form. However, the powder X-ray diffraction (PXRD) analysis of the microcrystalline material of **1a**, reveals high crystalline nature of the material, with a totally new PXRD pattern not related to either **1**, or **a** as well as not of **1a**, as shown in Figure 4.2. Thus, it shows that, a new phase of **1a** might have been obtained.

Further, the solid also appears to be homogeneous as Differential Scanning Calorimetric (DSC) analysis shows a sharp endothermic peak at 180 °C, as shown in Figure 4.3a, which corresponds to melting of the material. Indeed, DSC analysis of freshly prepared sample of **1a** reveals an endotherm, which is exactly correlated with the melting point observed for microcrystalline solid, (see Figure 4.3b).



**Figure 4.2.** Comparison of powder X-ray diffraction patterns of (a) acid **1**, (b) 4,7-phenanthroline, (c) co-crystals of **1a**, (d) microcrystalline solid of **1a** after exposure to atmosphere.



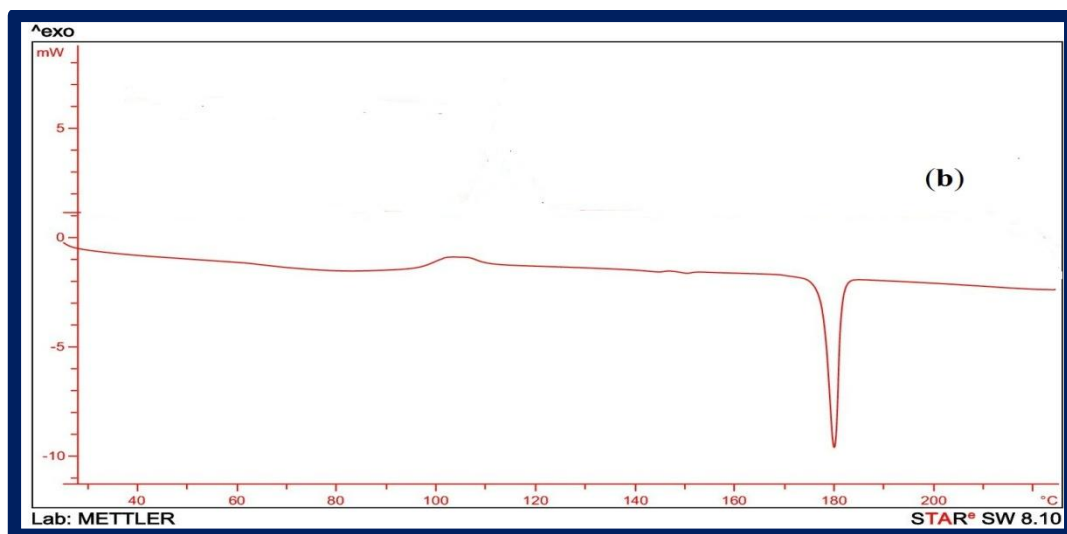


**Figure 4.3.** DSC plots of solid material of **1a**, (a) after exposure to atmosphere, (b) freshly prepared.

Further, Thermogravimetric analysis (TGA) on freshly prepared sample of **1a**, shows weight loss as shown in Figure 4.4. Thus, from the thermal analysis it may be concluded that **1a** undergoes dehydration and subsequently yielding a new phase. For the purpose of discussion, this new phase is labeled as **1a'**.

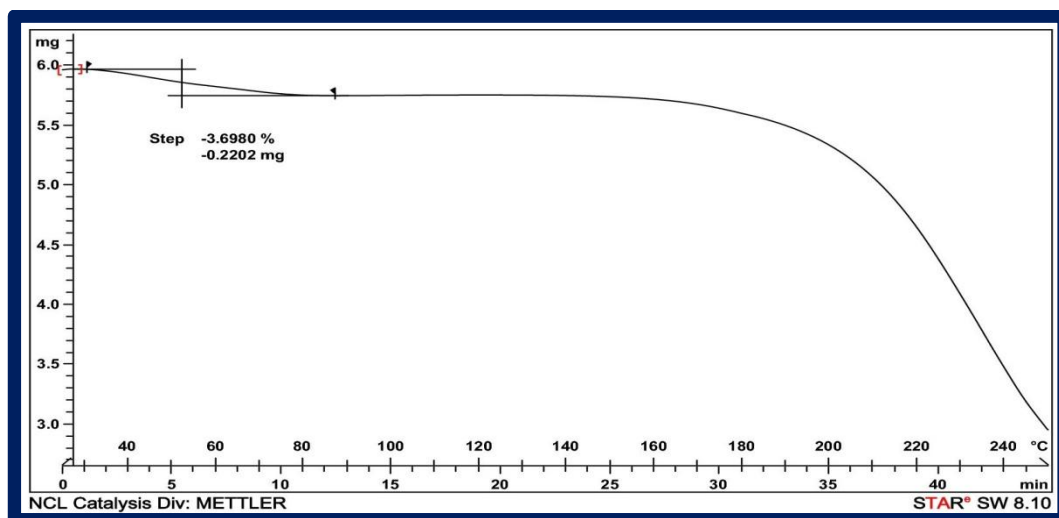


**Figure 4.4.** TGA plot for freshly prepared sample of **1a**.

To further substantiate the thermal analysis, in situ PXRD measurement has been carried out on co-crystals of **1a**. The resultant diffractograms recorded at different temperatures are shown in Figure 4.5.

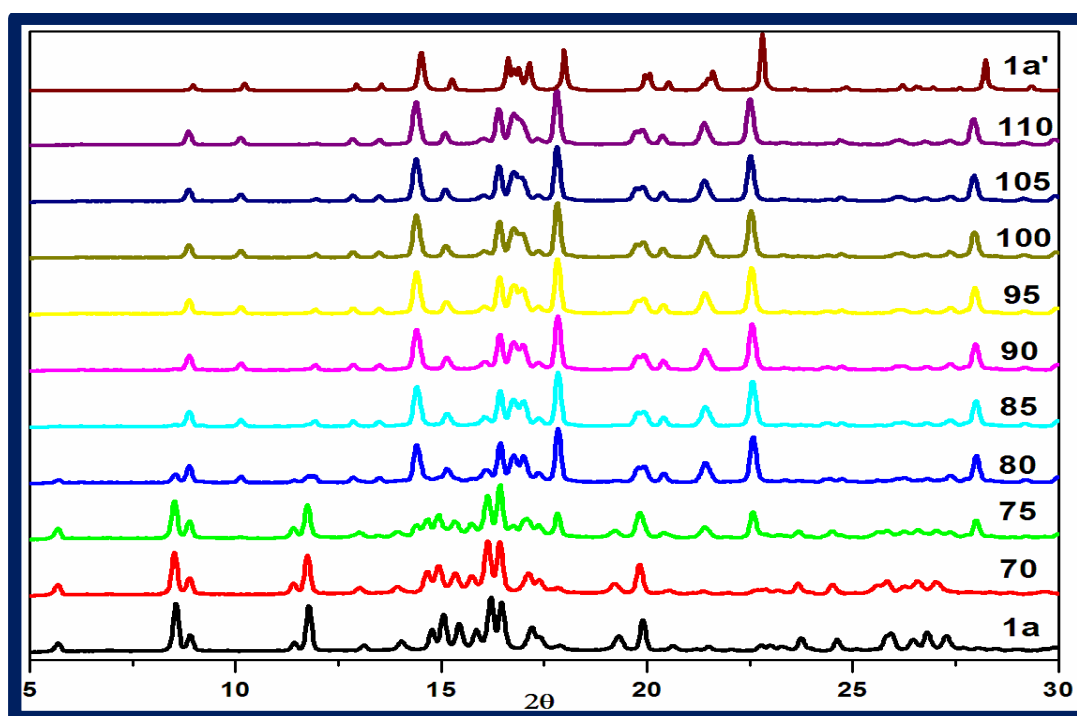


**Figure 4.5.** Different PXRD patterns of **1a** obtained at different temperatures.

It appears that the phase transition in fact is initiated at 75°C, but notable changes that are prominent and exact matching with the pattern obtained for **1a'**, around 85°C, which is closely related to the observation of phase change in the range of 90°C in DSC. Interestingly, solid state neat grinding of acid **1** and phenanthroline, **a**, indeed gave microcrystalline powder, with PXRD pattern exactly matching with that of **1a'**, as shown in Figure 4.6.

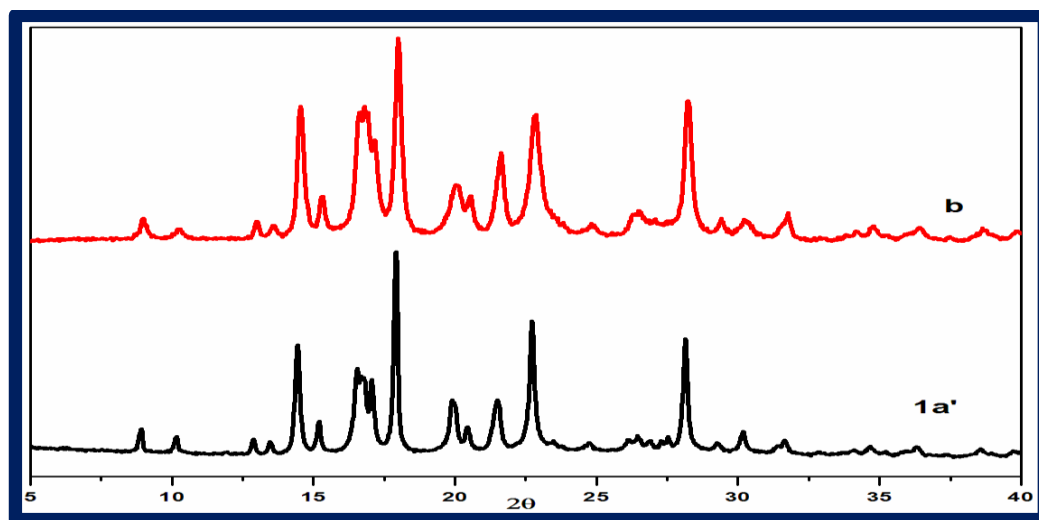


**Figure 4.6.** Comparison in the PXRD patterns of **1a'** and (b) obtained by solid state neat grinding of acid **1** and **a**.

Thus observation suggested that **1a'** may be an anhydrous form of **1a**. Although the observed new phase shows highly crystalline nature, with the well resolved intensity PXRD pattern, taken into account the complexity associated with structure determination with intensity data from powder X-ray diffractometer, preparation of **1a'** in the form of single crystal is attempted, to establish its structure in order to understand arrangement of constituting molecules in crystals. However, many attempts towards co-crystallization of acid **1** and phenanthroline, **a**, gave only co-crystals of **1a** from different solvent systems, as characterized by PXRD patterns. Nevertheless, the crystals obtained from either dimethylsulfoxide (DMSO) or dimethylformamide (DMF) even in the presence of water interestingly gave single crystals for which the PXRD pattern match with **1a'**, as shown in Figure 4.7.

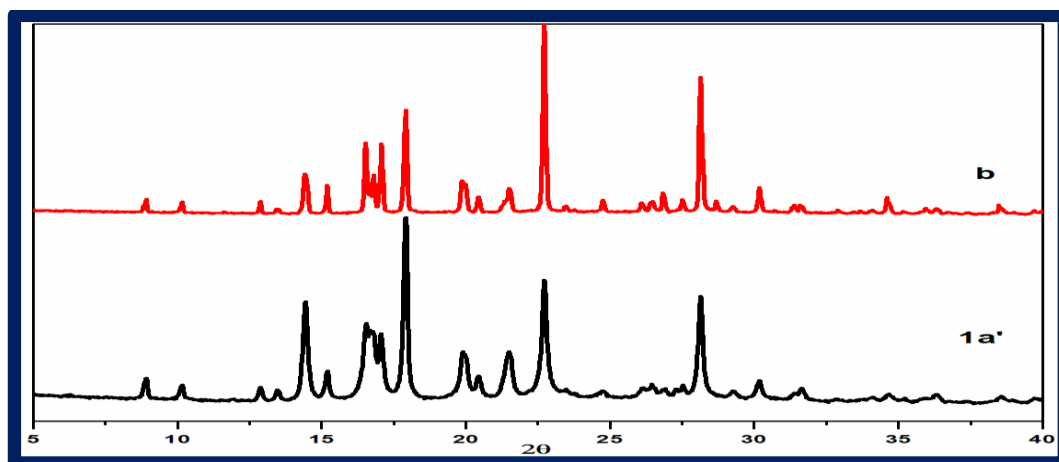


**Figure 4.7.** Comparison in the PXRD patterns of **1a'** (black) and obtained from single crystal of **1a'**(red).

The good quality single crystals of **1a'**, thus obtained were used for structural determination by single crystal X-ray diffraction method. The analysis reveals that, **1a'** is composed of molecules of 1,3-adamantanedicarboxylic acid (**1**) and 4,7-phenanthroline (**a**) with the constituents in the asymmetric unit in a 1:1 ratio, and most significant and noteworthy point is that it does not contain any water molecule(s). Thus, the **1a'** is anhydrous form of **1a**. The ORTEP diagram is shown in Figure 4.8. The complete crystallographic details are given in Table 4.1.

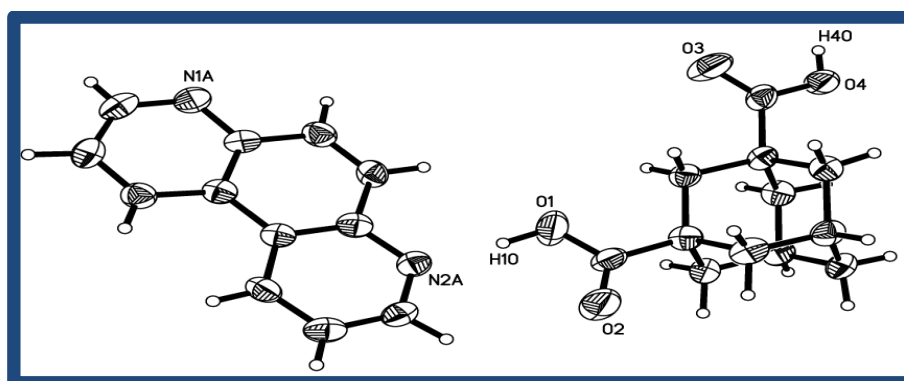


**Figure 4.8.** ORTEP of the co-crystal **1a'**.

Structural analysis reveals that two of each molecules of **1** and **a** are held together through a pair-wise  $R_2^2(7)$  and  $R_2^2(8)$  patterns, in cyclic network, as an ensemble of quartet molecules, like in the hydrated co-crystal **1a**, through O-H $\cdots$ N and C-H $\cdots$ O hydrogen bonds. Complete characteristics of hydrogen bonds are listed in Table 4.3. The ensemble observed in **1a'** is shown in Figure 4.9.

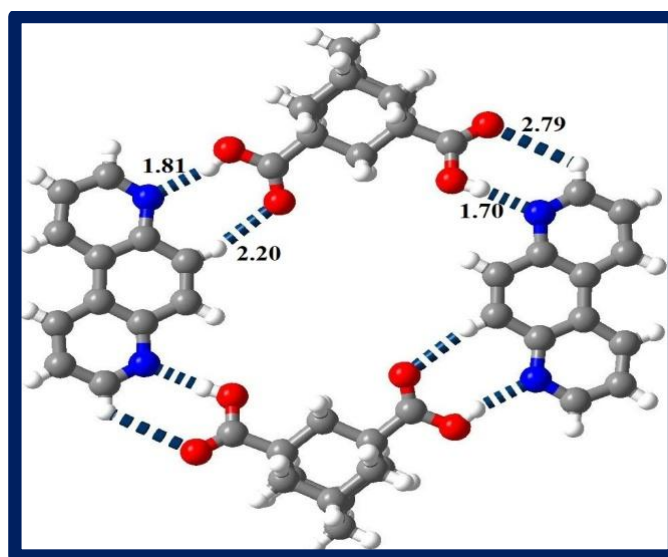


**Figure 4.9.** A cyclic network of quartet of molecules of **1** and **a**, in the co-crystals of **1a'**.

Such ensembles further stabilized in three-dimensional arrangement with the cavity being filled by the molecules from the adjacent layer. Such arrangement is shown in Figure 4.10.

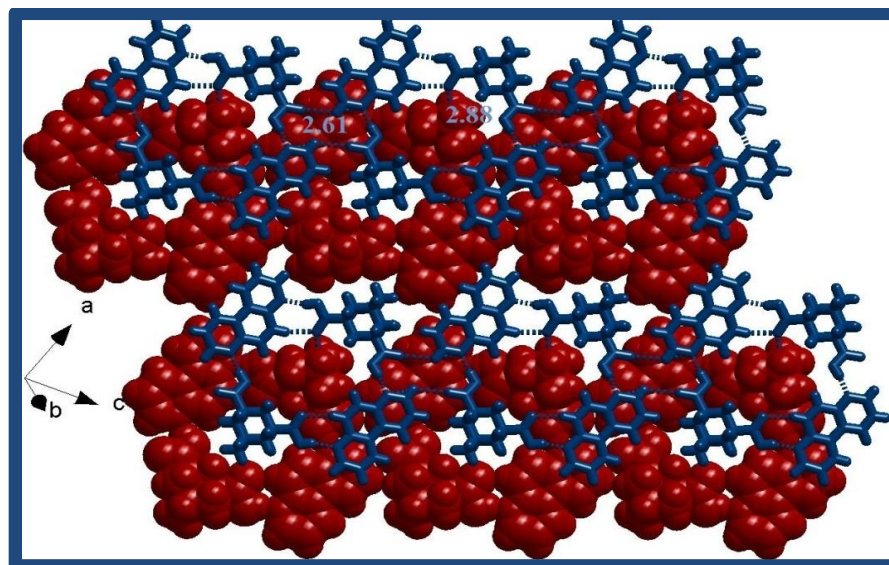


**Figure 4.10.** Three-dimensional packing observed in the co-crystals of **1a'**.

Thus, in the crystal structure of **1a'**, the voids are present only in two-dimensional arrangement unlike in its hydrated structure, where in such voids transform into channels with the alignment along the stacking direction.

In order to carry out further comparative structural analysis of corresponding hydrated and anhydrous forms, and also analyze the transformation, preparation of the co-crystals of 1,3-adamantanedicarboxylic acid with other aza donors as listed in Chart 4.1 is continued by replacing phenanthroline with DABCO.



### 4.3 Structural Analysis of Hydrated and Anhydrous Forms of Co-crystal of 1,3-Adamantanedicarboxylic Acid (**1**) and DABCO (**b**):

A tetrahydrofuran (THF) solution of 1,3-adamantanedicarboxylic acid (**1**) and DABCO (**b**) gave good quality single crystals, by slow evaporation method, which are labelled as **1b**. The crystals have been characterised by single crystal X-ray diffraction method. The analysis reveals that, crystals are composed of molecules of acid **1**, DABCO and water in 1:1:1 ratio, as shown in Figure 4.11, an asymmetric unit in the form of ORTEP. The complete crystallographic details are given in Table 4.1.

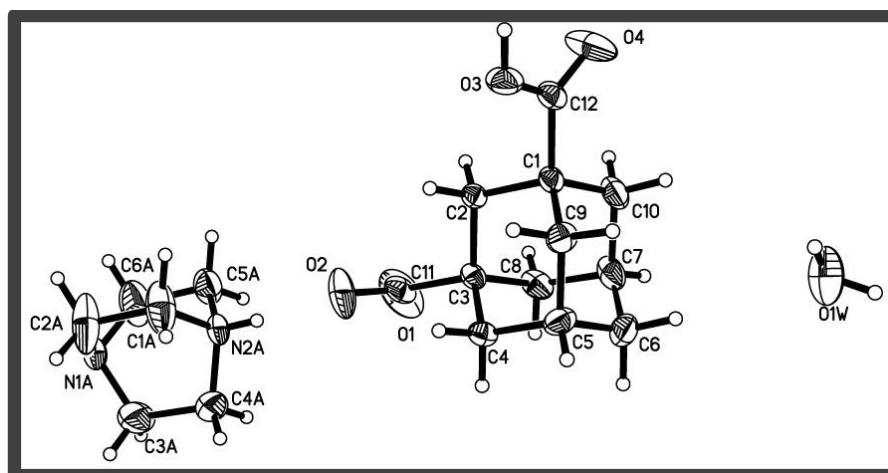


**Figure 4.11.** ORTEP of the co-crystals of **1b**.

It is apparent that **1b** is an adduct with proton of one of the  $-\text{COOH}$  groups being transferred to DABCO. Structural analysis highlights that each of the molecules of acid **1** and DABCO in the form of ions, along with two water molecules form a hexameric ensemble, through series of hydrogen bonds. In each ensemble, while acid molecules are held together directly by  $\text{O}-\text{H}\cdots\text{O}^-$  hydrogen

bonds, with a H $\cdots$ O distance being 1.55 Å, forms a chain. Such chains are held together by DABCO and water through N-H $\cdots$ O as well O-H $\cdots$ O hydrogen bonds. Complete characteristics of hydrogen bonds are listed in Table 4.3. A typical ensemble is shown in Figure 4.12. Thus, each ensemble possesses void space of dimension 8 x 14 Å<sup>2</sup>, in which water molecules are embedded through O-H $\cdots$ O (O $\cdots$ H, 1.93 Å) hydrogen bonds, (see Figure 4.16). Further, in a typical layer, the ensembles are held together by O-H $\cdots$ O hydrogen bonds formed between the carbonyl groups of molecules of acid **1** present in juxtaposed ensembles.

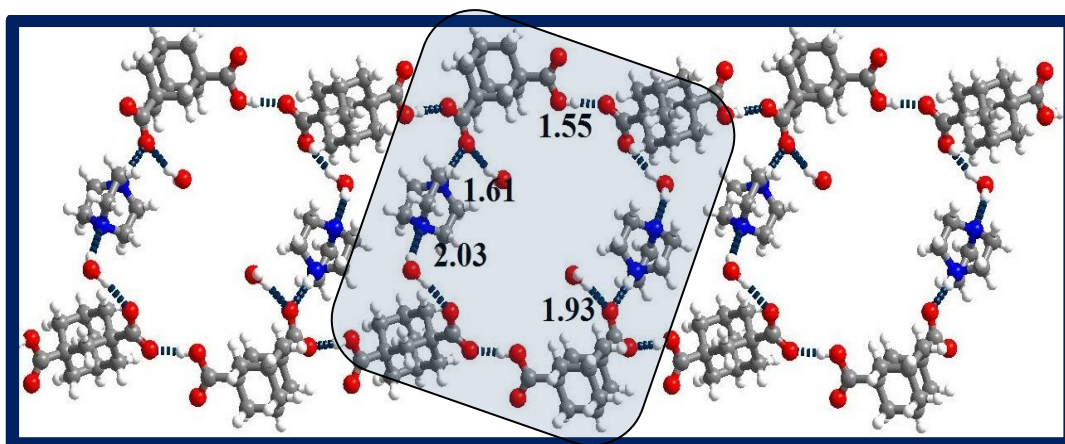


**Figure 4.12.** Arrangement of molecules in a typical layer with hexameric ensembles.

When the crystals of **1b** are exposed to the atmosphere at ambient temperature, it is observed that, the single crystals lost integrity after a period of time, as observed in **1a**, and resulted in a microcrystalline material. However, unlike the observations made in **1a**, the analysis of the diffraction pattern obtained from powder X-ray diffractometer reveals that, **1b** is intact with the pattern is exactly matched with the pattern obtained for the freshly prepared **1b**, the

comparison is shown in Figure 4.13. Nevertheless, to understand thermal stability of **1b**, analysis of it has been carried out by TGA and DSC, and results are found to be quite encouraging as described below.

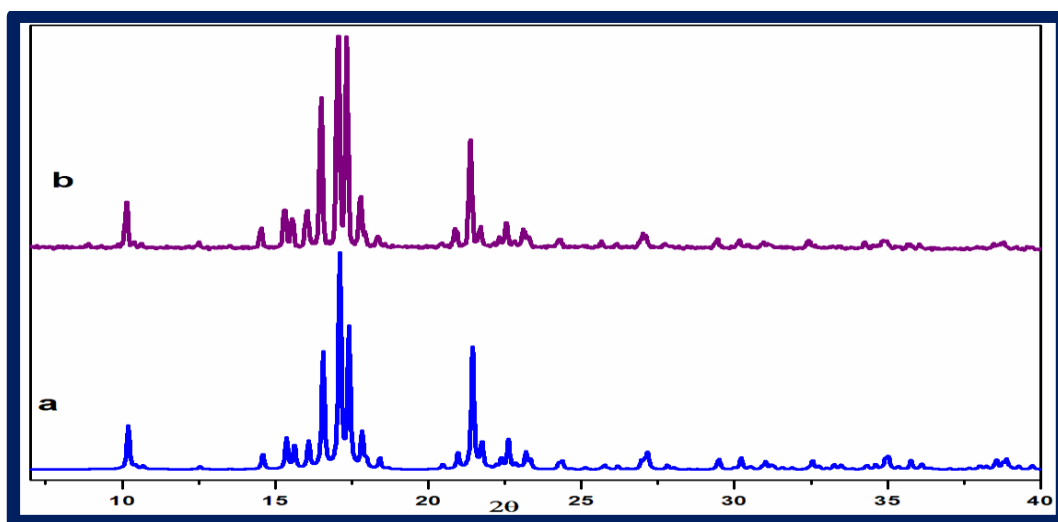


**Figure 4.13.** Comparison in the PXRD patterns of a) **1b** (freshly prepared), b) the crystals of **1b** after exposure to atmosphere at ambient condition.

In TGA analysis, carried out by heating the crystals of **1b** in inert atmosphere at the rate of 10° C gave a thermogram with a weight loss of 5% as shown in Figure 4.14. In fact, the weight loss corresponds to the loss of water present in the crystal lattice. However, continuation of further heating did not show any further weight loss till around 140°C at which decomposition of the material is observed, (see Figure 4.14).

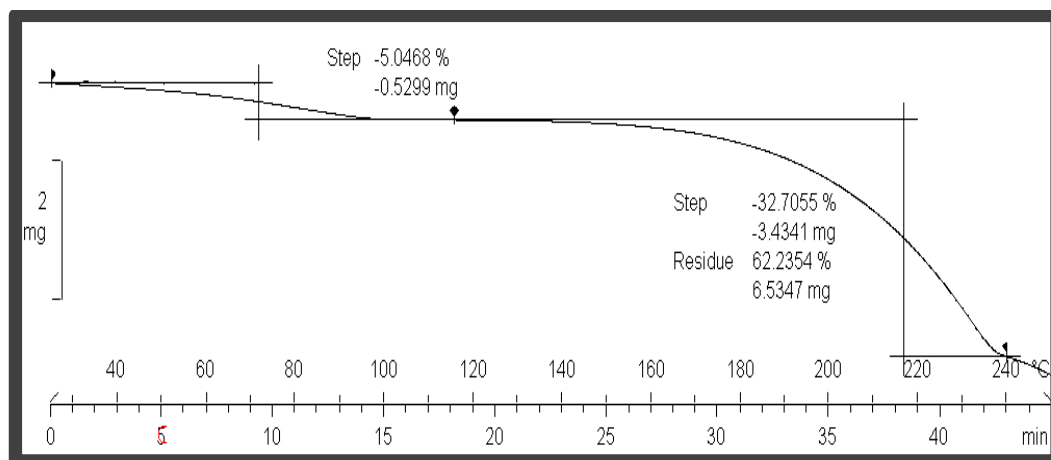


**Figure 4.14.** TGA analysis of co-crystal **1b**.

Analysis carried out by DSC, on a freshly prepared sample of **1b** shows two endothermic peaks at around 80 and 145°C, as shown in Figure 4.15. While the peak at around 80°C is broad and be related to the loss of water (as observed in TGA analysis), the peak at 145°C, neither corresponds to melting of **1** (m.p., 276-278°C) nor **b** (m.p., 156-160°C), could be related to the material, possibly a melting point of a new phase, **1b'**, formed after water is lost.

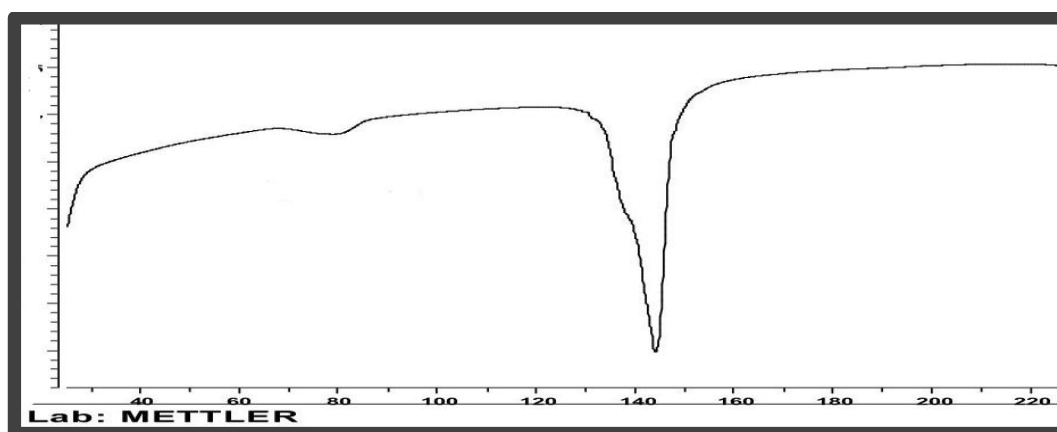


**Figure 4.15.** DSC analysis of co-crystal **1b**.

Thus, although at ambient conditions, **1b** appears to be stable, thermal analysis indicates the formation of a new phase at higher temperature. To observe the phase change in-situ, variable temperature powder X-ray diffraction experiment is carried out. The different diffractograms corresponding to patterns at different temperatures are compiled and shows in Figure 4.16. It is observed that the patterns at ambient temperature, represented at the bottom in Figure 4.16, remains intact till 75°C and since the peak around  $2\theta$  value of  $10^\circ$  started diminishing its intensity and finally vanished at 90 °C, suggesting the formation of a new phase at this junction, which is also reflected around the same temperature in DSC analysis. It is noteworthy to mentioned that the pattern after 90°C does not match with neither of acid 1 nor DABCO, thus, confirming the appearance of the new phase **1b'**.

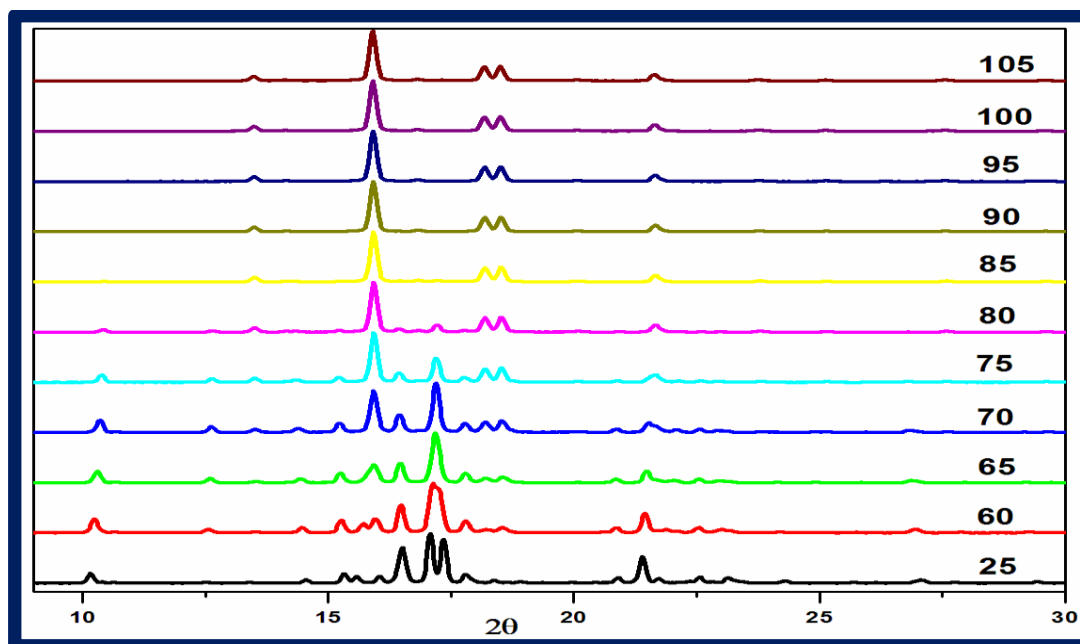


**Figure 4.16.** Comparison in PXRD patterns obtained at various temperatures for freshly prepared sample of **1b**.

As mentioned for **1a'**, due to the daunting exercise to determine the structure of a material from X-ray intensity data from powder X-ray diffractometer, experiment were directed to prepare single crystals of **1b'**. As we were successful in obtaining **1a'** from DMSO or DMF, acid **1** and DABCO were also dissolved in DMF and allowed for slow evaporation at ambient conditions. In about 48hr good quality single crystals were obtained which were found to be co-crystals of **1** and DABCO in a 1:1 ratio without water by single crystal X-ray diffraction analysis. The contents of the anhydrous co-crystal **1b'** within the asymmetric unit are shown in Figure 4.17. The complete crystallographic details are given in Table 4.1.

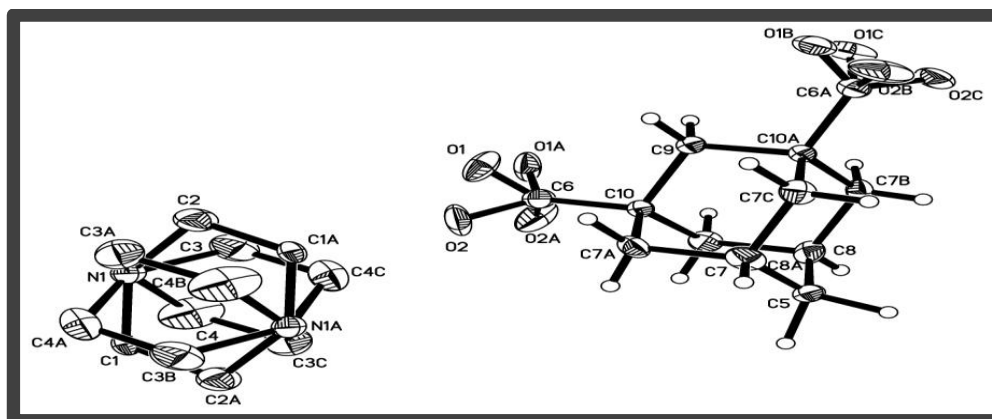


**Figure 4.17.** Thermal ellipsoid plot (ORTEP) of the co-crystal **1b'**.

Structural analysis shows that, the molecules of **1** and **b** interacts to each other through O-H $\cdots$ N or N $^+$ -H $\cdots$ O $^-$  hydrogen bonds in the form of a corrugated tape, as shown in Figure 4.18. Complete characteristics of hydrogen bonds are listed in Table 4.3. It is apparent from Figure 4.18 that such one-dimensional tapes are juxtaposed within a layer, which are further stacked in three dimensional arrangement, as shown in Figure 4.19.

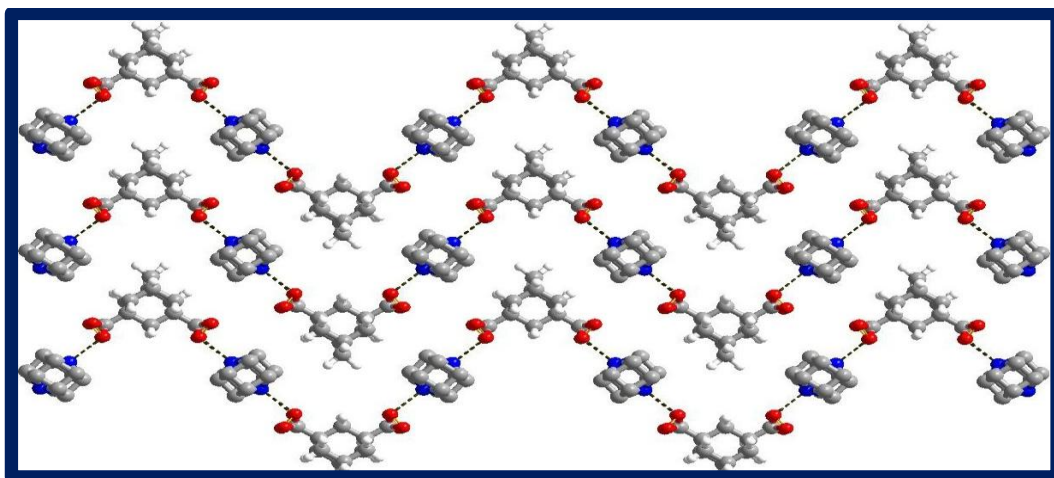


**Figure 4.18.** The arrangement of molecules in a typical layer in **1b'**.

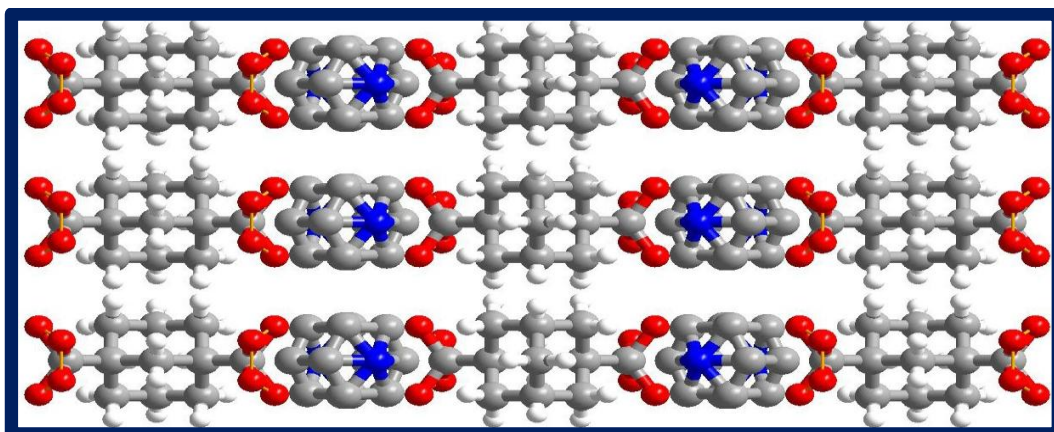


**Figure 4.19.** Three-dimensional arrangement of constituent in **1b'**.

Thus, the structures of **1b** and **1b'** are distinctly different by all means of interaction, packing etc. An interesting feature, further associate with **1b'** is that upon exposure to atmosphere for few days, it readily get converted to **1b**, by absorbing water from the atmosphere, as confirmed by powder X-ray diffraction patterns depicted in Figure 4.20. However, such transformation was not observed between **1a** and **1a'**.

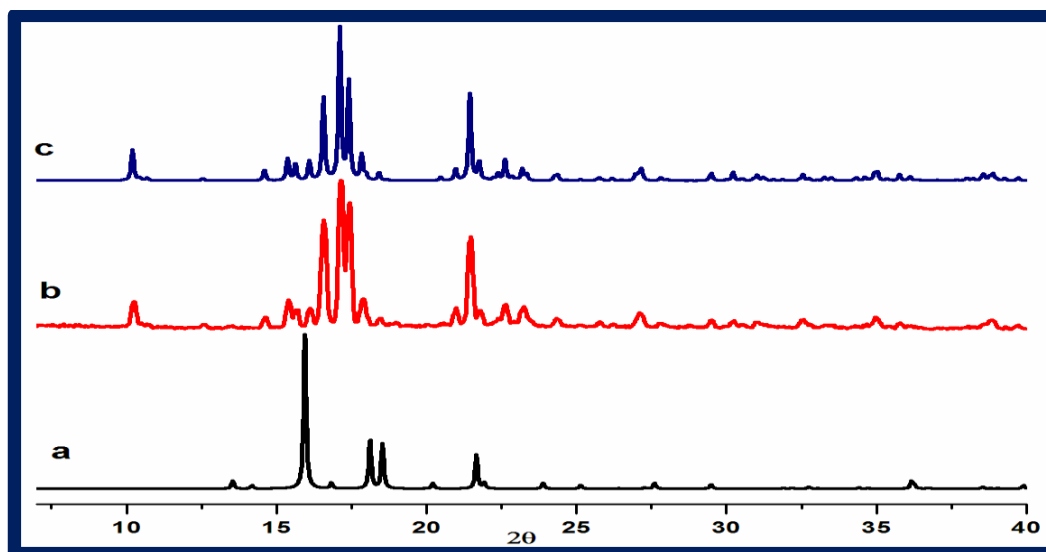


**Figure 4.20.** Comparison in PXRD patterns, a) **1b'** b) **1b'** after exposure to atmosphere at ambient conditions, c) **1b**.

#### **4.4 Preparation and Structural Analysis of Hydrated and Anhydrous Co-crystal of 1,3-Adamantanedicarboxylic Acid (**1**) and Piperazine (**c**):**

Crystals obtained from a methanol solution of 1,3-adamantanedicarboxylic acid (**1**) and piperazine (**c**) have been characterized by X-ray diffraction methods. The crystal structure is determined by single crystal X-ray diffraction method. Analysis reveals that, the crystals are composed of molecules of acid **1**, piperazine and water in a 2:1:2 ratio. ORTEP of the contents within the asymmetric unit of co-crystals of **1c** is shown in Figure 4.21. The complete crystallographic details are given in Table 4.2.



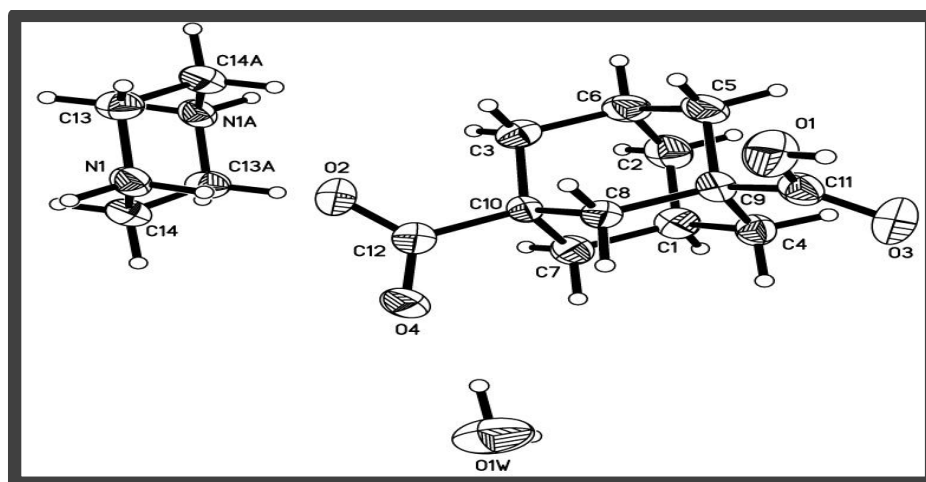


**Figure 4.21.** ORTEP of the asymmetric unit of co-crystals **1c**.

Analysis of packing of molecules shows that out of two  $\text{-COOH}$  groups on acid **1**, one of it is deprotonated and the proton is transferred to piperazine, **c**. Such ionic species are held together by  $\text{N}^+\text{-H}\cdots\text{O}^-$  hydrogen bonds, yielding an ensemble of quartet of molecules comprising of two of each molecules of acid **1** and **c**, by a  $R_4^4(12)$  pattern. Complete characteristics of hydrogen bonds are listed in Table 4.3. In fact, the ensembles form a one-dimensional columnar unit, as depicted in Figure 4.22. Such columnar units are further held together by  $\text{O-H}\cdots\text{O}$  hydrogen bonds formed by  $\text{-COOH}$  group on acid, **1** with  $\text{H}\cdots\text{O}$  distance of  $1.65\text{\AA}$ , leading to the formation of layers.

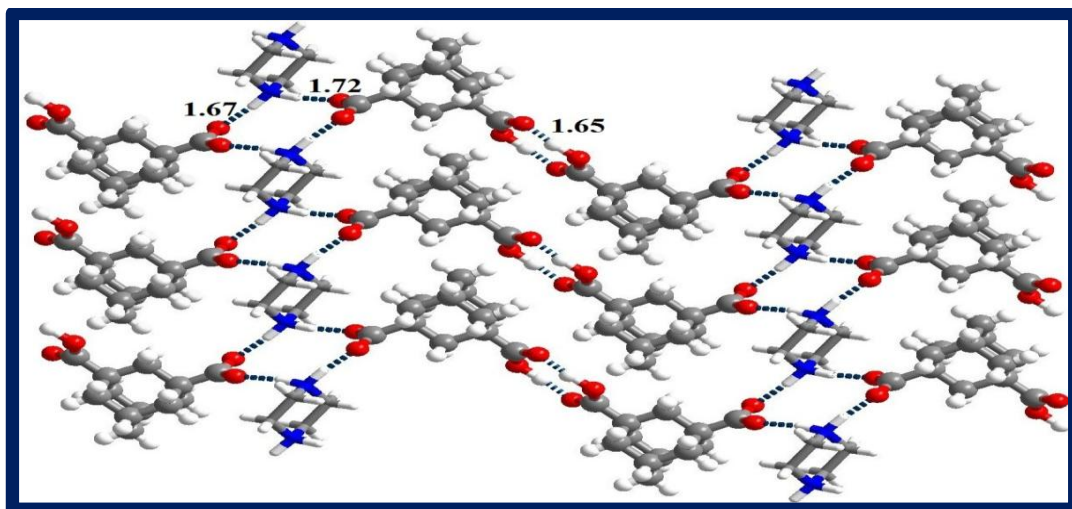


**Figure 4.22.** Arrangement of molecule of **1** and **c** in a layer, within the crystal lattice of **1c**.

In three-dimensional arrangement the layers are stacked along a crystallographic axis, with water molecules holding the adjacent layers by O-H $\cdots$ O hydrogen bonds with H $\cdots$ O distances 1.80 and 1.88 Å. The arrangement is shown in Figure 4.23.

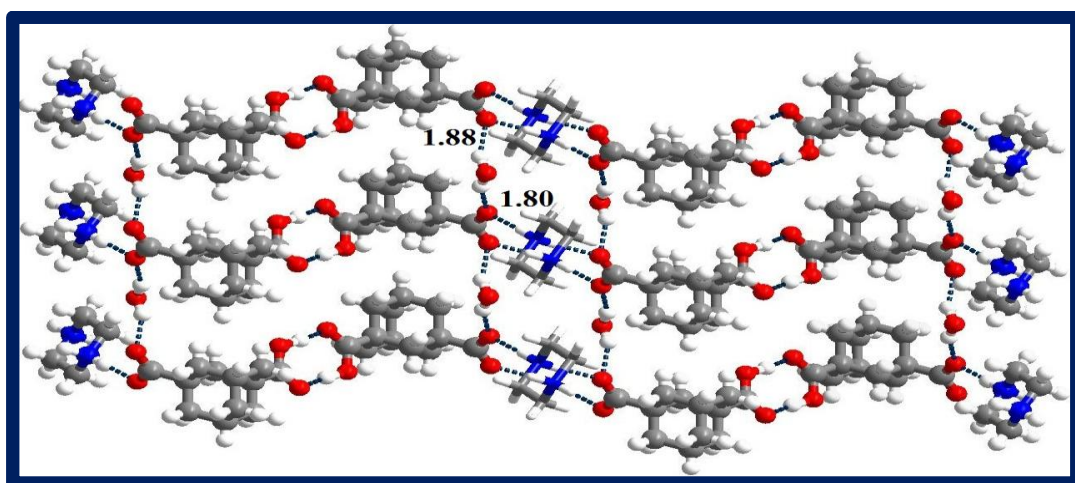


**Figure 4.23.** In three-dimensional arrangement, the layers are held together by water molecules.

The crystals of **1c** are also converted to microcrystalline material, when they are exposed to the atmosphere at ambient condition. The obtained material has been characterized by PXRD, which reveals that, it is a new crystalline phase, as found in **1a** and **1b**, with the diffraction pattern does not contain any reflections belonging to neither co-crystal component **1** and **c** nor co-crystal **1c**, as shown in Figure 4.24.

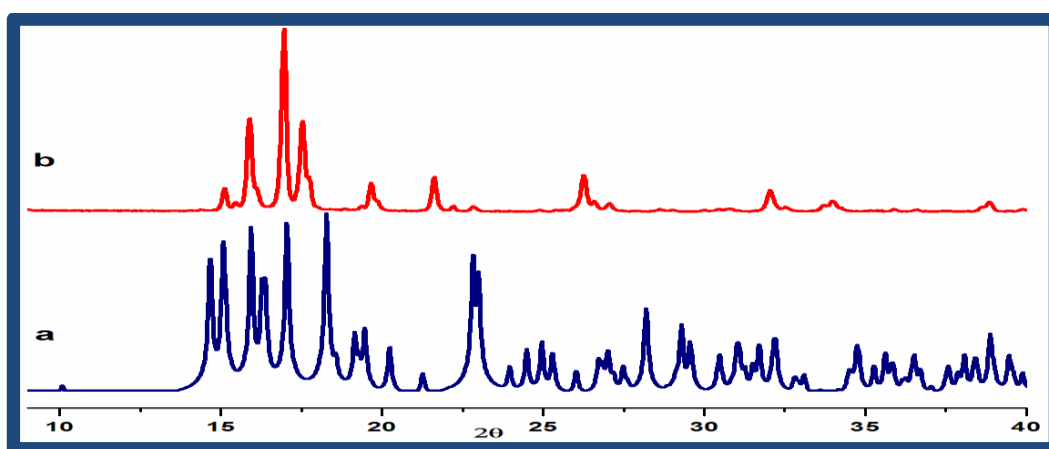


**Figure 4.24.** Comparison in the PXRD patterns, (a) **1c**, (b) microcrystalline material obtained with the exposure of **1c** to atmosphere.

Taken into account the observations and conclusions with **1a**, **1a'**, **1b** and **1b'**, the new phase of **1c** may be regarded as its anhydrous form. To demonstrate it, preparation of single crystals of **1c'** has been attempted by diffusion of a methanol solution of **c** into DMSO solution of **1**. The analysis of obtained good quality single crystals by X-ray diffraction method reveals that, the crystals are composed of molecules of acid **1** and piperazine in a 1:1 ratio without any solvent of crystallization. Asymmetric unit of crystal lattice, **1c'** is shown in Figure 4.25. The pertinent crystallographic data for **1c'** is given in Table 4.2.

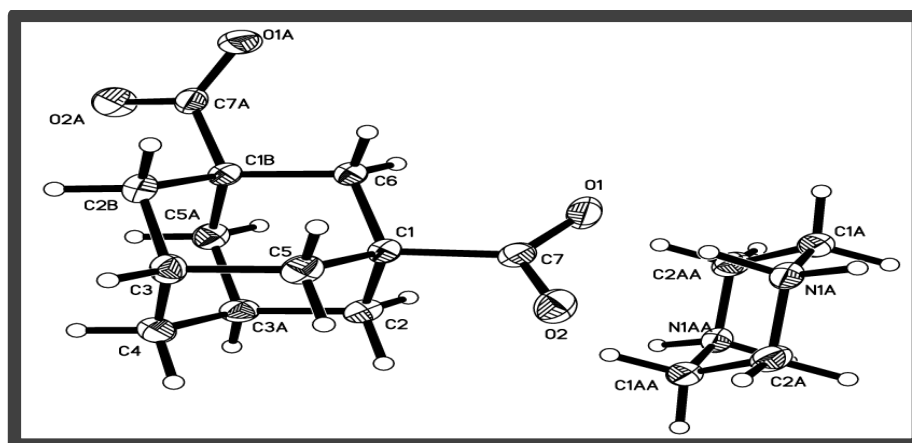


**Figure 4.25.** ORTEP drawing for the asymmetric unit of **1c'**.

Further analysis shows that, both the carboxylic acid groups of **1** are deprotonated in the crystals of **1c'**. Such molecules of **1**, interestingly interact with the molecules of piperazine in the same pattern as that of **1c**, so, in two-dimensional arrangement in **1c'** also, each of two molecules of **1** in the form of ions form quartet ensembles with two of molecules of **c**. Such ensembles are in fact associated with the  $R_4^4(12)$  hydrogen bonding patterns as observed in **1c** but with different type of hydrogen bonds. The details of hydrogen bonds are given in Table 4.3. Interestingly, the ensembles did not form columnar units as observed in **1c**, but extended in two-dimensional layer by forming similar ensemble through appropriate hydrogen bonds, as shown in Figure 4.26, using the second acid functionality on **1**. Such layers are stacked ultimately in the crystal lattice, with the layer being connected together directly by C-H $\cdots$ O $^-$  hydrogen bonds. The stacking of the layers is shown in Figure 4.27.

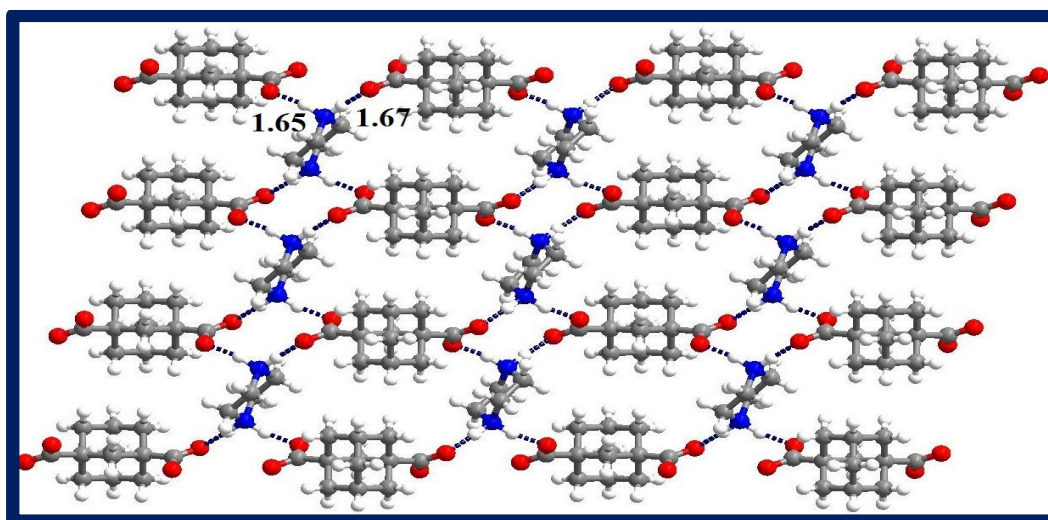


**Figure 4.26.** The arrangement of molecules of **1** and **c** held together through  $R_4^2(12)$  hydrogen bonding patterns in the crystal lattice **1c'**.

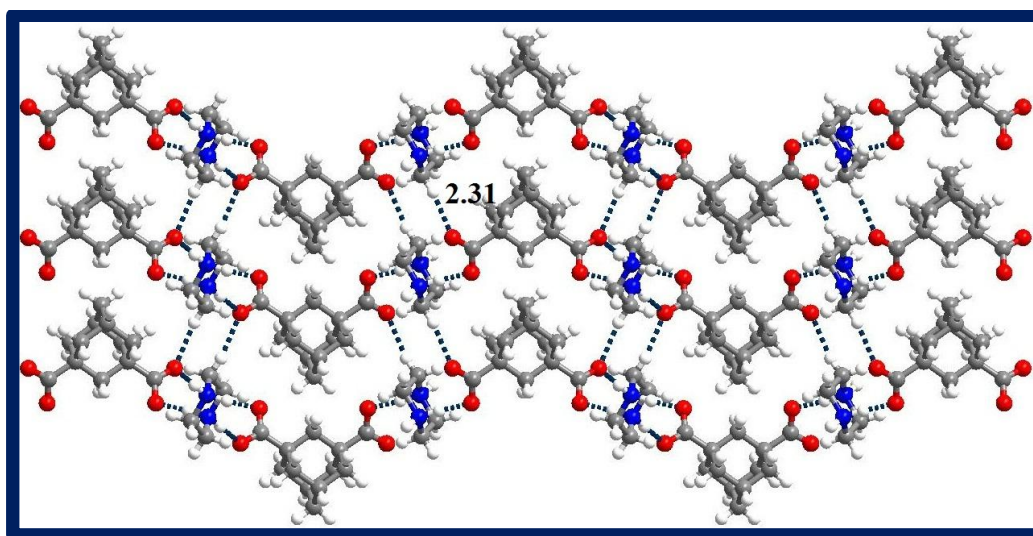


**Figure 4.27.** Packing of layers in **1c'**, with layers being held together by C-H...O hydrogen bonds.

To ensure that the structure of **1c'** is same as that of microcrystalline material obtained from **1c** upon exposure to atmosphere, the experimental powder pattern of the material is compared with the powder pattern of **1c'** simulated from

the single crystal data and the compilation is shown in Figure 4.28. The comparison clearly establishes the similarity between two patterns, thus, confirming the formation of anhydrous phase by **1c** upon exposure to atmosphere.

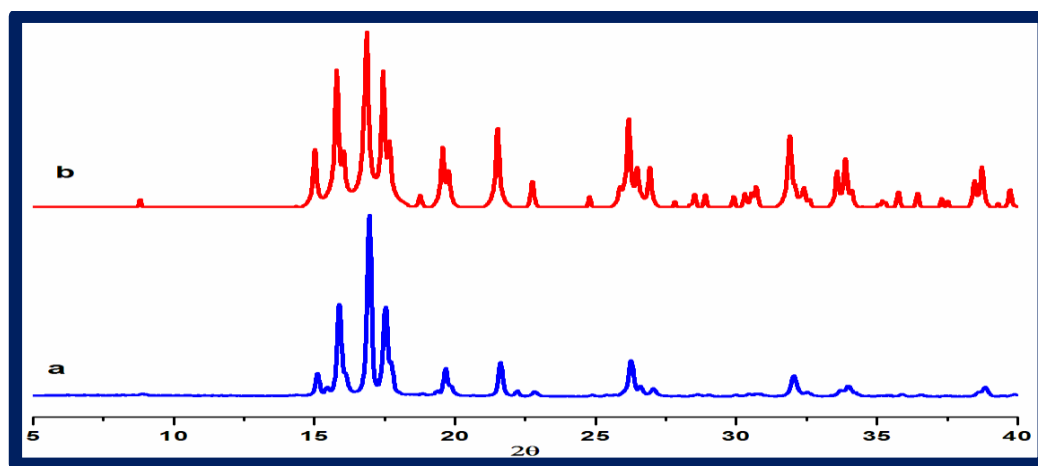


**Figure 4.28.** Comparison in the PXRD patterns, (a) the material obtained upon decomposition of the crystals of **1c**, (b) **1c'** (simulated from single-crystal X-ray diffraction data).

The solvated adducts or solids have immersive effect in pharmaceuticals with wide range of variations in the preparations of APIs. Taken into account the recent attention to develop co-crystals of pharmaceutically important substrates, the solvated co-crystals may be of potential targets for elegant and exotic exploration. Hence further studies in the series has been extended to an API which has pyridyl moiety to interact with acid functionality on **1**, thus, co-crystallization of **1** with norfloxacin has been carried out.

#### 4.5 Preparation and Structural Analysis of Hydrated and Anhydrous Co-crystal of 1,3-Adamantanedicarboxylic Acid (**1**) and Norfloxacin (**d**):

Co-crystallization of 1,3-adamantanedicarboxylic acid (**1**) and norfloxacin (**d**) has been carried out by slow evaporation of aqueous solution of co-crystal components. The solution is prepared by dissolving the solid mixture of **1** and **d** obtained by grinding in mortar and pestle, and allowing the resultant solution for slow evaporation. Good quality single crystals are obtained within 48hr, which were used for characterization by single crystal X-ray diffraction method. The analysis reveals that, the crystals are composed of molecules of acid **1**, norfloxacin and water, which may be regarded as a hydrate of co-crystal of **1** and **d** and it has been labeled as **1d** for the discussion purpose. The asymmetric unit of **1d** contains two symmetry independent molecules of each of **1**, **d** and water. ORTEP drawing for the asymmetric unit is shown on Figure 4.29. The pertinent crystallographic data for **1d** is given in Table 4.2.

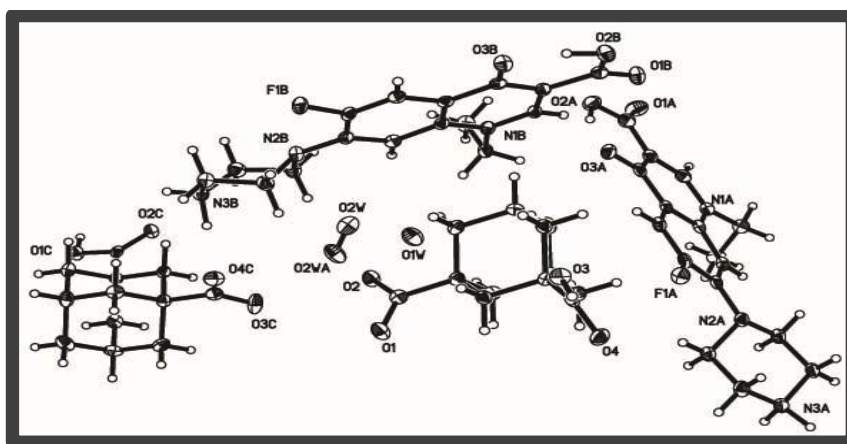
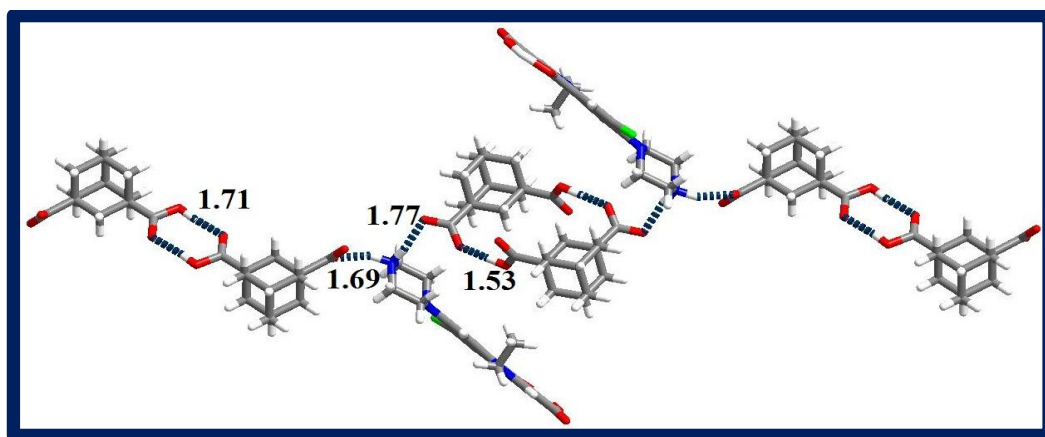


Figure 4.29. ORTEP of the contents in the asymmetric unit of **1d**.



Crystal structure analysis further reveals that, one of the carboxylic acid groups of both independent molecules of **1** are deprotonated. The ionic species are held together such that each of the molecules of **d** is connected to two acid molecules by N-H $\cdots$ O $^-$  hydrogen bonds yielding a triplet molecular unit. Such units are further linked to the adjacent units by two different modes through interaction between the -COOH groups present on the juxtaposed units. While, one of the -COOH groups formed well known R $_2^2(8)$  hydrogen bonding pattern, at the other end, the adjacent -COOH groups are held together by O-H $\cdots$ O hydrogen bonding but still yielding a dimer. The typical arrangement is shown in Figure 4.30. Hydrogen bond distances and other characteristics are compiled in Table 4.3.



**Figure 4.30.** The arrangement of molecules of components in the one-dimensional tape in **1d**.

Such an association forms an infinite chains, which are further held together constituting layers structure. However within a layer, the infinite chains exist as binary tapes that holding each other through the molecules of **d**, which in turn, are



connected to each other through water molecules. A schematic representation of a layer is shown in Figure 4.31.

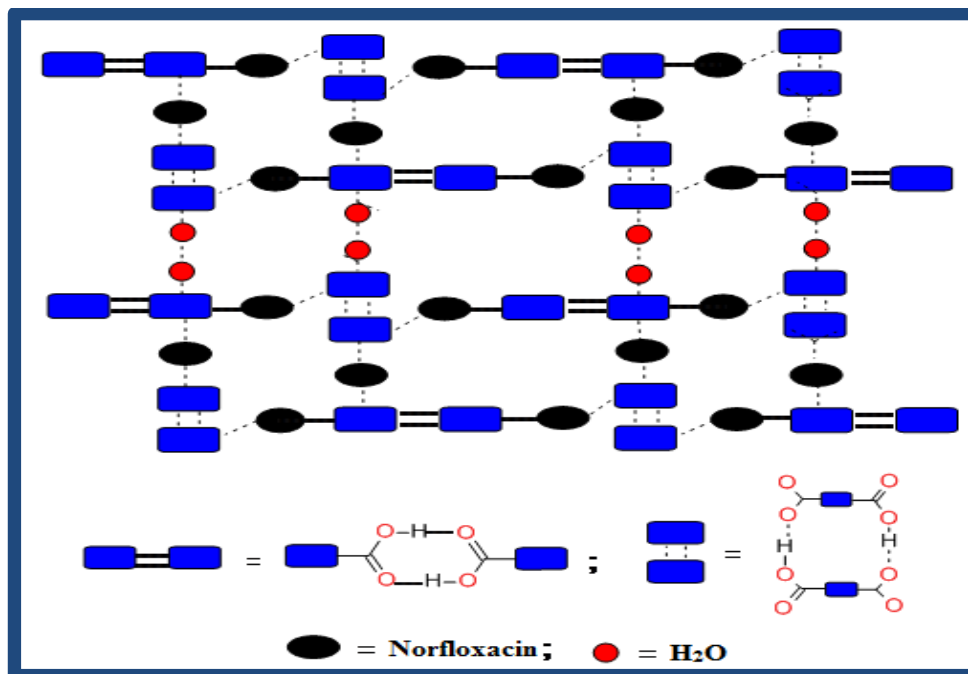


**Figure 4.31.** A schematic representation of a layer in the co-crystals of **1d**.

In contrast to **1a-1c**, crystals of **1d** are found to be intact even after prolonged exposure to atmosphere at ambient condition. But, variable temperature to PXRD in the temperature range 25-240 °C, as shown in Figure 4.32, shows a clear transformation **1d** into a new phase around the temperature 180 °C, with the appearance of totally new pattern without any correlation to either acid **1** or **d** also **1d**.

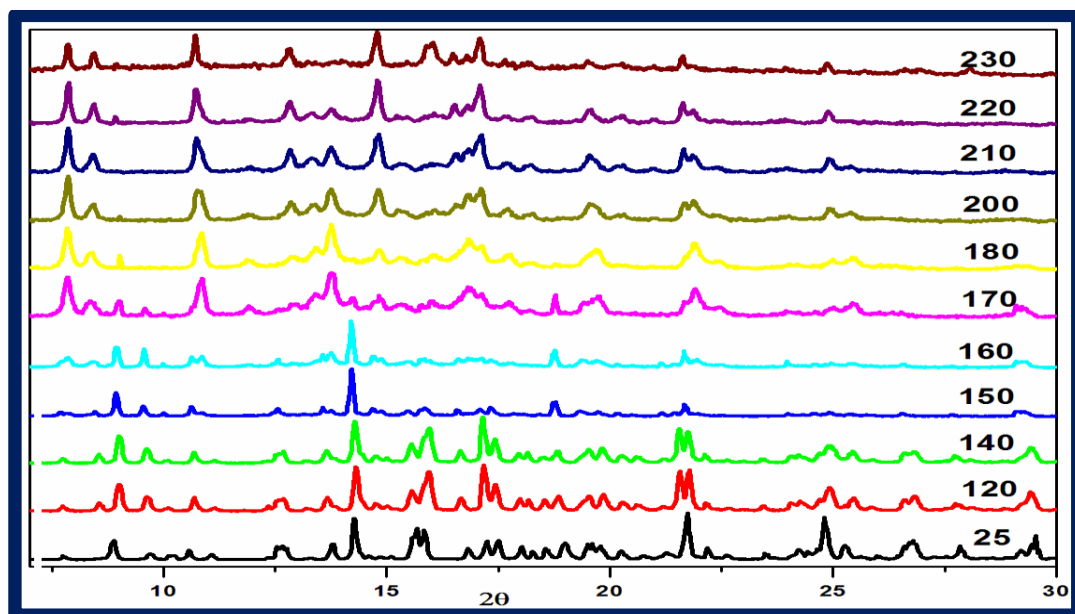


**Figure 4.32.** Comparison of PXRD patterns obtained at various temperatures for **1d**.

Based on the results discussed in the earlier section, the phase is considered to be anhydrous form of **1d** and attempts have put forward to obtain single crystals of it for structure determination unambiguously. Single crystal obtained from a DMSO solution of **1** and **d**, have been found to be different from that of **1d** with different unit cell dimension. Structure determination reveals that, the crystals are composed of molecules of **1** and **d**, without any solvent of crystallization. Further, the characterization of these single crystals by PXRD have shown similar pattern as that of the pattern found at 180°C in variable temperatures PXRD studies. Thus, the high temperature form could be regarded as anhydrous form of **1d**. The new crystals are labeled as **1d'** for the purpose of discussion. The anhydrous co-crystals,

**1d'** has asymmetric unit with the co-crystal components in a 1:1 ratio, as shown in Figure 4.33. The pertinent crystallographic data for **1d'** is given in Table 4.2.

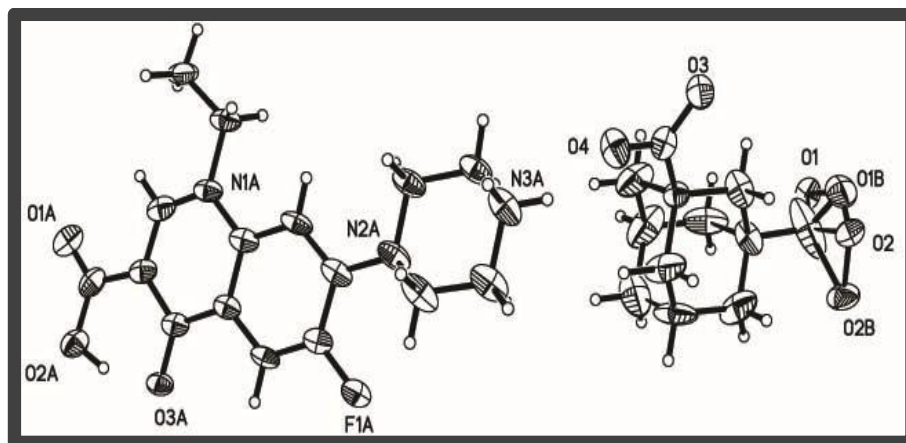


**Figure 4.33.** ORTEP of the contents in the asymmetric unit of **1d'**.

Packing analysis, further levels that, one of the carboxylic acid groups of **1** is deprotonated and forms an anion and a norfloxacin cation. In the structure, the ionic species interact with each other through  $N^+ \cdots H \cdots O^-$  hydrogen bonds, as observed in **1d**, with each norfloxacin molecule connects to two acid molecules. Complete characteristics of hydrogen bonds are listed in Table 4.3. These ensembles are further extended to form infinite one-dimensional tape in the crystal lattice of **1d'** through interaction established between the adjacent molecules of **1** with the aid of single  $O-H \cdots O$  hydrogen bond, in the form of cyclic ensemble. The typical arrangement in the tape is shown in Figure 4.34. The layers, in turn, are packed in three-dimensional array by  $\pi \cdots \pi$  interactions, as depicted in Figure 4.35.

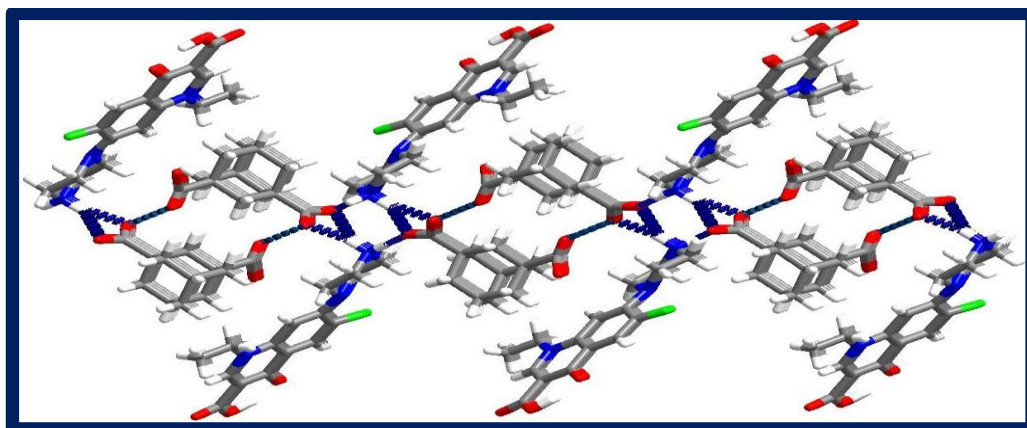


**Figure 4.34.** The typical two-dimensional layer obtained by the aggregation of the tapes.

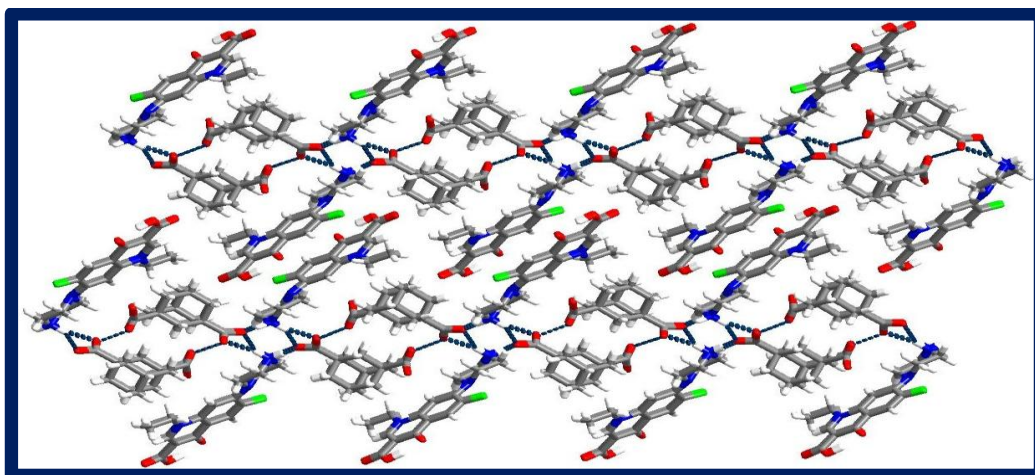


**Figure 4.35.** Three-dimensional arrangement in **1d'**.

## 4.6 Conclusions

In summary, hydrated (**1a-1d**) and anhydrous (**1a'-1d'**) co-crystals formed by 1,3-adamantanedicarboxylic acid with compounds **a-d** have been prepared by varying the solvent of crystallization. The solvents such as DMSO/DMF apparently are directing the formation of anhydrate co-crystals of the corresponding hydrated co-crystals, in the form of single crystals. The structural analysis of all the co-crystals has been carried out by single crystal X-ray diffraction method. The analysis of the co-crystals is revealed that, the crystal structure packing of corresponding anhydrous co-crystals is changed because of presence of water.

The crystals of **1a** and **1c** undergo phase transition to the corresponding anhydrous co-crystals **1a'** and **1c'**, even at ambient condition, while the crystals of **1b** and **1d** transformed to **1b'** and **1d'**, upon thermal treatment. Further, **1a'** and **1c'** are found to be irreversible, while **1b'** and **1d'** were transformed to **1b** and **1d**, respectively, when they were exposed to the atmosphere at ambient condition.

## **4.7 Experimental Section**

### **4.7.1 Synthesis of Co-crystals 1a-1d and 1a'-1d'**

All chemicals used in this study were obtained from Sigma Aldrich and used as such without any further purification. The solvents employed for the co-crystallization purpose were of spectroscopy grade of highest available purity. Co-crystals of **1a-1d** and **1a'-1d'** (except **1c'**) have been prepared by slow evaporation of corresponding solutions of the co-crystals components in the 1:1 ratio. However, **1c'** was prepared by diffusion of methanol solution of piperazine into DMSO solution of 1,3-adamantanedicarboxylic acid. Single crystals of good quality were obtained over a period of 48 h which are suitable for characterization by single crystal X-ray diffraction method.

### **4.7.2 X-ray Structure Determination**

Good quality single crystals of **1a-1d** and **1a'-1d'** were carefully selected using Leica microscope and glued to a glass fibre using an adhesive (cyanoacrylate). In all the cases, the crystals were smeared in the adhesive solution to prevent decomposition of crystals. The intensity data were collected on a Bruker single-crystal X-ray diffractometer, equipped with an APEX detector. Subsequently, the data were processed using the Bruker suite of programs (SAINT), and the convergence was found to be satisfactory with good  $R_{ini}$  parameters.<sup>19</sup> Absorption corrections were applied using SADABS package.<sup>19</sup> The structure determination by direct methods and refinements by least-squares methods on  $F^2$

were performed using the SHELXTL-PLUS package. The processes were smooth without any complications. All non-hydrogen atoms were refined anisotropically, while hydrogen atoms are treated isotropically. All the intermolecular interactions were computed using PLATON.<sup>20</sup> All packing diagrams are generated using Diamond software.<sup>21</sup>

#### **4.7.3 X-ray Powder diffraction Measurements**

X-ray Powder diffraction (XPRD) data were collected on a PANalytical diffractometer with Cu-K $\alpha$  radiation ( $\lambda = 1.5406$ ). The power of the X-ray generator was set to 40 kV and 30 mA with step size 0.017 ( $2\theta$ ) in a continuous scanning mode.

#### **4.7.4 Thermogravimetric measurements**

Thermogravimetric analyses (TGA) were performed on a Mettler Toledo TGA/SDTA 851e module. Co-crystals samples placed in open alumina pans for TGA experiments. Sample size is in the range of 1-7mg. The samples were heated in the temperature range 25-250°C at a rate of 10°C/min. The samples were purged with flow dry nitrogen at 150 ml/min.

#### **4.7.5 Differential Scanning Calorimetric measurements**

Differential Scanning Calorimetric analyses (TGA) were performed on a Mettler Toledo 822. Sample used for DSC analysis is in the range of 1-5 mg. The samples were heated in the temperature range 25-350°C at a rate of 10°C/min.

**Table 4.1.** Crystallographic data and structure refinement parameters for the co-crystals **1a'**, **1b** and **1b'**

	<b>1a'</b>	<b>1b</b>	<b>1b'</b>
formula	$C_{12}H_{16}O_4:C_{12}H_8N_2$	$C_{12}H_{16}O_4:C_6H_{12}N_2$ : $H_2O$	$C_{12}H_{16}O_4:C_6H_{12}N_2$
formula wt	404.45	354.44	173.17
crystal system	triclinic	monoclinic	orthorhombic
space group	$P\bar{1}$	$P2_1/n$	$Cmcm$
$a/\text{\AA}$	7.000(3)	11.334(3)	9.787(5)
$b/\text{\AA}$	10.048(5)	12.132(3)	8.780(4)
$c/\text{\AA}$	14.200(7)	13.092(4)	21.060(1)
$\alpha^\circ$	79.46(7)	90	90
$\beta^\circ$	79.34(8)	91.38(5)	90
$\gamma^\circ$	79.68(8)	90	90
$V/\text{\AA}^3$	953.9(8)	1799.5(9)	1809.8(2)
$Z$	2	4	8
$D_c/\text{g cm}^{-3}$	1.408	1.308	1.271
$\mu/\text{mm}^{-1}$	0.096	0.095	0.090
$2\theta$ range[ $^\circ$ ]	50.48	50.18	50.10
$T/\text{K}$	120	100	293
$F(000)$	428	768	720
$\lambda/\text{\AA}$	0.71073	0.71073	0.71073
$\Delta\rho_{\text{min,max}}/e \text{\AA}^{-3}$	-0.193, 0.258	-0.292, 0.599	0.398, -0.222
total reflections	9383	15506	6259
unique reflections	3455	3198	878
reflections used	2565	2394	652
no. of parameters	279	299	111
$R_1, I > 2\sigma(I)$	0.0384	0.0755	0.1077
$wR_2, I > 2\sigma(I)$	0.0937	0.2223	0.3036



**Table 4.2.** Crystallographic data and structure refinement parameters for the co-crystals **1c**, **1d** and **1a'**, **1d'**.

	<b>1c</b>	<b>1c'</b>	<b>1d</b>	<b>1d'</b>
<b>formula</b>	$C_{12}H_{16}O_4 \cdot 0.5(C_2H_5N)$ :H <sub>2</sub> O	$C_{12}H_{16}O_4 \cdot C_4H_{10}N_2$	$C_{12}H_{16}O_4 \cdot C_{16}H_{18}N_3FO_3$ :H <sub>2</sub> O	$C_{12}H_{16}O_4 \cdot C_{16}H_{18}N_3FO_3$
<b>formula wt</b>	285.33	310.39	559.58	542.57
<b>crystal system</b>	triclinic	monoclinic	triclinic	monoclinic
<b>space group</b>	<i>P</i> $\bar{1}$	<i>C</i> 2/ <i>c</i>	<i>P</i> $\bar{1}$	<i>P</i> 2 <sub>1</sub> / <i>c</i>
<b><i>a</i>/Å</b>	6.622(1)	6.322(3)	12.917(3)	17.055(6)
<b><i>b</i>/Å</b>	6.690(1)	12.332(5)	14.424(3)	7.005(2)
<b><i>c</i>/Å</b>	17.791(4)	20.154(8)	14.616(3)	23.388(7)
<b><math>\alpha^\circ</math></b>	98.10(4)	90	102.27(3)	90
<b><math>\beta^\circ</math></b>	91.43(4)	95.45(7)	97.03(4)	115.190(19)
<b><math>\gamma^\circ</math></b>	113.76(4)	90	93.76(3)	90
<b><i>V</i>/Å<sup>3</sup></b>	711.2(3)	1564.1(1)	2629.1(9)	2528.4(14)
<b><i>Z</i></b>	2	4	4	4
<b><i>D<sub>c</sub></i>/g cm<sup>-3</sup></b>	1.332	1.318	1.414	1.425
<b><math>\mu</math>/mm<sup>-1</sup></b>	0.101	0.094	0.109	0.108
<b>2<math>\theta</math> range[°]</b>	50.06	50.00	50.58	50.56
<b><i>T</i>/K</b>	100	293	120	120
<b><i>F</i>(000)</b>	308	672	1184	1148
<b><math>\lambda</math>/Å</b>	0.71073	0.71073	0.71073	0.71073
<b><math>\Delta\rho_{\min.\max}</math>/e Å<sup>-3</sup></b>	-0.180, 0.169	-0.176, 0.172	-0.212, 0.626	-0.408, 0.486
<b>total reflections</b>	6908	5564	26064	11881
<b>unique reflections</b>	2500	1384	9516	4591
<b>reflections used</b>	1431	1093	7169	2952
<b>no. of parameters</b>	270	153	763	371
<b><i>R</i><sub>1</sub>, <i>I</i> &gt; 2<math>\sigma</math>(<i>I</i>)</b>	0.0543	0.0534	0.0413	0.0639
<b><i>wR</i><sub>2</sub>, <i>I</i> &gt; 2<math>\sigma</math>(<i>I</i>)</b>	0.0896	0.1077	0.1056	0.1622

**Table 4.3.** Characteristics of hydrogen bond distances (Å) and angles (°) observed in the co-crystals **1a - 1d** and **1a' - 1d'**.

Complexes	O-H...N			C-H...O			O-H...O			N-H...O		
	H...N	O...N	O-H...N	H...O	C...O	C-H...O	H...O	O...O	O-H...O	H...O	N...O	N-H...O
<b>1a</b>	1.79	2.77	172	2.73	3.61	138						
				2.77	3.40	117						
<b>1a'</b>	1.70	2.67	172	2.20	3.25	161						
	1.81	2.77	162	2.61	3.29	120						
				2.79	3.44	118						
				2.88	3.47	114						
<b>1b</b>	2.03	2.98	163				1.55	2.53	173	1.61	2.61	175
							1.93	2.90	167			
<b>1c</b>							1.65	2.63	171	1.72	2.71	169
							1.80	2.75	160	1.67	2.68	174
							1.88	2.80	154			
<b>1c'</b>				2.31	3.31	153				1.65	2.64	170
										1.67	2.68	177
<b>1d</b>							1.53	2.51	176	1.69	2.69	177
							1.71	2.68	173	1.73	2.69	158
										1.77	2.74	161
										1.78	2.73	155
<b>1d'</b>										1.73	2.67	153
										1.88	2.84	157
										2.17	3.00	138

## 4.8 References

1. Vishweshwar, P.; McMahon, J. A.; Bis, J. A.; Zaworotko, M. J. *J. Pharm. Sci.* 2006, *95*, 499–516.
2. Wohler, F. *Annalen Chem. Pharm.* 1844, *51*, 145.
3. Stahly, G. P. *Cryst. Growth. Des.* 2009, *9*, 4212.
4. (a) Gutov, O. V.; Rusanov, E. B.; Kudryavtsev, A. A.; Garasevych, S. G.; Slobodyanyuk, O. V.; Yashchuk, V. M.; Chernega, A. N. *Crystengcomm* 2011, *13*, 1373-1377; (b) Cheney, M. L.; McManus, G. J.; Perman, J. A.; Wang, Z. Q.; Zaworotko, M. J. *Cryst. Growth. Des.* 2007, *7*, 616-617; (c) Desiraju, G. R., *Crystal Engineering: The Design of Organic Solids*. Elsevier: Amsterdam: 1989; (d) Seddon, K. R.; Zaworotko, M. J., *Crystal Engineering: The Design and Application of Functional Solids*. NATO-ASI Series; Kluwer: Dordrecht, The Netherlands: 1999; Vol. 539; (e) Kuroda, R.; Sato, T.; Imai, Y. *Crystengcomm* 2008, *10*, 1881-1890; (f) Pan, F.; Wong, M. S.; Gramlich, V.; Bosshard, C.; Gunter, P. *J. Am. Chem. Soc.* 1996, *118*, 6315-6316; (g) Childs, S. L.; Chyall, L. J.; Dunlap, J. T.; Smolenskaya, V. N.; Stahly, B. C.; Stahly, G. P. *J. Am. Chem. Soc.* 2004, *126*, 13335-13342; (h) Remenar, J. F.; Morissette, S. L.; Peterson, M. L.; Moulton, B.; MacPhee, J. M.; Guzman, H. R.; Almarsson, O. *J. Am. Chem. Soc.* 2003, *125*, 8456-8457; (i) Perumalla, S. R.; Suresh, E.; Pedireddi, V. R. *Angew. Chem., Int. Ed.* 2005, *44*, 7752-7757; (j) Remenar, J. F.; Morissette, S. L.; Peterson, M.

- L.; Moulton, B.; MacPhee, J. M.; Guzman, H. R.; Almarsson, O. *J. Am. Chem. Soc.* 2003, *125*, 8456-8457.
5. (a) Trask, A. V.; Motherwell, W. D. S.; Jones, W. *Cryst. Growth. Des.* 2005, *5*, 1013-1021; (b) Aakeroy, C. B.; Forbes, S.; Desper, J. *J. Am. Chem. Soc.* 2009, *131*, 17048; (c) Karki, S.; Friscic, T.; Jones, W.; Motherwell, W. D. S. *Mol. Pharm.* 2007, *4*, 347-354; (d) Jones, W.; Motherwell, S.; Trask, A. V. *Mrs Bull* 2006, *31*, 875-879; (e) Shiraki, K.; Takata, N.; Takano, R.; Hayashi, Y.; Terada, K. *Pharmaceut. Res.* 2008, *25*, 2581-2592.
6. (a) Shen, J. P.; Duan, X. H.; Luo, Q. P.; Zhou, Y.; Bao, Q. L.; Ma, Y. J.; Pei, C. H. *Cryst. Growth. Des.* 2011, *11*, 1759-1765; (b) Wei, C. X.; Huang, H.; Duan, X. H.; Pei, C. H. *Propell. Explos. Pyrot.* 2011, *36*, 416-423.
7. (a) Hulliger, J.; Konig, O.; Hoss, R. *Adv. Mater.* 1995, *7*, 719-721; (b) Hulliger, J.; Konig, O.; Hoss, R. *Adv. Mater.* 1995, *7*, 719-721.
8. (a) Talwelkar, M.; Pedireddi, V. R. *Tetrahedron Lett.* 2010, *51*, 6901-6905; (b) Delori, A.; Suresh, E.; Pedireddi, V. R. *Chem.-Eur. J.* 2008, *14*, 6967-6977; (c) Marivel, S.; Suresh, E.; Pedireddi, V. R. *Tetrahedron Lett.* 2008, *49*, 3666-3671.
9. (a) James, S. L.; Adams, C. J.; Bolm, C.; Braga, D.; Collier, P.; Friscic, T.; Grepioni, F.; Harris, K. D. M.; Hyett, G.; Jones, W.; Krebs, A.; Mack, J.; Maini, L.; Orpen, A. G.; Parkin, I. P.; Shearouse, W. C.; Steed, J. W.; Waddell, D. C. *Chem. Soc. Rev.* 2012, *41*, 413-447; (b) Delori, A.; Friscic, T.; Jones, W. *Crystengcomm* 2012, *14*, 2350-2362; (c) Pedireddi, V. R.;

- Jones, W.; Chorlton, A. P.; Docherty, R. *Chem. Commun.* 1996, 987-988; (d) Friscic, T.; Trask, A. V.; Jones, W.; Motherwell, W. D. S. *Angew. Chem., Int. Ed.* 2006, 45, 7546-7550.
10. Ranganathan, A.; Pedireddi, V. R.; Rao, C. N. R. *J. Am. Chem. Soc.* 1999, 121, 1752-1753.
11. Selvaraj, S. L.; Xavier, F. P. *J. Cryst. Growth.* 2001, 225, 168-172.
12. (a) Reddy, L. S.; Bhatt, P. M.; Banerjee, R.; Nangia, A.; Kruger, G. J. *Chem-Asian J* 2007, 2, 505-513; (b) Harings, J. A. W.; van Asselen, O.; Graf, R.; Broos, R.; Rastogi, S. *Cryst. Growth. Des.* 2008, 8, 2469-2477; (c) Dhumal, R. S.; Kelly, A. L.; York, P.; Coates, P. D.; Paradkar, A. *Pharmaceut. Res.* 2010, 27, 2725-2733.
13. Varughese, S.; Desiraju, G. R. *Cryst. Growth. Des.* 2010, 10, 4184-4196.
14. Khankari, R. K.; Grant, D. J. W. *Thermochim Acta* 1995, 248, 61-79.
15. Karki, S.; Friscic, T.; Jones, W.; Motherwell, W. D. S. *Mol. Pharm.* 2007, 4, 347-354.
16. Allen, F. H.; Kennard, O. *Chem. Des. Automate. News* 1993, 31-37.
17. Kadirvelraj, R.; Umarji, A. M.; Robinson, W. T.; Bhattacharya, S.; Row, T. N. G. *Chem. Mater.* 1996, 8, 2313-2323.
18. Marti-Rujas, J.; Morte-Rodenas, A.; Guo, F.; Thomas, N.; Fujii, K.; Kariuki, B. M.; Harris, K. D. M. *Cryst. Growth. Des.* 2010, 10, 3176-3181.
19. (a) G. M. Sheldrick, *SHELXTL-PLUS*, Program for Crystal Structure Solution and Refinement, University of Gottingen, Gottingen, Germany,

1997. (b) Siemens, *SMART System*. Siemens Analytical X-ray Instruments Inc., Madison, WI, 1995.
20. Spek, A. L. *PLATON*, Molecular Geometry Program; University of Utrecht: The Netherlands, 1995.
21. Diamond—Crystal and Molecular Structure Visualization, Version 3.1f, Crystal Impact, Brandenburg & Putz, Bonn 2008.

## List of Research Publications

1. "Co-Crystals of 1,3-Adamantanedicarboxylic Acid with N-oxide and Aza Compounds". Manjare, Y.; Pedireddi, V. R. *Cryst. Growth Des.*, **2011**, *11* (11), pp 5079–5086.
2. "Sandwich Type Supramolecular Assemblies: Molecular Adducts of Oxalic Acid with Aniline and 4-MethoxyAniline". Manjare, Y.; Pedireddi, V. R.; Harris, K. D. M.; Babu, K. R.; Kariuki, B. (Manuscript under preparation)
3. "Designer Host-Guest Complexes: Co-crystals of 1,3-Adamantanedicarboxylic Acid and 4,7-Phenanthroline". Manjare, Y.; Pedireddi, V. R. (Manuscript under preparation)
4. "Preparation and Analysis of Anhydrous and Hydrated Forms of Co-crystals of 1,3- Adamantanedicarboxylic Acid with Aza Compounds". (Manuscript under preparation)

## Symposia/Poster presentation

1. XX International Conference on the Chemistry of the Organic Solid State ICCOSS XX, Indian Institute of Science, Bangalore, India, 25-30<sup>th</sup> June, 2011.
2. Workshop on "X-Ray techniques for Materials Research" IIT Bombay, 4<sup>th</sup> and 5<sup>th</sup> December, 2009.
3. Annual meeting of the American Crystallographic Association in Toronto, Canada, July 25 - 30, 2009.
4. 38<sup>th</sup> National Seminar on Crystallography, Mysore, India, 11-13<sup>th</sup> February, 2009.
5. 4<sup>th</sup> J-NOST Conference, Madurai Kamaraj University, Madurai, 6-9<sup>th</sup> December, 2008.
6. SERC Summer School in Modelling and Informatics in Drug Designing, 30<sup>th</sup> -18 July, 2008.